
***National Nanotechnology Coordinated
Infrastructure (NNCI)***

Research and Education Highlights

Year 4 (October 2018 – September 2019)



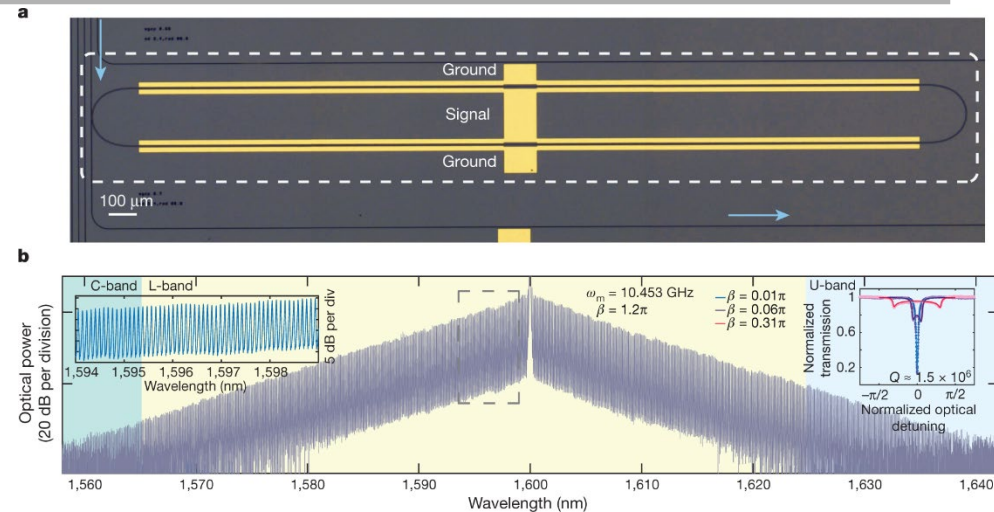
Table of Contents

Center for Nanoscale Systems (CNS)	3
Cornell Nanoscale Science and Engineering Facility (CNF)	11
Kentucky Multi-Scale Manufacturing and Nano Integration Node (KY MMNIN)	17
Mid-Atlantic Nanotechnology Hub (MANTH)	26
Midwest Nanotechnology Infrastructure Corridor (MINIC)	35
Montana Nanotechnology Facility (MONT)	43
Nanotechnology Collaborative Infrastructure Southwest (NCI-SW)	54
Nebraska Nanoscale Facility (NNF)	67
NNCI Site @ Stanford (nano@stanford)	75
Northwest Nanotechnology Infrastructure (NNI)	82
Research Triangle Nanotechnology Network (RTNN)	97
San Diego Nanotechnology Infrastructure (SDNI)	106
Soft and Hybrid Nanotechnology Experimental (SHyNE) Resource	112
Southeastern Nanotechnology Infrastructure Corridor (SENIC)	119
Texas Nanofabrication Facility (TNF)	134
Virginia Tech National Center for Earth and Environmental Nanotechnology Infrastructure (NanoEarth)	144
Education and Outreach	151

Center for Nanoscale Systems (CNS)

Broadband electro-optic frequency comb generation in a lithium niobate microring resonator

Optical frequency combs consist of equally spaced discrete optical frequency components and are essential tools for next generation quantum optical communication, precision metrology, timing and spectroscopy. Here the Loncar team has realized an integrated EO comb generator in a thin-film lithium niobate photonic platform that features a large EO response, ultralow optical loss and highly co-localized microwave and optical fields, while enabling dispersion engineering. Their measured EO comb spans more frequencies than the entire telecommunications L-band (over 900 comb lines spaced about 10 gigahertz apart), and they show that future dispersion engineering can enable octave-spanning combs. Furthermore, they demonstrate the high tolerance of our comb generator to modulation frequency detuning, with frequency spacing finely controllable over seven orders of magnitude (10 hertz to 100 megahertz), and they use this feature to generate dual-frequency combs in a single resonator.



a, Micrograph of a fabricated lithium niobate microring resonator (a shorter device is shown here for illustration purposes). The black lines are etched optical waveguides and the yellow regions are gold microelectrodes. The gold electrodes are driven so that the phase shifts on the two sides of the microresonator are opposite, which is required to break the symmetry of different azimuthal order optical modes, enabling efficient frequency conversion. **b**, Measured output spectrum of the EO comb generated from the microring resonator, demonstrating a bandwidth exceeding 80 nm and more than 900 comb lines with a slope of 1 dB nm⁻¹. The left inset shows a magnified view of several comb lines, with a line-to-line power variation of about 0.1 dB. The right inset shows the measured transmission spectrum for several different modulation indices β .

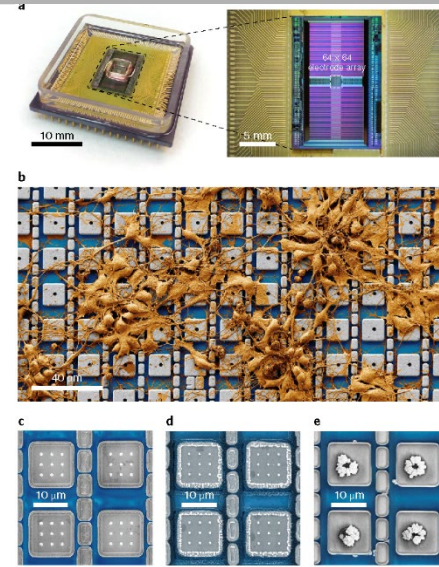
Mian Zhang, Brandon Buscaino, Cheng Wang, Amirhassan Shams-Ansari, Christian Reimer, Rongrong Zhu, Joseph M. Kajm, and Marko Loncar. Work performed at Center for Nanoscale Systems.

This work was supported by NSF ECCS-1541959; ECCS-1609549; ECCS-1740291 E2CDA; ECCS-1740296 E2CDA; DMR-1231319. *Nature Comm* (2019) 10:978; *Appl. Phys. Lett.*, 115, 12108 (2019)

National Research Priority: NSF-Quantum Leap

A nanoelectrode array for obtaining intracellular recordings from thousands of connected neurons

Current electrophysiological or optical techniques cannot reliably perform simultaneous intracellular recordings from more than a few tens of neurons. The Ham group developed a nanoelectrode array that can simultaneously obtain intracellular recordings from thousands of connected mammalian neurons in vitro. The array consists of 4,096 platinum-black electrodes with nanoscale roughness fabricated on top of a silicon chip that monolithically integrates 4,096 microscale amplifiers, configurable into pseudocurrent-clamp mode (for concurrent current injection and voltage recording) or into pseudovoltage-clamp mode (for concurrent voltage application and current recording). We used the array in pseudovoltage-clamp mode to measure the effects of drugs on ion-channel currents. In pseudocurrent-clamp mode, the array intracellularly recorded action potentials and postsynaptic potentials from thousands of neurons.



a, A CMOS-activated PtB electrode array packaged with a microfluidic well (left) in which neurons are cultured. Its CMOS IC (right) contains an array of 64×64 pixel pads ($20 \mu\text{m}$ pitch) at its centre. On each pad PtB-coated Pt electrodes are built. **b**, False coloured scanning electron microscope image of neurons cultured on top of the electrode array of an example CNEI device. Actual recording experiments are performed with much higher neuron densities containing three to six cell layers covering the entire electrode array

Jeffrey Abbott, Tianyang Ye, Keith Krenek, Rona S. Gertner, Steven Ban, Youbin Kim, Ling Qin, Wenxuan Wu, Hongkun Park, and Donhee Ham. Work performed at Center for Nanoscale Systems.

This work was supported in part by ARO W911NF-15-1-0565; W911NF-17-1-0425; NIH #1-U01-MH105960-01. *Nature Biomedical Engineering* (2019)

National Research Priority: NSF-Understanding the Rules of Life

Photon-mediated interactions between quantum emitters in a diamond nanocavity

Photon-mediated interactions between quantum systems are essential for realizing quantum networks and scalable quantum information processing. The Loncar and Lukin groups have demonstrated such interactions between pairs of silicon-vacancy (SiV) color centers coupled to a diamond nanophotonic cavity. When the optical transitions of the two-color centers are tuned into resonance, the coupling to the common cavity mode results in a coherent interaction between them, leading to spectrally resolved superradiant and subradiant states. They use the electronic spin degrees of freedom of the SiV centers to control these optically mediated interactions. Such controlled interactions will be crucial in developing cavity-mediated quantum gates between spin qubits and for realizing scalable quantum network nodes.

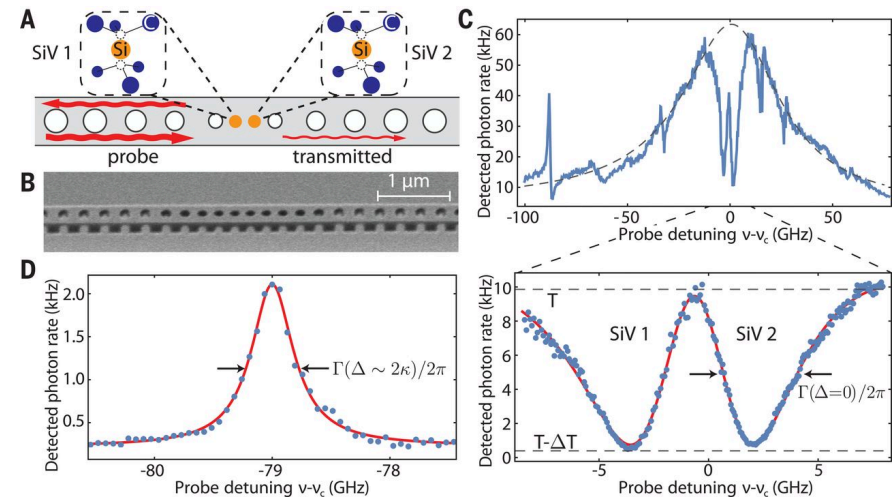


Fig. 1 High cooperativity SiV-photon interface. (A) Schematic of a diamond nanocavity containing two SiV centers. (B) Scanning electron micrograph of a nanocavity. (C) Transmission spectrum of the coupled SiV-cavity system (blue). The broad Lorentzian response of an empty cavity (dashed) is modulated by cavity-coupled SiVs. Near the cavity resonance (lower panel), two SiVs each result in greater than 95% extinction in transmission

R.E. Evans, R. E.; Bhaskar, M. K.; Sukachev, D. D.; Nguyen, C. T.; Sipahigil, A.; Burek, M. J.; Machielse, B.; Zhang, G. H.; Zibrov, A. S.; Bielejec, E.; Park, H.; Loncar, M.; Lukin, M. D ; Work performed at Center for Nanoscale Systems.

This work was supported by NSF ECCS-1541959; DOE-SC DE-NA-0003525. *Science* 362, 662-665, 2018

National Research Priority: NSF-Quantum Leap

Cryo-EM structures and dynamics of substrate-engaged human 26S proteasome

The proteasome is an ATP-dependent, 2.5-megadalton molecular machine that is responsible for selective protein degradation in eukaryotic cells. Here we present cryo-electron microscopy structures of the substrate-engaged human proteasome in seven conformational states at 2.8–3.6 Å resolution, captured during breakdown of a polyubiquitylated protein. These structures illuminate a spatiotemporal continuum of dynamic substrate–proteasome interactions from ubiquitin recognition to substrate translocation, during which ATP hydrolysis sequentially navigates through all six ATPases.

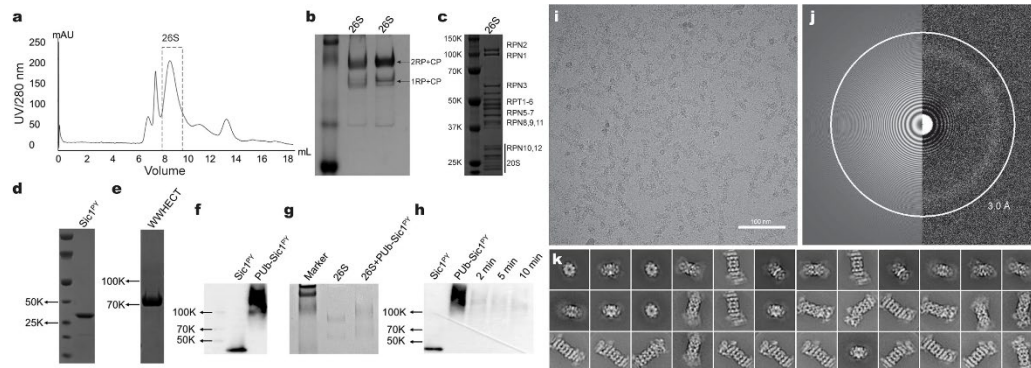


Fig. 1 Characterization and structure determination of the substrate-engaged human proteasome. a, FPLC purification of the human 26S proteasome on Superose 6 10/300 GL. The dashed box shows the fraction taken for structural analysis. b, Native PAGE analysis of proteasome purified as in a. c, SDS–PAGE analysis of proteasome purified as in a. d, SDS–PAGE analysis of Sic1PY purified through a Superdex 75 column. e, SDS–PAGE analysis of WW-HECT purified through Superdex 75. b–e, Stained with Coomassie blue. f, SDS–PAGE/western blot analysis of polyubiquitinated Sic1PY. After ubiquitination, the samples were applied to a SDS–polyacrylamide gel, followed by western blotting with anti-T7 antibody. The result suggests that almost all Sic1PY is ubiquitinated. g, Native PAGE analysis of proteasomes crosslinked to PUB-Sic1PY. Left, no-substrate control. With the addition of the PUB-Sic1PY, the proteasomes ran slower than without PUB-Sic1PY, indicating that the substrate had been captured by the proteasome but not totally degraded when samples were prepared for cryo-EM analysis. h, SDS–PAGE/western blot analysis of the degradation of PUB-Sic1PY, which was visualized with anti-T7 antibody. This experiment confirms that PUB-Sic1PY is readily degraded by our proteasome samples. i, Typical cryo-EM micrograph of the substrate-engaged human proteasome after motion correction. All experiments in a–i were repeated independently at least three times with similar results. j, Power spectrum evaluation of the micrograph shown in i. k, Gallery of unsupervised class averages calculated by ROME54 using machine-learning-based clustering.

Yuanchen Dong, Shuwen Zhang, Zhaolong Wu, Xuemei Li, Wei Li Wang, Yanan Zhu, Svetla Stoilova-McPhie, Ying Lu, Daniel Finley & Youdong Mao. Initial cryo-EM screening was performed at the Center for Nanoscale Systems.

This work was supported by National Natural Science Foundation of China #11774012 and #91530321, NIH GM43601, NSF NNCI-1541959 and NIH AI100645. *Nature*, 565, p. 49 (2019)

Electron-phonon instability in graphene revealed by global and local noise probes

Understanding and controlling nonequilibrium electronic phenomena is an outstanding challenge in science and engineering. By electrically driving ultraclean graphene devices out of equilibrium, we observe an instability that is manifested as substantially enhanced current fluctuations and suppressed conductivity at microwave frequencies. Spatial mapping of the nonequilibrium current fluctuations using nanoscale magnetic field sensors reveals that the fluctuations grow exponentially along the direction of carrier flow. Our observations, including the dependence on density and temperature, are consistently explained by the emergence of an electron-phonon Cerenkov instability at supersonic drift velocities. These results offer the opportunity for tunable terahertz generation and active phononic devices based on two-dimensional materials.

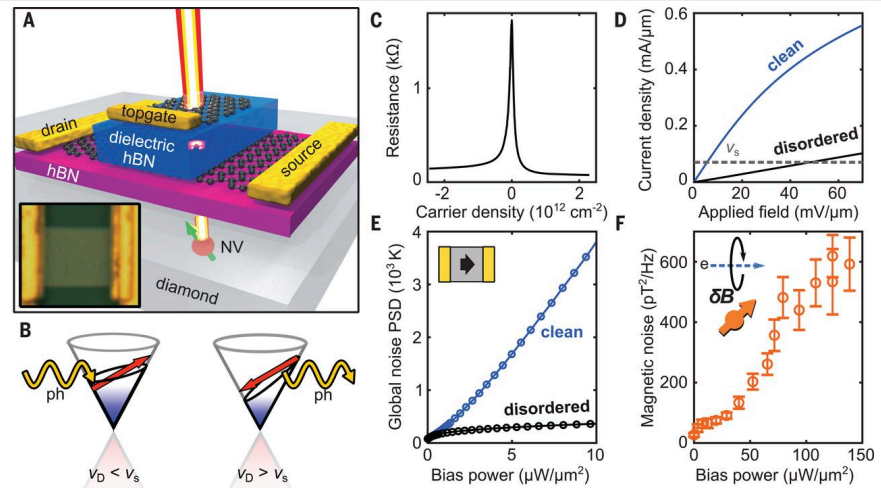


Fig. 1 Nonequilibrium dynamics in graphene, probed both globally and locally. **(A)** Device schematic: hBN-encapsulated graphene device on diamond substrate containing NV centers for nanomagnetometry. (Inset) Optical image of clean hBN-encapsulated device A1 (6 μm by 5.4 μm). **(B)** Condition for Cerenkov emission of phonons: when $v_D > v_s$, stimulated phonon (ph) emission dominates over absorption (right). **(C)** Two-probe resistance versus carrier density of device A1 ($T = 10$ K). **(D)** Current density as a function of applied electric field ($T = 80$ K) in clean device A1 (blue) and disordered device B1 (7 μm by 18 μm , black). The gray dashed line indicates where $v_D = v_s$ for the longitudinal acoustic mode. **(E)** Global electronic noise PSD (averaged over 100 to 300 MHz) as a function of bias power in devices A1 (blue) and B1 (black). Blue curve satisfies $v_D > v_s$ for $P > 0.12$ $\mu\text{W}/\mu\text{m}^2$. **(F)** Local magnetic noise (measured by NV nanomagnetometry) versus applied bias power in clean device C1 on diamond substrate.

T.I. Andersen, B.L. Dwyer, J.D. Sanchez-Yamagishi, J.F. Rodriguez-Nieva, K. Agarwal, K. Watanabe, T. Taniguchi, E.A. Demler, P. Kim, H. Park, M.D. Lukin. This work was performed at Center for Nanoscale Systems.

This work was supported by NSF ECCS-1541959, Elemental Strategy Initiative conducted by the MEXT, Japan and the CREST (JPMJCR15F3), and ARO W911NF-17-1-0574. *Science* 364, pp. 154-157 (2019)

National Research Priority: NSF Quantum Leap

Coherent control of a hybrid superconducting circuit made with graphene-based van der Waal heterostructures

Quantum coherence and control is foundational to the science and engineering of quantum systems. In van der Waals materials, the collective coherent behaviour of carriers has been probed successfully by transport measurements. However, temporal coherence and control, as exemplified by manipulating a single quantum degree of freedom, remains to be verified. Here the team demonstrates such coherence and control of a superconducting circuit incorporating graphene-based Josephson junctions. Furthermore, we show that this device can be operated as a voltage-tunable transmon qubit, whose spectrum reflects the electronic properties of massless Dirac fermions travelling ballistically. In addition to the potential for advancing extensible quantum computing technology, our results represent a new approach to studying van der Waals materials using microwave photons in coherent quantum circuits.

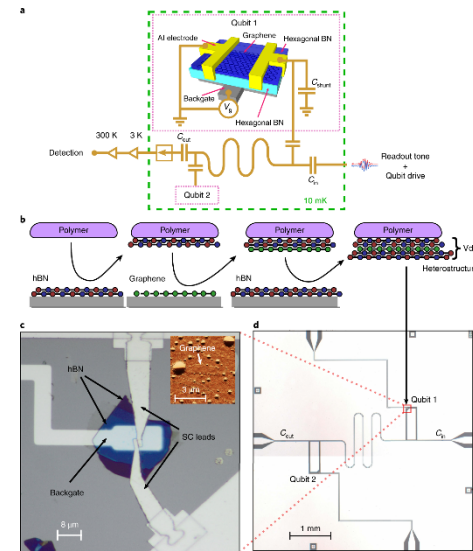


Fig. 1 *a*, Schematic of the hBN-encapsulated S–G–S junctions embedded in a cQED system. *b*, Assembly of vdW heterostructures using a dry polymer-based pick-up and transfer technique. *c*, Optical micrograph of the graphene transmon qubit. SC, superconducting. Inset, atomic force microscopy image of the encapsulated graphene before making electrical contact to the superconducting electrodes. *d*, Qubit chip made of high-quality aluminium. Each shunting capacitor is cut out at the corner (red box; see *c*) to host the assembled vdW stack. Bonding pads on the top and bottom of the chip are used for backgate control.

J. Wang, D. Rodan-Legrain, L. Bretheau, D.L. Campbell, B. Kannan, D. Kim, M. Kjaergaard, P. Krantz, G.O. Samach, F. Yan, J.L. Yoder, K. Watanabe, T. Taniguchi, T.P. Orlando, S. Gustavsson, P. Jarillo-Herrero, and W.D. Oliver. Work performed at CNS.

This work was supported by ARO #W911NF-17-S-0001, MIT Lincoln Lab Air Force #FA8721-05-C-0002, Gordon and Betty Moore Foundation's EPIQS Initiative #GBMF4541, Agence Nationale de la Recherche # ANR-18-CE47-0012, NSF DMR-14-19807 and ECCS-1541959. *Nature Nanotechnology*, 14, pp. 120-125 (2019).

Giant intrinsic photoresponse in pristine graphene

When the Fermi level is aligned with the Dirac point of graphene, reduced charge screening greatly enhances electron-electron scattering. In an optically excited system, the kinematics of electron-electron scattering in Dirac fermions is predicted to give rise to novel optoelectronic phenomena. Here reported is the observation of an intrinsic photocurrent in graphene, which occurs in a different parameter regime from all the previously observed photothermoelectric or photovoltaic photocurrents in graphene: the photocurrent emerges exclusively at the charge neutrality point, requiring no finite doping. Unlike other photocurrent types that are enhanced near p - n or contact junctions, the photocurrent observed in this work arises near the edges/corners. It is shown that the phenomenon stems from the unique electron-electron scattering kinematics in charge-neutral graphene.

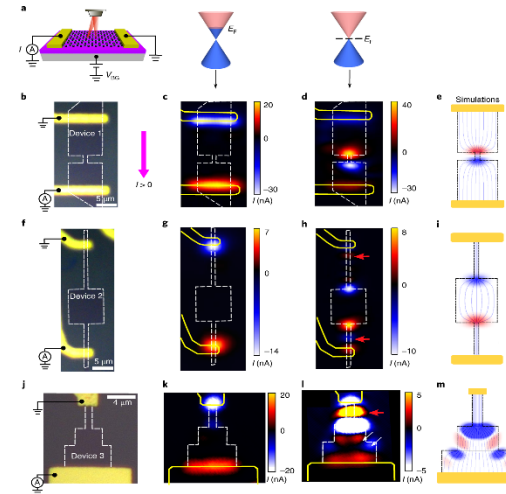


Fig. 1 *a*, Schematic of a back-gated graphene device with scanning laser excitation. The photocurrent is measured in a short-circuit configuration. *b-d*, Optical image (*b*) and scanning photocurrent images (*c,d*) of Device 1 with a narrower middle graphene channel. At high charge density (*c*), the photocurrent is mainly generated at the contact areas. At the CNP (*d*), however, significant photocurrent emerges at the two ends of the middle graphene region. *e*, Simulation of the photocurrent image for Device 1. *f-i*, Similar figures to *b-e*, for Device 2 with a wider middle graphene section. *j-m*, Similar figures to *b-e*, for Device 3 with three rectangular graphene regions with increasing widths. The white arrows in *I* indicate that the photocurrent is generated from the graphene edge. The red arrows in *h* and *I* denote the photocurrent along the straight edges, which cannot be accounted for by our simple model, but can be captured with some modifications.

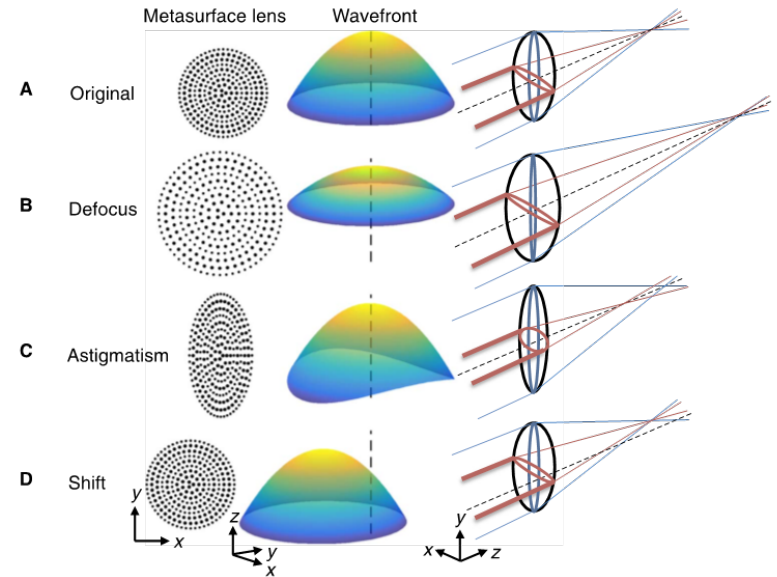
Q. Ma, C.H. Lui, J.C.W. Song, Y. Lin, J.F. Kong, Y. Cao, T.H. Dinh, N.L. Nair, W. Fang, K. Watanabe, T. Taniguchi, S.-Y. Xu, J. Kong, T. Palacios, N. Gedik, N.M. Gabor, and P. Jarillo-Herrero. Work performed at CNS.

This work was supported by NSF #DMR-14-19807, ECCS-1541959, STC Center for Integrated Quantum Materials, DMR-1231319. *Nature Nanotechnology* 14, pp. 145-150 (2019).

Cornell Nanoscale Science and Engineering Facility (CNF)

Adaptive metalenses with simultaneous electrical control of focal length, astigmatism, and shift

Focal adjustment and zooming are universal features of cameras and advanced optical systems. Recent advent of ultrathin planar lenses based on metasurfaces (metalenses), opens the door to future drastic miniaturization of mobile devices such as cell phones and wearable displays and mandates fundamentally different forms of tuning based on lateral motion rather than longitudinal motion. They demonstrate electrically tunable large-area metalenses controlled by artificial muscles capable of simultaneously performing focal length tuning (>100%) as well as on-the-fly astigmatism and image shift corrections, which until now were only possible in electron optics. Their results demonstrate the possibility of future optical microscopes that fully operate electronically, as well as compact optical systems that use the principles of adaptive optics to correct many orders of aberrations simultaneously



Adaptive metalenses with simultaneous electrical control of focal length, astigmatism, and shift.

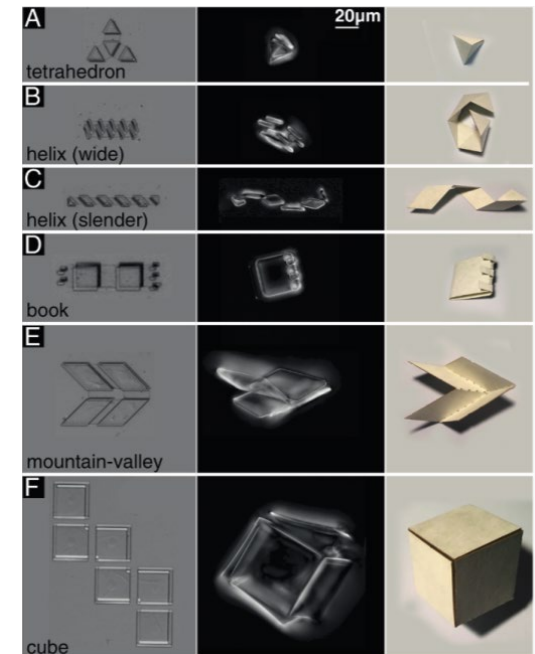
Clarke, Cappasso and coworkers (Harvard), J. Treichler, A. Windsor, G. Bordonaro, K. Musa, and D. Botsch Cornell Nanoscale Facility. Work performed at the Cornell Nanoscale Facility.

This work was supported by AFOSR MURI: FA9550-12-1-0389. NSF CMMI-1333835; MRSEC DMR 1420570. CNS ECCS-0335765. *Sci. Adv.* 2018;4:eaap9957

National Research Priority: NSF-Growing Convergence Research

Graphene-based bimorphs for micron-sized, autonomous origami machines

This presents an attractive platform for miniaturizing machines: thinner layers of folding material lead to smaller devices, provided that key functional aspects, such as conductivity, stiffness, and flexibility, are preserved. They show origami fabrication at its ultimate limit by using 2D atomic membranes as a folding material. As a prototype, they bond graphene sheets to nanometer-thick layers of glass to make ultra-thin bimorph actuators that bend to micrometer radii of curvature in response to small strain differentials. Although the graphene bimorphs are only nanometers thick, they can lift these panels, the weight equivalent of a 500-nm-thick silicon chip. These machines change shape in fractions of a second when crossing a tunable pH threshold, showing that they sense their environments, respond, and perform useful functions on time and length scales.



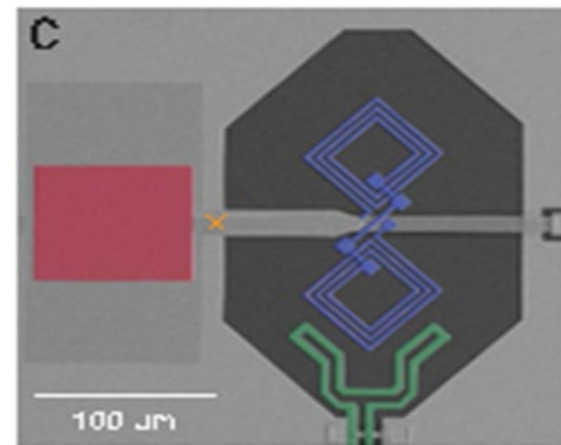
Marc Z. Miskin, Kyle J. Dorsey, Baris Bircan, Yimo Han, David A. Muller, Paul L. McEuen and Itai Cohen, Cornell University. Work performed at the Cornell Nanoscale Facility

This work was supported by NSF DMR-1719875, DMR-1429155, DMR-1435829, AFSOR MURI FA2386- 13-1-4118; (NNCI-1542081). *PNAS*, 115(3), 466–470, 2018

National Research Priority: NSF-Growing Convergence Research

Measurement of a superconducting qubit with a microwave photon counter

Fast, high-fidelity measurement is a key ingredient for quantum error correction. They introduce an approach to measurement based on a microwave photon counter demonstrating raw single-shot measurement fidelity of 92%. Conventional approaches to the measurement of superconducting qubits, involving linear amplification of a microwave probe tone followed by heterodyne detection at room temperature, do not scale well to large system sizes. Moreover, the intrinsic damping of the photon counter is used to extract the energy released by the measurement process, allowing repeated high-fidelity quantum nondemolition measurements. Their scheme provides access to the classical outcome of projective quantum measurement at the millikelvin stage and could form the basis for a scalable quantum-to-classical interface.



Superconducting Qubit with microwave photon counter

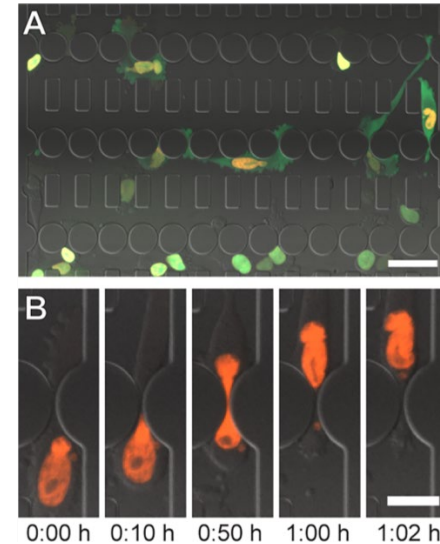
McDermott (University Wisconsin), Plourde (Syracuse University) and coworkers. Work performed at the Cornell Nanoscale Facility.

This work was supported by ARO W911NF-14-1-0080 and W911NF-15-1-0248. (NNCI-1542081).
Science, 361, 1239–1242 (2018)

National Research Priority: NSF-Quantum Leap

Automated analysis of cell migration and nuclear envelope rupture in confined environments

Recent *in vitro* and *in vivo* studies have highlighted the importance of the cell nucleus in governing migration through confined environments. Devices that mimic narrow interstitial spaces have emerged as important tools to study cellular dynamics during confined migration, including the consequences of nuclear deformation and nuclear envelope rupture. Studies that compare large numbers of cell types and conditions require automated image analysis to achieve sufficiently high throughput. Applying the program to specific biological examples, they demonstrate its ability to detect differences in nuclear transit time between cells with different levels of the nuclear envelope proteins lamin A/C, which govern nuclear deformability, and to detect an increase in nuclear envelope rupture duration in cells.



Automated analysis of cell migration and nuclear envelope rupture in confined environments

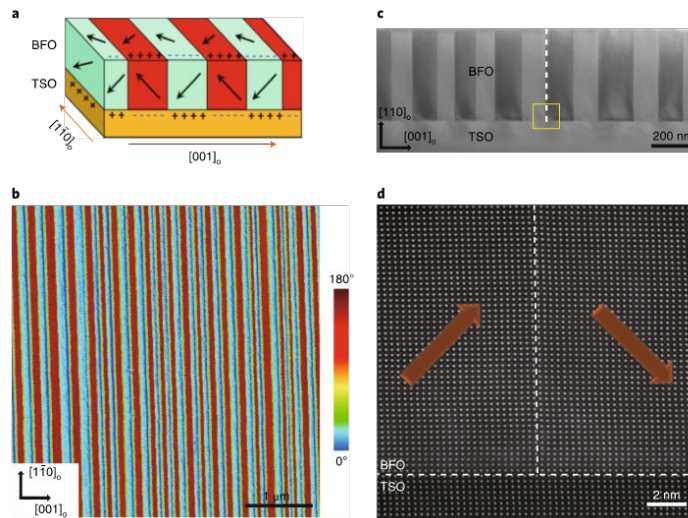
Lammerding (Cornell University) and coworkers. Work performed at the Cornell Nanoscale Facility

This work was supported by NIH [R01 HL082792 and U54 CA210184]; DoD Breakthrough Award BC150580, NSF CAREER CBET-1254846; NSF GRFP DGE-1144153, (NNCI-1542081). *PLoS ONE* 13(4): e0195664

National Research Priority: NSF-Understanding the Rules of Life

Anisotropic polarization-induced conductance at a ferroelectric–insulator interface

By probing the local conductance and ferro-electric polarization over a cross-section of a $\text{BiFeO}_3\text{-TbScO}_3$ (BFO/TSO) (001) heterostructure, they demonstrated that this interface is conducting along the 109 domain stripes in BFO, whereas it is insulating in the direction perpendicular to these domain stripes. Depending on the polarization orientation, either electrons or holes are transferred to the interface, to form either a 2DEG or two-dimensional hole gas (2DHG). Electron energy-loss spectroscopy and theoretical modelling suggest that the anisotropy of the interfacial conduction is caused by an alternating polarization associated with the ferroelectric domains, producing either electron or hole doping of the BFO/TSO interface.



Pan and coworkers (University of California, Irvine, University of Nebraska, Nanjing University, Penn State University, Cornell University). Work performed at the Cornell Nanoscale Facility

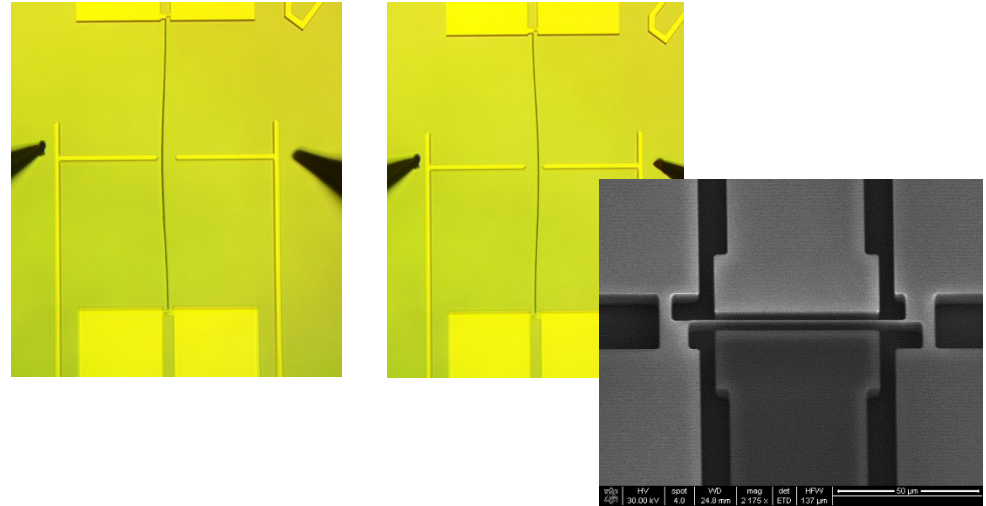
This work was supported by DOE BES DE-SC0014430; NSF DMR-1506535, DMR-1629270, NSF MRSEC DMR-1420645. DOE-BES DE-272 FG02-05ER46237 DOE DE-FG02-07ER46417; NSF EEC-1160504 (NNCI-1542081).
Nature Nanotechnology, 13, 1132–1136 2018

National Research Priority: NNI Signature Initiative-Nanoelectronics 2020 and Beyond

Kentucky Multi-Scale Manufacturing and Nano Integration Node (KY MMNIN)

MEMS Memory Element for Rad-Hard Memory

This MEMS memory element is using a bistable clamped-clamped beam for applications that require rad-hard memory. Most memory technology is based on the storage of electrical charge, including DRAM and Flash memory. The amount of charge on a bit is easily disrupted from ionizing radiation. For rad-hard applications, a mechanical element is desired for which ionizing radiation will not affect the bit value. The bit is stored using a clamped-clamped silicon beam that is oxidized to provide compressive strain. This compressive strain causes the beam to buckle along its length. Since the beam can buckle in one of two stable states, a memory element can be formed. Reading the bit is performed by observing the resistance change in an asymmetric piezoresistor at either end of the beam. Writing the bit is performed electrostatically by applying a voltage to an electrode on either side of the beam



Top: Photographs of a bistable beam that can be mechanically actuated. (Left) Bistable beam is latched in the "left" position. (Right) Bistable beam is latched in the "right" position.

Bottom: SEM of a memory element. The bistable beam extends through the center of the device, with stress sensors on either end of the beam to electrically determine the beam position (read operation). Electrodes are placed on either side of the beam for actuation (write operation)

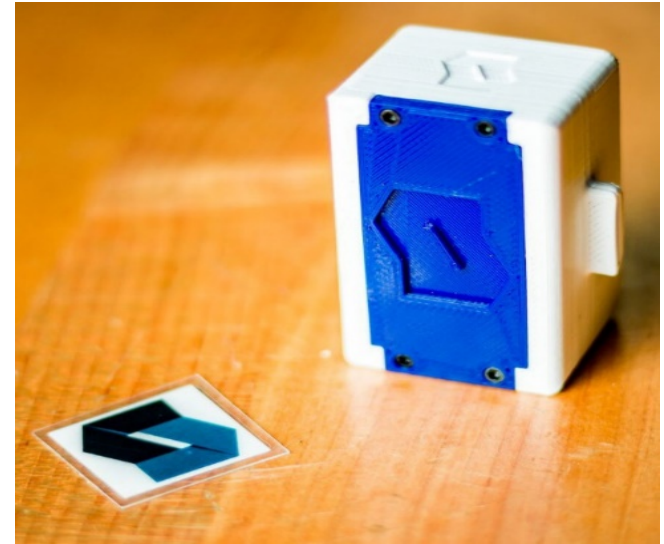
Bruce Alphenaar, Shamus McNamara, Kevin Walsh, Electrical and Computer Engineering, University of Louisville. Work partially performed at the University of Louisville Micro/Nano Technology Center.

The work was supported by DTRA grant no. HDTRA1-15-0027.

National Research Priority: NSF-Windows on the Universe

Pascal Tags

This project uses patent-pending flexible conductive-based antenna-based inventory tags with custom detectors to build a system that can achieve detection with ambient RF waves from Wi-Fi, 4G or even 5G. This technology allows one to put tags directly into finished goods or products requiring only one inventory tag for a products life. These tags are detected via custom detectors built to detect and secure product information through a novel approach. To achieve the technical challenges, existing networks such as the system transmitter are used to achieve the functionality needed. Moreover, requiring no additional transmitter or chip/battery for the passive tag improves the cost effectiveness that previous solution have struggled to achieve for widespread adoption. This technology directly tackles the over \$800B that is lost every year from inadequate inventory systems with the current technologies of Barcode and RFID. The technology was developed using the resources of KY Multiscale and is being commercialized by a startup called Pascal Tags.



Example Tag and Receiver

Druffel, T. and B. Young, University of Louisville. Work partially performed at the University of Louisville KY Multiscale Core Facilities

National Research Priority: NSF-Harnessing the Data Revolution

3D Printing of Surgical Instruments for Space Flight

Given the impracticality of resupplying a deep space exploration mission directly from Earth, additive manufacturing (aka 3-D printing) technology can provide a novel capability to fabricate hardware and instruments as-needed to generate and resupply necessary medical hardware. The team successfully designed and 3-D printed three surgical instruments : hemostat, scalpel handle (two variants for #10, #11 and #15 blades) and forceps.

The three instruments were used successfully in an animal research study with the surgeons providing feedback that the instruments offered acceptable performance. Also, the 3-D printed instruments were provided to the project's robotics team in order to accomplish their aim of programming Robonaut 2 to perform instrument recognition, pickup, and handoff to a human surgeon.



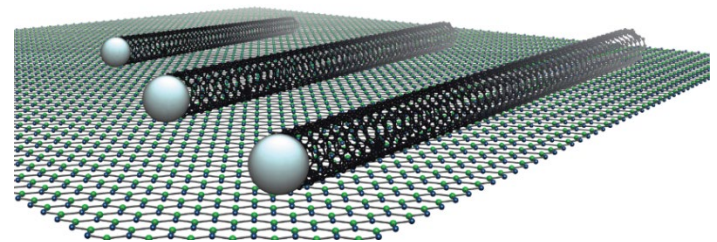
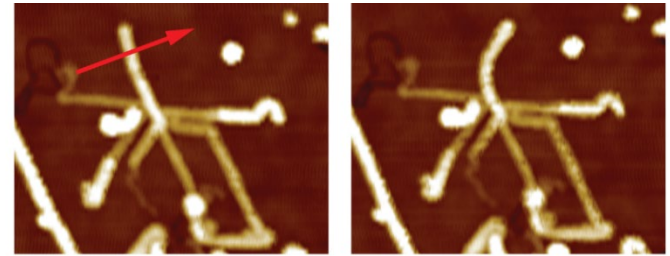
George Pantalos, Ed Tackett, and others, University of Louisville. This work was performed in the Rapid Prototyping Center.

This work was supported by NASA Cooperative Agreement NNX16AO69A.

National Research Priority: NSF-Work at the Human-Technology Frontier

Growing Carbon Nanotubes Aligned to Hexagonal Boron Nitride

One and two dimensional materials show exceptional promise for a variety of electronic, photonic, and mechanical applications. Recently, Professor Strachan's group at U.K. combined materials, carbon nanotubes and hexagonal boron nitride (hBN), with dissimilar properties and dimensions having nearly the same lattice spacing to form ordered interfaces along specific crystal directions. The nanotubes show clear preference to align to specific crystal directions of the hBN substrate during growth processing. The direct integrated growth of components consisting of contrasting material properties and dimensionalities provides an important step to developing high-performance nanoscale electrical circuits on these ideal insulating substrates.



Top: Crystallographically-aligned nanotubes shown that were grown on a boron nitride (hBN) surface. There are three clear preferred growth directions along the hBN lattice. The nanotubes can be pushed along the surface of the hBN, as they are van der Waals coupled to it.

Bottom: Illustration of one-dimensional carbon nanotubes aligned on a two-dimensional hBN substrate.

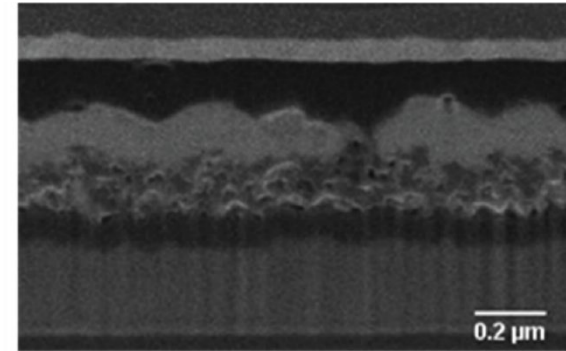
Douglas Strachan, Physics, University of Kentucky. Work partially performed at the University of Kentucky Center for Nanoscale Science and Engineering.

The work was supported by the Department of Energy No. 0000223282, with additional coordinated funds from the Kentucky EPSCoR Program. *Advanced Materials Interfaces* (2018): 1800793

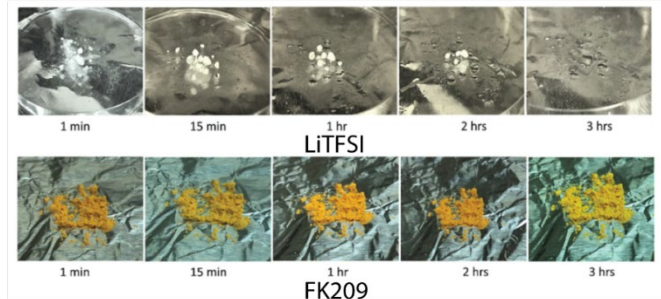
National Research Priority: NSF-Quantum Leap

Fabrication of Perovskite Solar Cells under Ambient Conditions

Perovskite solar cells have remarkable potential in terms of performance and cost. However, the materials for these cells are often sensitive to manufacturing conditions, particularly moisture, and require highly controlled fabrication environments. This level of control adversely affects manufacturing costs. Professors Chen and Singh at the University of Kentucky have recently demonstrated that an alternative, LiTFSI free, hole transport material enables the fabrication of solar cells with power conversion efficiencies of 13% *entirely* under ambient conditions with humidity above 36%. This includes preparation and storage of all solutions. Moreover, they discovered that exposure of samples to both air and light are important for maximizing current density and fill factor.



Cross-section of perovskite solar cell fabricated entirely under ambient conditions.



Comparison of moisture sensitivity of hole transport materials.

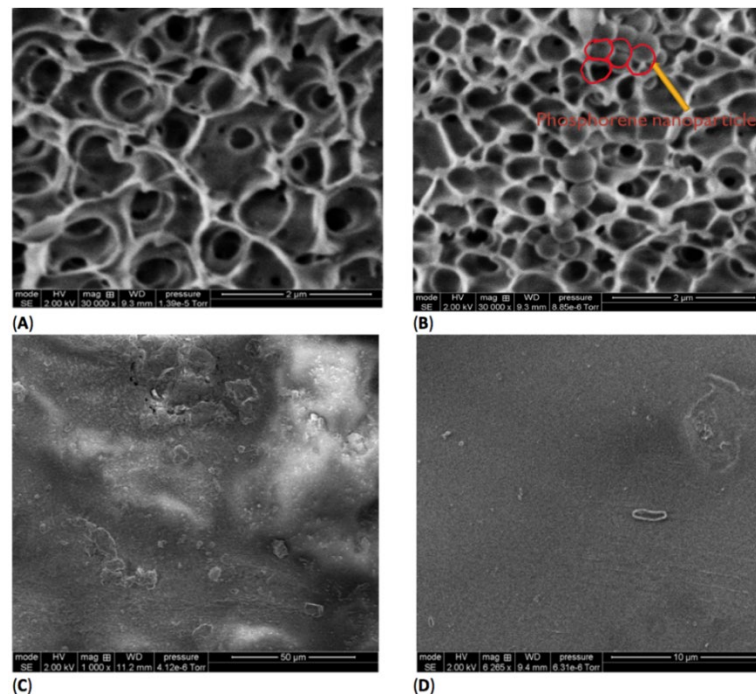
Zhi Chen and Vijay Singh, Electrical Engineering, University of Kentucky. Work partially performed at the University of Kentucky Center for Nanoscale Science and Engineering and Electron Microscopy Center.

Supported in part by Advanced Semiconductor Processing Technology LLC, China Scholarship Council, and National Natural Science Foundation of China Grants 61421002, 61574029, and 61371046. *IEEE Journal of Photovoltaics* 8.4 (2018): 1051-1057.

National Research Priority: NSF-Quantum Leap

Self-Cleaning Nanocomposite Membranes with Phosphorene-Based Pore Fillers for Water Treatment

This group has been the first to successfully fabricate nanocomposite membranes incorporating phosphorene. Phosphorene lends the membrane self-cleaning characteristics when either deposited on the membrane surface or embedded into the membrane polymer matrix. This creates a self-cleaning membrane useful in applications benefitting from a material that can degrade organic compounds—this includes preventing the formation of biofilms and water treatment. Figure A,B shows the cross-section of the pore structure of SPEEK membranes before and after the addition of phosphorene, respectively, while Figure C,D shows the surface images of both membranes before filtration. By comparing the two images, it was confirmed that phosphorene was successfully immobilized onto the membranes. The phosphorene membranes showed spherical-looking structures present in the pores, which upon analysis by EDX, were confirmed to come from phosphorus. After performing reverse-flow filtration experiments to mimic pure water cleaning, it was found that the average recovered flux of phosphorene-modified membranes was four times higher than that of unmodified membranes.



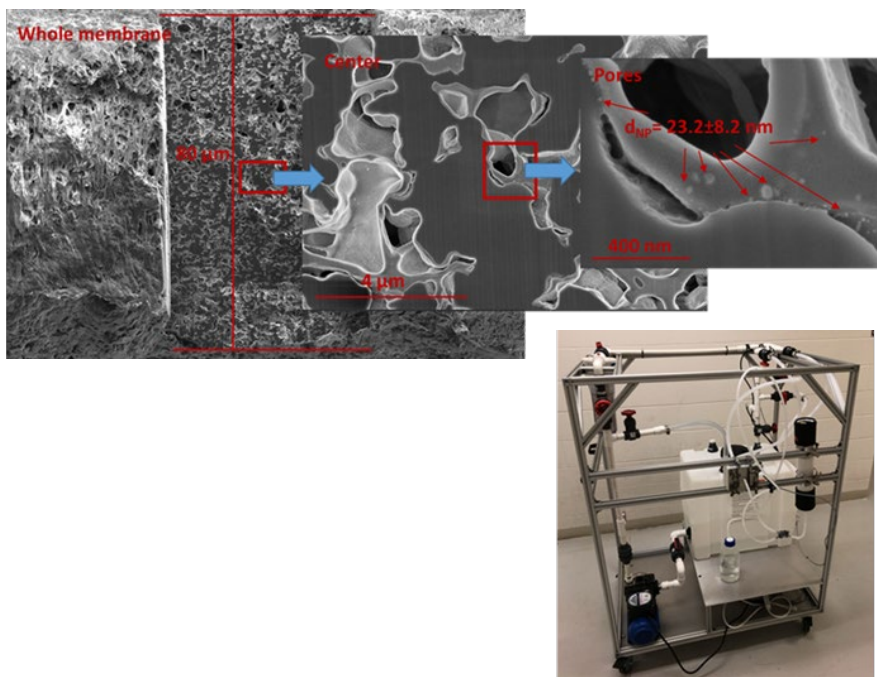
Cross-section SEM analyses of (A) SPEEK membranes and (B) phosphorene-membranes with some of the phosphorene nanoparticles marked in red, and surface SEM analyses of (C) SPEEK membranes (50-micron magnification) and (D) phosphorene-membranes (10-micron magnification) before filtration.

Eke Joyner, Katherine Elder, Isabel Escobar, University of Kentucky. Work performed at University of Kentucky's KY Multiscale Cores

National Research Priority: NSF-Growing Convergence Research

Reactive Membrane Unit for the Detoxification of Chlorinated Organics in Groundwater

Prof. Bhattacharyya in cooperation with an environmental consulting firm is working on a pilot reactive membrane unit for the remediation of groundwater. A commercial membrane cartridge, house water filter, is functionalized and incorporated with iron and palladium nanoparticles for the detoxification of toxic chlorinated organics in water, such as trichloroethylene and carbon tetrachloride. To disclose the nanoparticles' properties inside the pores of membranes, cross-section samples of membrane were made by FIB milling (Figure 33). Since the beam size is around 2-5 nm, the smooth and clear cross-section was made with less damage. The nanoparticle size, as well as element compositions, were then quantified with various depths underneath the membrane surface. The depth profile indicates that particle size was uniform inside membrane pores (23 ± 8 nm) but slightly smaller than those nanoparticles located on the surface (39 ± 9 nm). These results were used in performance simulation and system optimization. This characterization work was performed in the UK EMC.



(Top) SEM image of FIB modified membrane cross-section sample. (Bottom) Pilot reactive membrane unit.

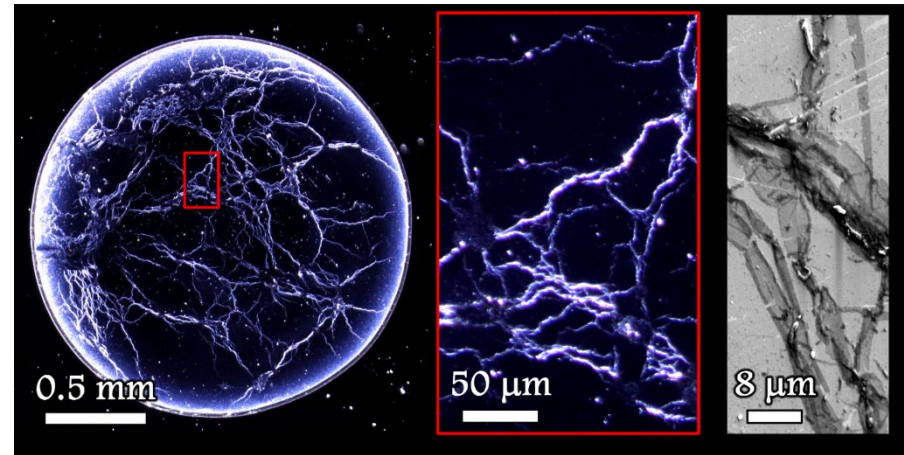
Prof. Bhattacharyya, University of Kentucky. Work performed at the University of Kentucky Electron Microscopy Center

National Research Priority: NSF-Growing Convergence Research

Analysis of Web-like Nanostructures of Evaporated Drops of Bourbon Whiskey

This work focuses on the analysis of self-assembled web-like structures that form when a drop of diluted bourbon whiskey is evaporated. These structures form when lipid-derived monolayers are at the liquid-air interface and are subsequently distorted and assembled via evaporation fluid dynamics.

We have found that through our fixed evaporation conditions (1.0 mL drop, 25% ABV) these patterns form only for new charred barrel products ($n = 65$) and not for other whiskeys ($n=12$) nor distillates ($n=5$). Further, patterns are repeatable and are distinctly unique between different brands of bourbon. Findings are used for simplistic analysis of intrinsic properties as well as counterfeit identification.



Microscopic (via light scattering) and SEM images of web-like structures resulting from an evaporated diluted (25% ABV) drop of Jack Daniel's Barrel Strength bourbon whiskey (unpublished).

Stuart J. Williams, University of Louisville. Work performed at University of Louisville's Micro/Nano Technology Center

National Research Priority: NSF-Growing Convergence Research

Mid-Atlantic Nanotechnology Hub (MANTH)

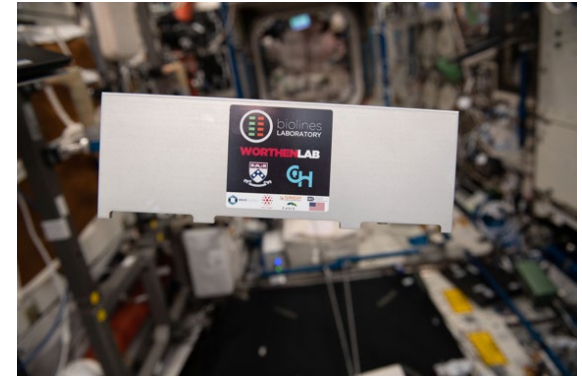
NIH/NCATS: Microfluidics in Space

NCATS- National Center for Translational Sciences

Collaboration between Penn Engineering (Dan Huh) and Children's Hospital of Philadelphia (Scott Worthen)

A little-known fact about space travel is that **astronauts often get sick with colds and lung infections** during their time away - much more frequently than on Earth.

Recruitment of the immune system to battle disease in space can be observed through microfluidically-enabled organs on a chip. The goal is to improve ability to protect astronauts during long voyages to the Moon, Mars, and beyond.



Andrei Georgescu, Scott Worthen, and Dan Huh, University of Pennsylvania. Work performed at the Singh Center for Nanotechnology.

This work was supported by a grant from NIH National Center for Advancing Translational Sciences, NASA, and Center for the Advancement of Science in Space.

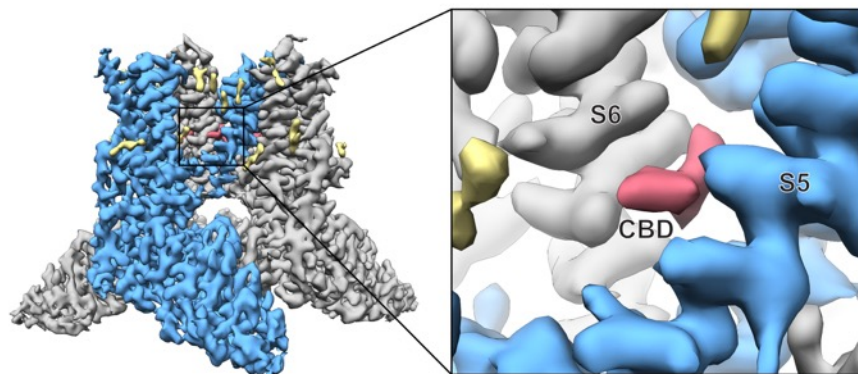
National Research Priority: NSF-Understanding the Rules of Life and Windows on the Universe

New Tool at MANTH used to Discover the Rules of Life

A new microscope lab for Life Sciences and Materials Research, the Krios Cryo-TEM at MANTH, is available to Penn and external academic research groups in the greater Philadelphia area. Researchers from Penn, Pfizer, and Rutgers University recently used the microscope to image a Transient Receptor implicated in the function of glioblastoma (a form of brain cancer). Transient receptor potential (TRP) channels play significant roles in human physiology and facilitate permeation of essential ions (Na^+ , Ca^{2+}) through the plasma membrane.

Cannabidiol (CBD), a natural product of the Cannabis sativa plant, is a TRPV2 agonist which has been recently used to demonstrate the important role of TRPV2 in the inhibition of glioblastoma multiforme cell proliferation. These findings place TRPV2 on the list of important anti-tumor drug targets.

These structural studies provide new molecular insights into TRPV2 channel gating and revealed a novel drug binding site in TRPV channels. This new information could be used to **guide therapeutic design to treat glioblastoma multiforme** and other TRPV2 channel associated pathophysiological processes.



Right; The Krios Cryo-TEM at MANTH.

Left; an image formed by the Krios of a transient receptor potential channel with CBD



Ruth A Pumroy, Amrita Samanta, Yuhang Liu, Taylor ET Hughes, Siyuan Zhao, Yevgen Yudin, Tibor Rohacs, Seungil Han, Vera Y Moiseenkova-Bell, Perelman School of Medicine, University of Pennsylvania; Pfizer Research and Development; New Jersey Medical School, Rutgers University. Work performed at the Singh Center for Nanotechnology.

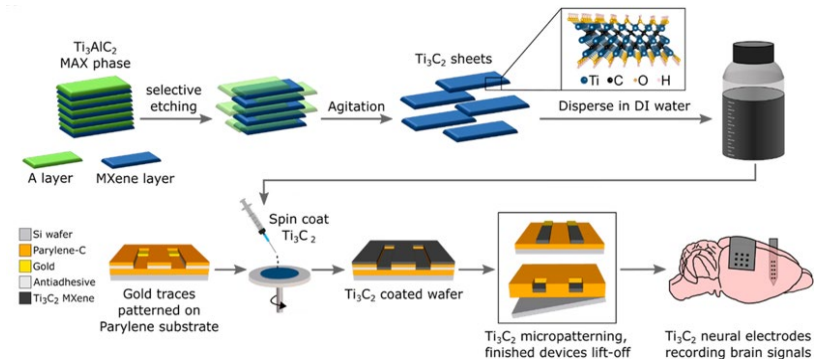
Life 2019;8:e48792

National Research Priority: NSF-Understanding the Rules of Life

Two-Dimensional Ti_3C_2 MXene for Neural Interfaces

High-resolution neural interfaces are essential tools for studying and modulating neural circuits underlying brain function and disease. Because electrodes are miniaturized to achieve higher spatial resolution and channel count, maintaining low impedance and high signal quality becomes a significant challenge. Nanostructured materials can address this challenge because they combine high electrical conductivity with mechanical flexibility and can interact with biological systems on a molecular scale.

Two-dimensional (2D) Ti_3C_2 MXene possesses a combination of remarkably high volumetric capacitance, electrical conductivity, surface functionality, and processability in aqueous dispersions distinct among carbon-based nanomaterials. A high-throughput microfabrication process for constructing Ti_3C_2 neuroelectronic devices was developed at MANTH. Ti_3C_2 electrodes exhibit a 4-fold reduction in interface impedance, lower baseline noise, higher signal-to-noise ratio, and reduced susceptibility to 60 Hz interference than gold electrodes.



In neuronal biocompatibility studies, neurons cultured on Ti_3C_2 are as viable as those in control cultures, and they can adhere, grow axonal processes, and form functional networks. These results indicate that Ti_3C_2 MXene microelectrodes **have the potential to become a powerful platform technology for high-resolution biological interfaces.**

Flavia Vitale and colleagues, Dept. of Neurology, Dept. of Bioengineering, Univ. of Pennsylvania, and Dept. of Neurosurgery, Drexel University. Work performed at the Singh Center for Nanotechnology.

ACS Nano, 12(10), pp.10419-10429 (2018).

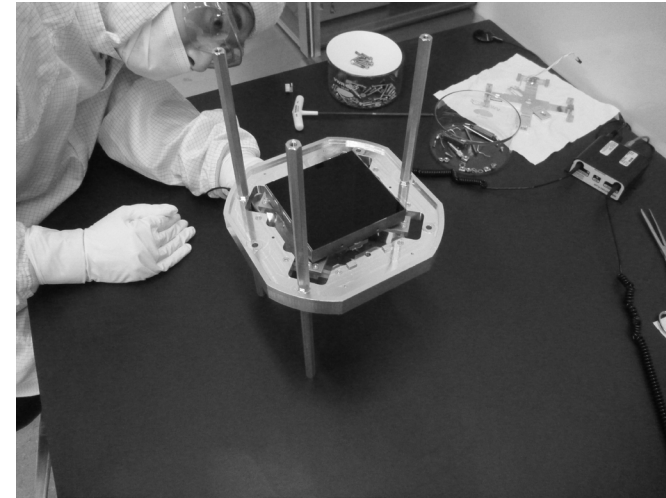
National Research Priority: NSF-Understanding the Rules of Life

CleanSpace Assembly for New Telescope Sensors

MANTH is used to handle and package Charge Coupled Device (CCD) imaging detectors for a NASA- and NSF-funded called project NASA-NSF Exoplanet Observational Research.

One of the main goals of this project is to build a new astronomical spectrometer sensitive enough to enable astronomers to detect the tiny acceleration an Earth-like exoplanet planet imparts on its host star by measuring Doppler shifts of the stellar spectral lines.

This new spectrometer, which will be deployed to the WIYN telescope at Kitt Peak (Arizona) and available to the entire U.S. user community, is designed to be capable of measuring the velocities of nearby stars with a precision of 30 cm/s, substantially better than what current facilities are capable of. At the heart of this new spectrometer is the world's largest commercially available monolithic digital detector, a silicon wafer-scale device having 9000 x 9000 pixels. This detector will record high-resolution stellar spectra covering the optical range (360 nm to 930 nm). These devices, which measure 90 mm on a side in their silicon carbide packages, are extremely sensitive to particulate contamination and electrostatic damage. The facility in **MANTH** **provides an ideal work environment** where Blake and his team can safely handle these devices to install them inside a portable test apparatus, which is then brought back to the Physics and Astronomy department where extensive electro-optical testing is carried out.



Cullen Blake and colleagues, Physics and Astronomy, Univ. of Pennsylvania. The NEID Doppler spectrometer at WIYN. Work performed at the Singh Center for Nanotechnology.

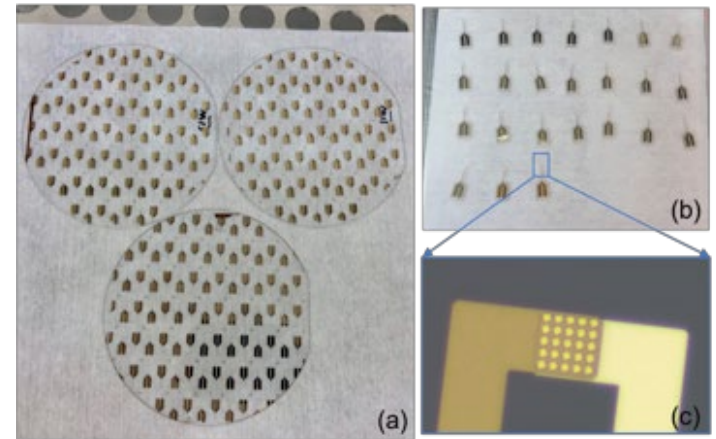
American Astronomical Society Meeting Abstracts #233, January 2019.

National Research Priority: NSF-Windows on the Universe

Microfabricated, Label Free Biosensors

Collaborating with Rutgers University, Penn researchers at MANTH are developing microfabricated, label-free, insertion-format sensors for biomarker detection. Electronic-based sensing is a promising approach for fM-level specific detection of proteins due to its low cost, ease of miniaturization, and label-free operation. One limitation of these previous sensors is that they do not have an insertion form factor for *in vivo* use.

Using the resources at MANTH, a wafer-level, microfabricated, needle-shaped impedance sensor for **rapid, label-free detection of cytokines and other biomarkers** was developed. The needle shape of the sensor allows for transdermal or transvascular sensing. The sensor, a micro-well array comprising 25 individual 2 μ m-diameter wells embedded in a sensing tip, is lithographically configured on a laser micromachined fused silica microneedle. Label-free specific detection is achieved via functionalizing the microwells with antibodies and monitoring the impedance change across the sensor electrodes due to the binding of target protein to the antibody. The figures show wafer-level fabricated functional sensors. A sensor yield of 80% is achieved.



(a) Microscopic images of batch fabricated sensors; (b) Sensors released from wafer post laser micromachining; (c) close view of microwells at sensor tip.

Mehdi Javanmard, Rutgers and Mark Allen, Penn. Work performed at the Singh Center for Nanotechnology.

This work is sponsored by DARPA. 2018 IEEE Micro Electro-Mechanical Systems (MEMS), Belfast, 2018, pp. 392-395.

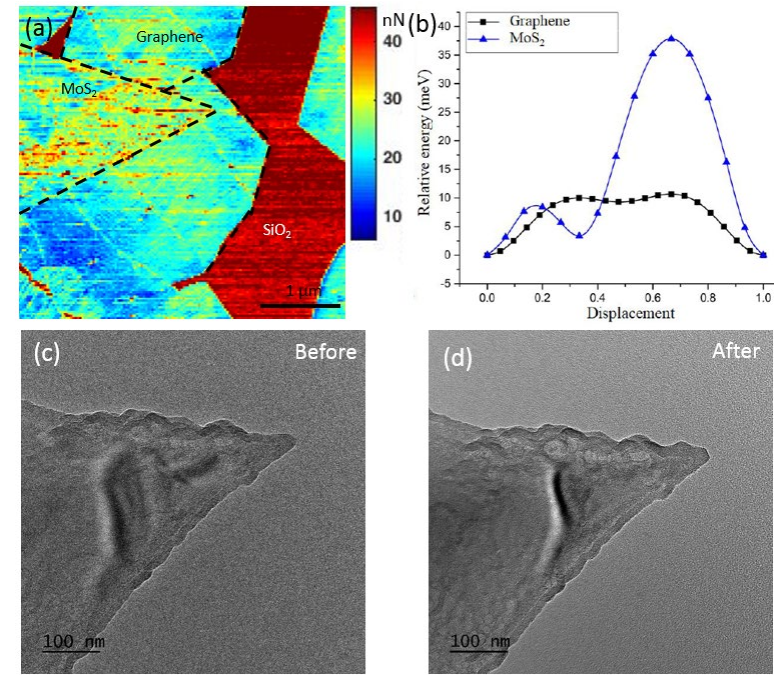
National Research Priority: NSF-Understanding the Rules of Life and Growing Convergence Research

Scanning Probe Research – Friction and 2D Materials

The friction of atomically-thin layered materials is characterized by single asperity contact measurements using the MANTH Asylum MFP-3D atomic force microscope (AFM). Friction between a nanoscale AFM tip and two materials - CVD-grown monolayer graphene and MoS₂ flakes supported on a SiO₂ surface - can be directly compared by scanning both co-deposited materials in one image. The friction image shown in (a) illustrates that the single crystalline MoS₂ and graphene regions have significantly reduced friction compared to the SiO₂ substrate, which demonstrates their potential as *nano lubricating films*.

Graphene also has lower friction than MoS₂. Simulations reveal that the fundamental mechanism for the friction contrast between graphene and MoS₂ surfaces is the different corrugations of the potential energy surfaces of each material; the corrugation provides a barrier to sliding and thus governs static friction. The calculated energy corrugation difference shown in (b), is attributed to the higher polarizability of the sulfur atoms in the MoS₂ compared to carbon atoms.

Furthermore, the AFM tip shape can be characterized in the MANTH JEOL F200 transmission electron microscope (TEM) as seen in (c) before and (d) after measurements to evaluate tip wear. Only a small amount of tip wear is observed, which helps validate the reliability of the data.



Robert W. Carpick's group at Penn, in collaboration with A.T. Charlie Johnson's at Penn, A. Martini's group at University of California, Merced, and E. Johnson's group at Dalhousie University. Work performed at the Singh Center for Nanotechnology.

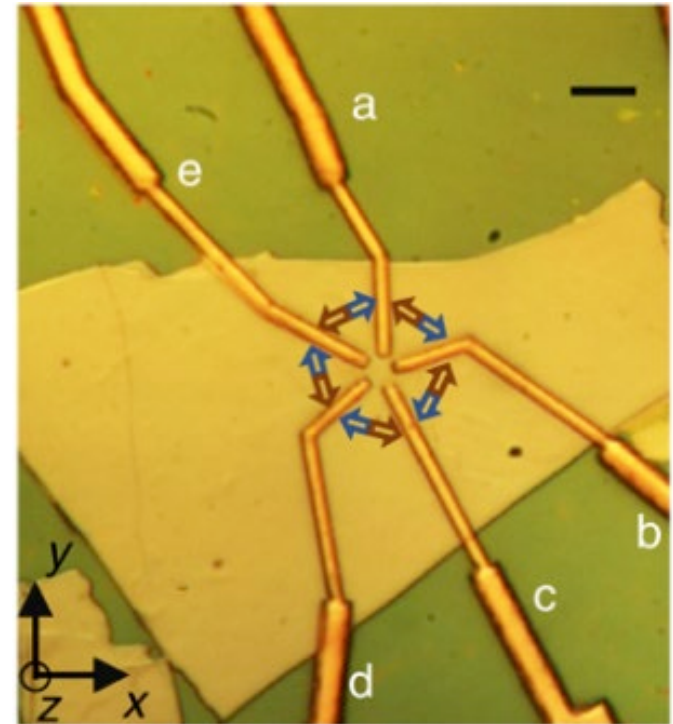
RAISE-EQuIP – Nanophotonics and Quantum

NSF Research Advanced by Interdisciplinary Science and Engineering (RAISE)

Engineering Quantum Integrated Platforms for Quantum Communication (EQuIP)

RAISE-EQuIP Grant: Integrated Higher-Dimensional Quantum Photonic Platform

Collaboration between Penn Engineering (Liang Feng and Ritesh Agarwal) and Stevens Institute of Technology (Stefan Strauf) for fabrication of nanophotonic devices with unique materials essential in advancing quantum communications research.



Liang Feng (PI), Ritesh Agarwal (Co-PI), Penn., and Stefan Strauf (Co-PI), Stevens Inst. of Tech. Work performed at the Singh Center for Nanotechnology.

This work was supported by NSF ECCS-1842612, RAISE-EQuIP: Integrated Higher-Dimensional Quantum Photonic Platform

National Research Priority: NSF-Growing Convergence Research and Quantum Leap

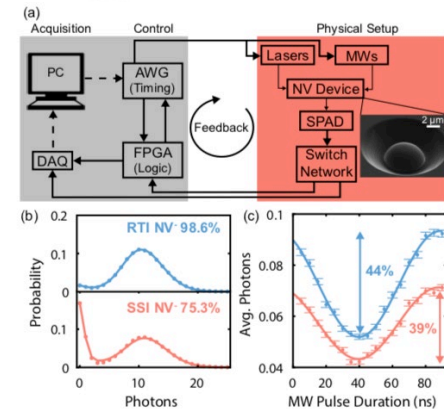
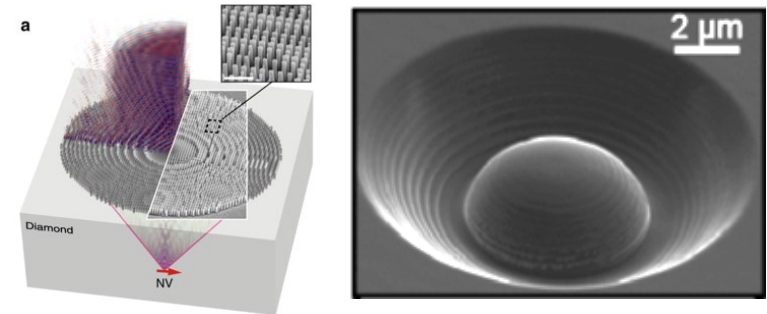
RAISE-EQuIP – Nanofabrication and Quantum

NSF Research Advanced by Interdisciplinary Science and Engineering (RAISE)

Engineering Quantum Integrated Platforms for Quantum Communication (EQuIP)

RAISE-EQuIP Grant: Chip-Scale Quantum Memories for Practical Quantum Communication Networks

Collaboration between Penn Engineering (Lee Bassett and Firooz Aflatouni) and Brown University (Rashid Zia) leveraging modern capabilities in materials science, nanofabrication, signal processing, and integrated systems-on-a-chip to harness the computational power and sensitivity of quantum-coherent systems for practical applications.



Lee Bassett (PI), Firooz Aflatouni (Co-PI), Penn. Engineering and Rashid Zia (Co-PI), Brown Univ. Work was performed at the Singh Center for Nanotechnology.

This work was supported by NSF ECCS-1842655 RAISE-EQuIP: Chip-Scale Quantum Memories for Practical Quantum Communication Networks.

National Research Priority: NSF-Quantum Leap and Growing Convergence Research

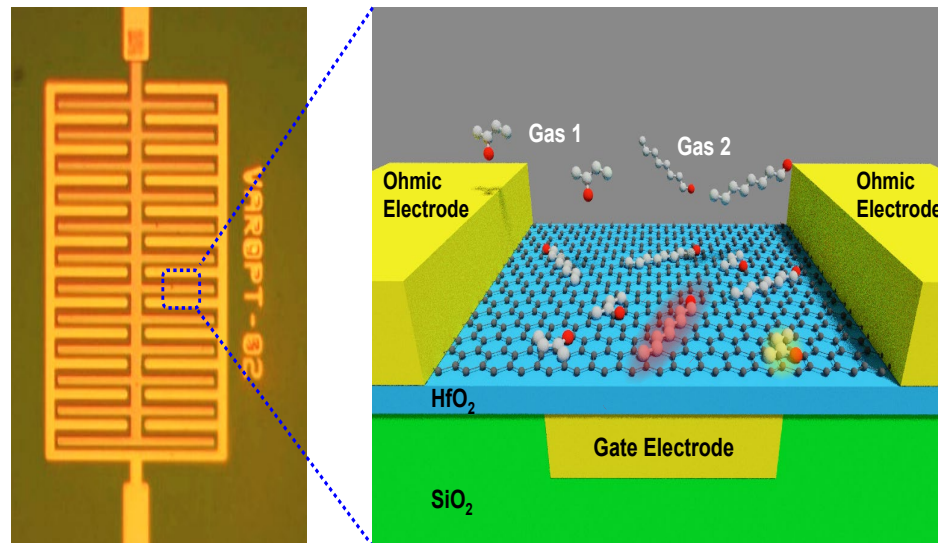
Midwest Nanotechnology Infrastructure Corridor (MINIC)



Graphene-Based High Sensitivity Remote Sensing Devices Now in Production

This work involves a remote sensing device made from an ungated graphene FET. Charged species adsorbing on the surface of the graphene shift the resonance frequency of the oscillator by changing the voltage at which the Dirac condition is reached. The device was developed by Steve Koester (ECE, UMN) and adopted by Boston Scientific who built prototypes in the MINIC facility.

The device has proven so successful that Boston Scientific has transferred the process to a CMOS foundry where the devices are being built on 200 mm wafers. The application is disease detection. The type of disease varies with the sensitizer coatings being applied to the graphene.



Optical micrograph and schematic of graphene sensor. The resonance frequency of the device shifts with charge on the surface making it a high sensitivity remote sensing device.

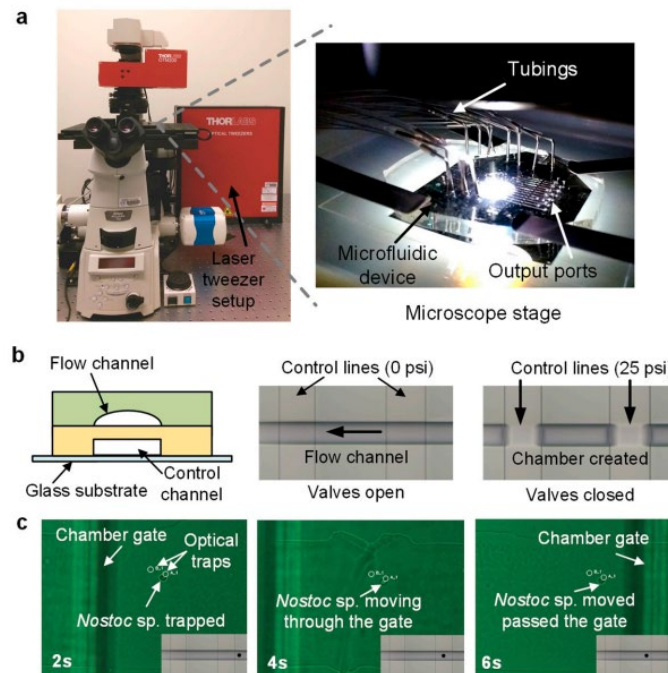
Steven Koester, ECE, UMN. Work performed at MINIC.

Supported by the Alice M. O'Brien Foundation. *ACS Appl. Mater. Interfaces* 2017, 9, 44.

National Research Priority: NSF-Future of Work at the Human-Technology Frontier

Bacterial Single-Cell Lysis Method for Whole Genome Amplification in Microfluidic Platforms

Single-cell sequencing is mostly coupled with microfluidic systems for cell manipulation and fluid handling. So far, single-cell sequencing has been focused on human cells. Challenges that bacterial species pose include the rigid bacterial cell walls and the need for an effective lysis protocol compatible with microfluidics. We developed a lysis protocol that can be used to extract genomic DNA without interfering with the amplification chemistry. Our protocol is based on thermal and chemical lysis. We consider 80% of single-cell replicates that lead to >5 ng DNA after amplification as successful attempts. The protocol was directly applied to *Gloeocapsa* sp. and the single cells of the eukaryotic *Sphaerocystis* sp. and achieved a 100% success rate.



Overview of the optofluidic single-cell whole genome amplification (SC-WGA) platform.

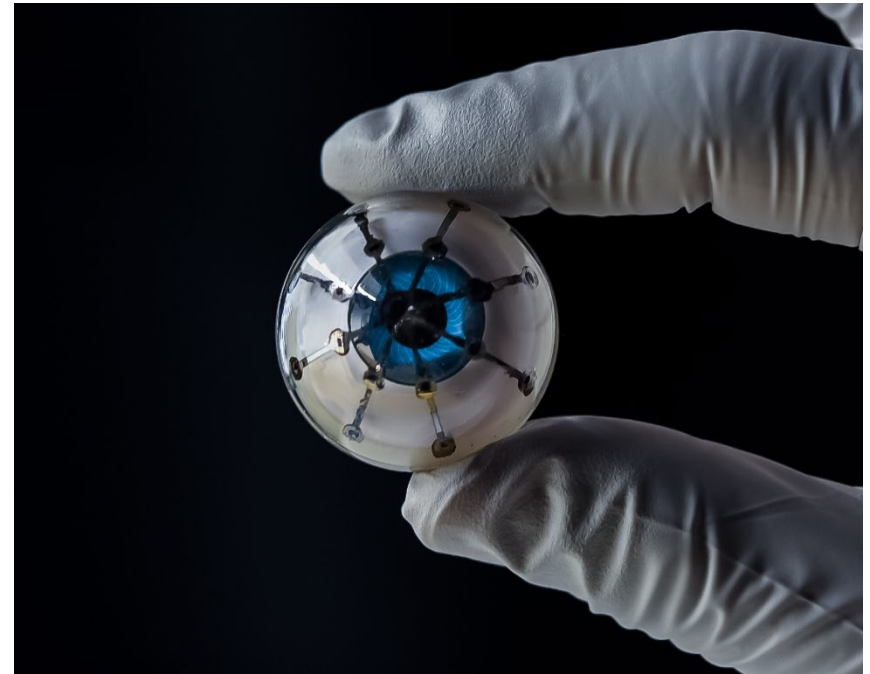
Marina Walther-Antonio, Surgery and ObGyn, Mayo. Work was performed at MINIC.

Micromachines, 9, 367, 2018.

National Research Priority: NSF-Future of Work at the Human-Technology Frontier

3D Printing of High Performance Integrated Active Electronic Materials and Devices

The **McAlpine Research Group** (UMN, Mechanical Engineering) has demonstrated polymer-based exhibiting high performance photodetectors that are fully 3D printed using a semiconducting polymer ink. The devices are integrated into image sensing arrays with high sensitivity and wide field of view, by 3D printing interconnected photodetectors directly on flexible substrates and hemispherical surfaces. 3D printed optoelectronic devices allow for flexibility in the design and manufacturing of next-generation wearable and 3D structured optoelectronics, and validate the potential of 3D printing to achieve high performance integrated active electronic materials and devices. Further, this work sets the foundation for future applications such as 'bionic eyes' which can potentially be implanted for vision restoration applications.



3D printed bionic eye that can include photodetectors with varying wavelength sensitivities.

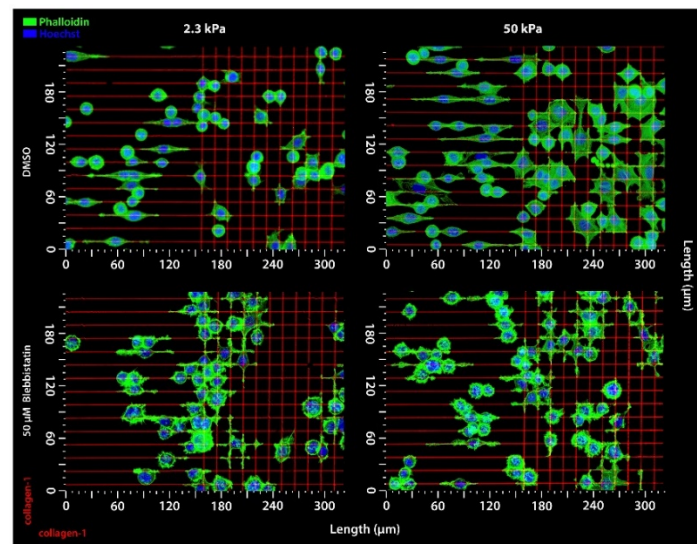
Mike McAlpine, ME, UMN. Work was performed at MINIC.

Advances in Materials and Manufacturing pp. 309-334 (2019).

National Research Priority: NSF-Future of Work at the Human-Technology Frontier

The Effect of Extracellular Matrix Behavior on the Regulator of Carcinoma Invasion and Metastasis

Contact guidance due to extracellular matrix architecture is a key regulator of carcinoma invasion and metastasis, yet our understanding of how cells sense and respond to contact guidance cues remains poorly understood. We have used MINIC to make micro- and nano-engineered platforms that facilitate uniaxial or biaxial extracellular matrix cues, or competing E-cadherin adhesions, on substrates with variable stiffness, and demonstrated distinct mechanoresponsive behavior during guidance sensing. Our data suggests that guidance sensing in carcinoma cells depends on both the architecture and mechanical properties of the environment and that targeting the bimodal responses may provide a rational strategy for disrupting metastatic behavior.



Breast carcinoma cells sensing and protruding along uniaxial collagen lines that mimic aligned fibers (left) and biaxial cues (right) on soft and stiff substrates under control or blebbistatin-treated conditions. Treated cells display a dendritic protrusion phenotype in response to both cues on both substrates, suggesting a bimodal response to these cues.

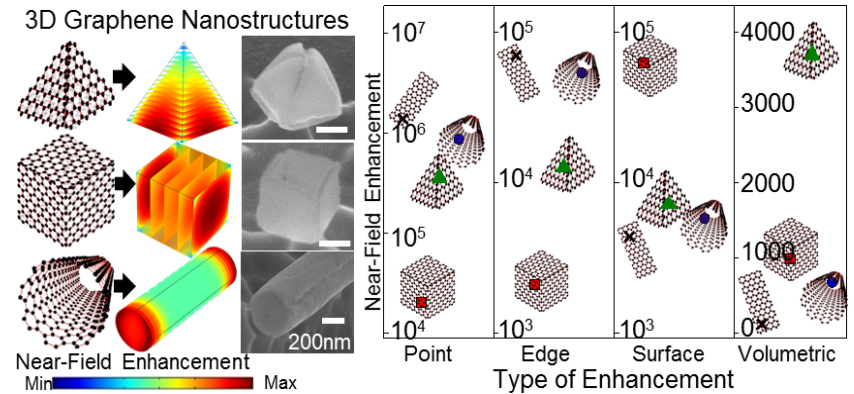
Jeong Cho, ECE, UMN. Work performed at MINIC.

This work was supported by the American Cancer Society (RSG-14-171-01-CSM) and the NIH (U54CA210190). *Nature Comm*, 20;9(1):4891, 2018.

National Research Priority: NSF-Understanding the Rules of Life

Self Assembled 3D Graphene Based Plasmonic Structures

The limited spatial coverage of the plasmon enhanced near-field in 2D graphene ribbons is a major hurdle in practical applications. Professor Cho's group is exploring diverse self-assembled 3D graphene architectures that induce hybridized plasmon modes by simultaneous in-plane and out-of-plane coupling. 3D architectures benefit from a fully symmetric 360° coupling at the apex of pyramidal graphene, orthogonal four-directional coupling in cubic graphene, and uniform cross-sectional radial coupling in tubular graphene. The hybridized modes introduced through the 3D coupling delivers nondiffusion limited sensors, high efficiency fuel cells, and extreme propagation length optical interconnects.



SEM images of self-assembled 3D graphene nanostructures and evaluation of plasmonic enhancement modes in 2D and 3D graphene nanostructures. Comparison between the highest intensity of the point-based, edge-based, surface-based, and volumetric near-field enhancement in the hollow 3D pyramidal, cubic, tubular graphene and 2D graphene ribbon.

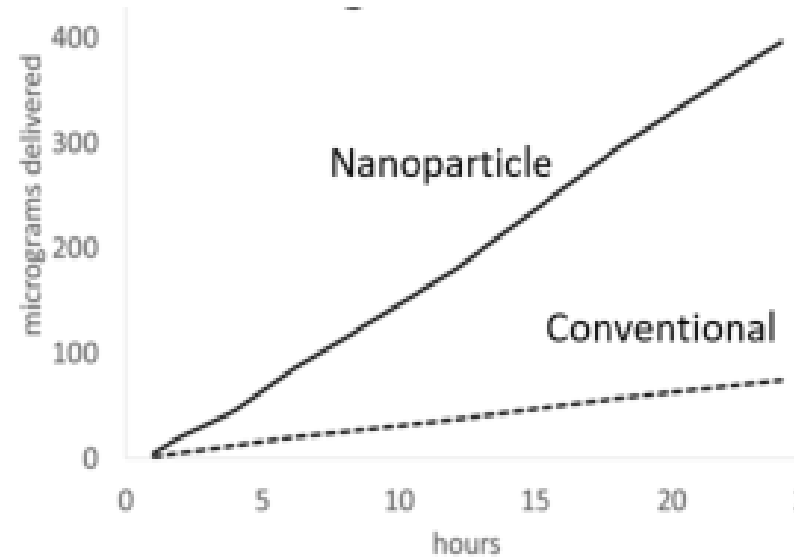
Jeong Cho, Electrical and Computer Engineering, University of Minnesota. Work performed at MINIC.

This work was supported by NSF (CMMI-1454293). *ACS Nano* 13(2), 1050-1059, 2018.

National Research Priority: NSF-Quantum Leap

Nanoparticle Modulated Transdermal Drug Delivery

One of MINIC's research strengths lies in the area of nanoparticle synthesis and characterization. This strength has been leveraged by **Dynation LLC**, a start-up company located in St. Paul MN. Dynation has received Phase 1 SBIR funding to successfully develop nanoparticles for a dermal drug delivery platform since such particles have much better permeation rates than conventional lipids. This work has now led to further funding from private sources to develop nanoparticles for encapsulating a variety of bio-derived chemicals for use in agricultural, nutraceutical, and personal care products.



Transdermal drug delivery is dramatically accelerated by nanoparticle attachment.

Dynation LLC. Work performed at the Minnesota Nano Center.

National Research Priority: NSF-Future of Work at the Human-Technology Frontier

MEMS-Based Sensors for Aerospace Applications

Collins Aerospace develops sensors for the aerospace market. The company has used the Minnesota Nano Center to assist in MEMS development projects since the production demand in their MEMS fab does not always allow for the interruption to try new processes.

A variety of equipment is used; photo tools, dry etching including, deep reactive ion etch (DRIE), reactive ion etch (RIE), ion milling and inductively coupled reactive ion etch (ICRIE), metal deposition tools and tube furnaces. The vast experience of the staff members is also a valuable asset. The staff has vast experience and have been a reliable source of information. Without the availability of this valuable resource their development efforts would be severely impacted.



Aerospace sensors made by Collins Aerospace, some of which were developed using MINIC facilities.

Collins Aerospace sensor development. Work performed at the Minnesota Nano Center.

National Research Priority: NSF-Windows on the Universe

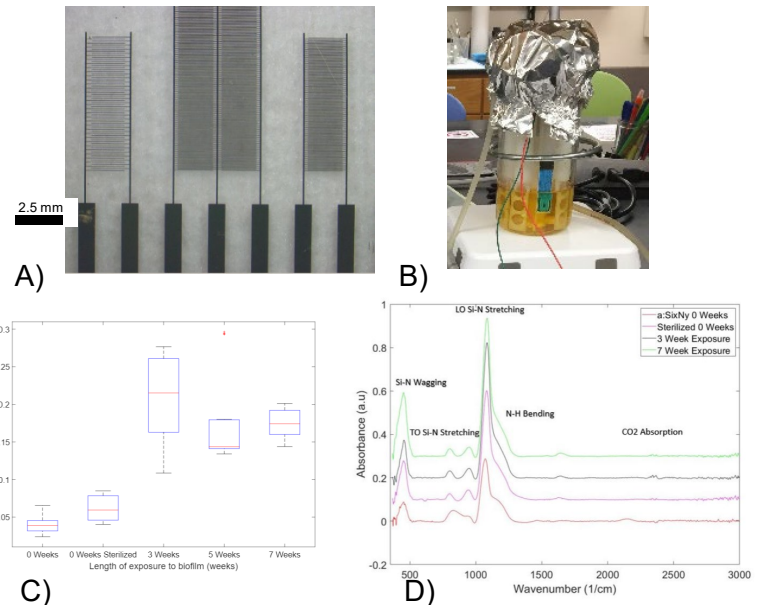
Montana Nanotechnology Facility (MONT)

Effects of Biofilm Growth on Thin Films

Biofilms can inhibit the performance of micro-fabricated water monitoring sensor platforms. A bacterial strain (*Escherichia coli* K12) that forms corrosive biofilms may alter surface and material properties and consequently sensor performance.

An inert interface between the active sensor surface and the aqueous media is required for reliable operation. This study investigates common thin films (Al, poly-Si, Au and $a\text{:Si}_x\text{N}_y\text{-H}$) regarding material degradation and studies how biofilm growth influences sensor performance such as impedance spectroscopy sensors to study microbial loads in groundwater.

Current work indicates that the biofilms inhibit the electrical conductivity due to deterioration. An inert encapsulation layer, such as SiN, is necessary for field deployment.



A) Micro-fabricated Impedance Spectroscopy sensor used to monitor biofilm growth (feature size: 30 μm). B) Biofilm reactor to control biofilm growth. C) Surface resistivity increase of Al due to prolonged biofilm exposure. D) FTIR of potential inert $a\text{:Si}_x\text{N}_y\text{-H}$ encapsulation layer (no changes in vibration modes after biofilm exposure).

M. Thomae, S. Warnat. Mechanical & Industrial Engineering. C. Foreman. Chemical & Biological Engineering, Montana State University. Work performed at Montana Microfabrication Facility.

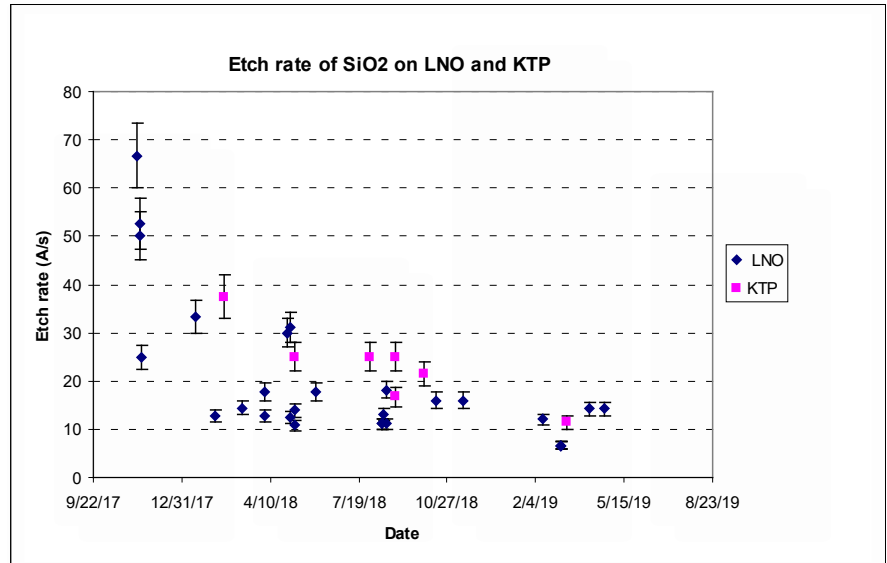
Funding support by MSU Startup (S. Warnat) and Thornton Excellence in Engineering Research (Warnat, Foreman). *Engineering Research Express*, in press (Dec.2019.) *IEEE Conference Proceedings*, in press (Dec 2019).

National Research Priority: NAE Grand Challenge-Provide Access to Clean Water

Increasing Quality and Consistency of SiO₂ films as etch mask material for LNO and KTP devices

The goal of this project is to increase the consistency and quality of e-beam and sputtered oxide films at MMF to increase the yield of devices patterned in oxide masks. Changes to the original process included new crystal monitor sensors, increased control of the deposition rate through tuning of the PID controller, tighter control of deposition pressure, and modifying the electron beam sweep pattern to increase melt uniformity.

These changes have resulted in improved edge roughness of patterned features and increased density of the coatings as shown through wet etch tests and device performance. Work is still ongoing to further improve the adhesion of sputtered films and the run to run thickness variation in e-beam deposited films.



Etch rate changes over time. Decreased etch rate of the films demonstrates an increased density of the coatings as development has progressed. This is supported by increased device performance seen at AdvR.

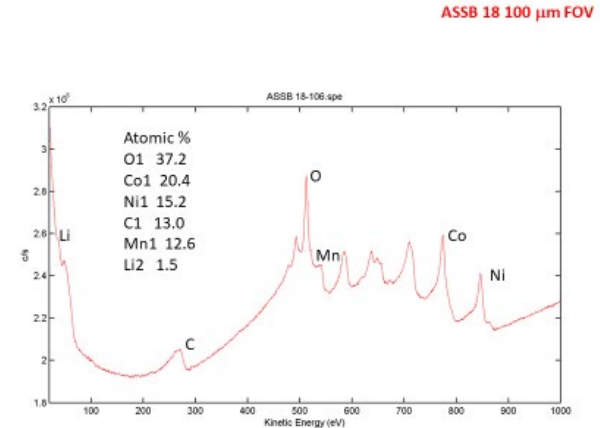
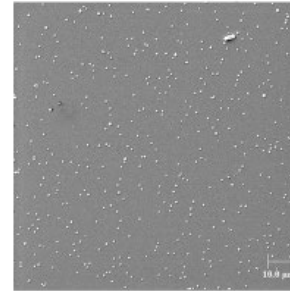


Sarah Mondl, AdvR, Inc. Work performed at Montana Microfabrication Facility

National Research Priority: NAE Grand Challenges-Individualized Learning, Virtual Reality, Health Informatics, Secure Cyberspace

NanoCoatings, Inc.

NanoCoatings, Inc. (NCI), a small business in Rapid City, SD, is involved in advanced coating and materials technology development. We are engaged in government supported R&D for DoD agencies. Under SBIR program with the Navy, All Solid State Batteries (ASSB). We are to develop the technology to fabricate solid-state battery components using Radio-Frequency Magnetron Sputtering (RFMS). ICAL performed XPS and Auger Nanoprobe analysis of co-deposited cathode material coatings that we fabricated using our RFMS technique to provide correlations of coating-composition with coating co-deposition parameters and reactive-gas flow ratios. This type of basic information is important for us to design and then fabricate the best performing cathode layers, an important part of the ASSB.



Quantitative Auger Nanoprobe analysis, e-beam technique that can detect and quantify Li.

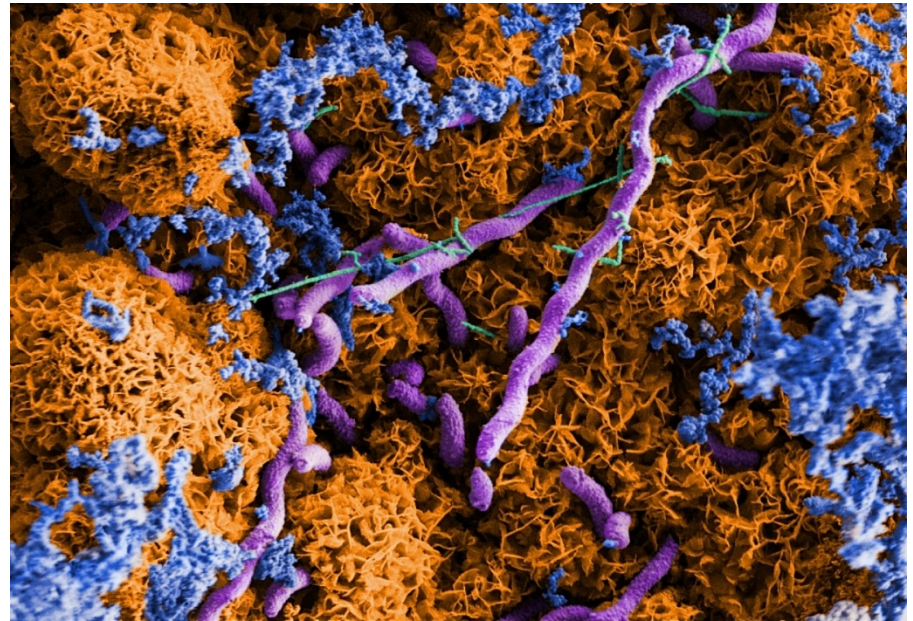
Frank Kustas, NanoCoatings, Inc. Work performed at Montana Nanotechnology Facility **ICAL**

DoD SBIR contract #N68335-17-C-0016

National Research Priority: NAE Grand Challenge-Make Solar Energy Economical

Steel Corrosion by Biofilm

- | Sulfate-Reducing Bacterial (SRB) biofilm on 1018 carbon steel.
- | **Orange:** FeS_x corrosion products
- | **Blue:** Carbohydrate
- | **Purple:** SRB cells
- | **Green:** Extracellular structures



Gregory Krantz, Kilean Lucas, Matthew Fields, Dept. of Chemical & Biological Eng, Montana State University. Work performed at MONT facility **ICAL**.

Department of Energy BER award: ENIGMA #DE-AC02-05CH11231. *Biofouling*, (2019) 35:6, 669-683.

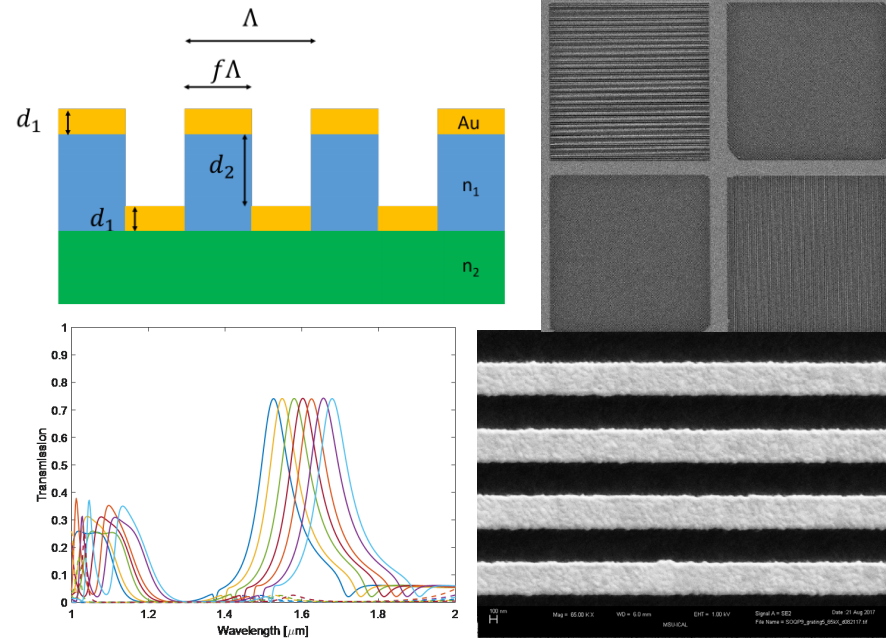
National Research Priority: NAE Grand Challenge-Restore and Improve Urban Infrastructure

Nanostructured Polarization Filters in Near-Infrared for Atmospheric Science

Metal-coated nanoscale gratings in Silicon or Silicon-on-Oxide substrates can realize polarization- and wavelength-selective filter elements for the near infrared.

Nanofabrication approach enables a tiled array of filters with customized polarizer orientation and center wavelength for each filter element which can be manufactured in parallel.

Filter array is being developed to aid in identification of cloud thermodynamic phase (whether ice or water) via ground-based passive polarimetric imaging. This has potentially important impacts in climate studies, atmospheric science, and remote sensing.



(Top-left): schematic drawing of nanostructured polarization filter; (Top-right): SEM image of fabricated structure; (Bottom-left): simulation results showing predicted filter transmissivity, tunable over a range of wavelengths; (Bottom-right): magnified SEM view of an example fabricated nanostructure.

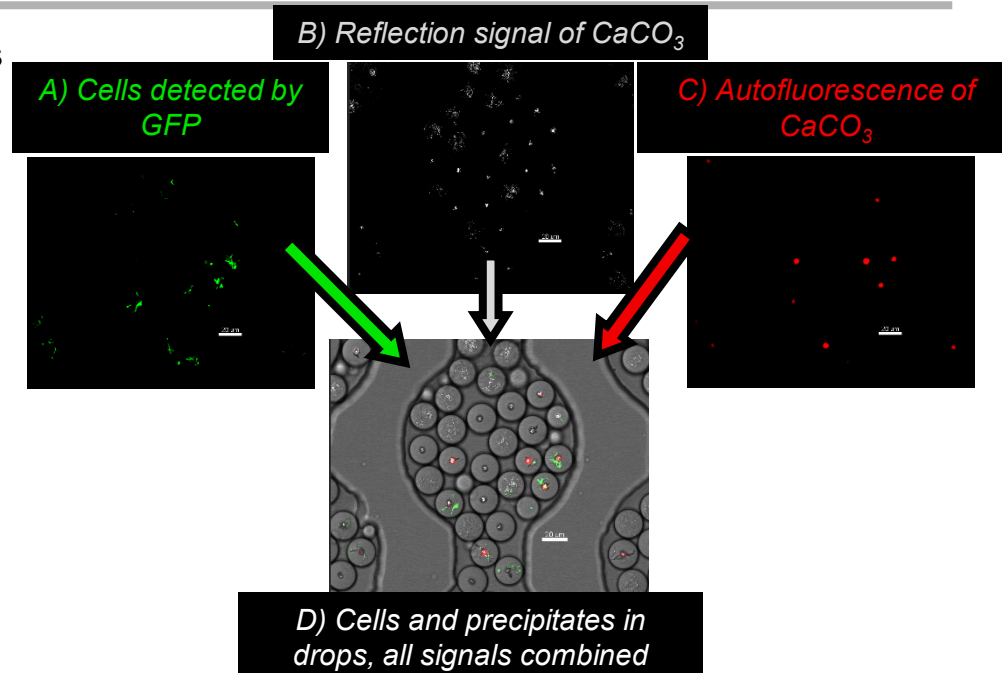
J. Hohne, B. Moon, C. L. Baumbauer, T. Gray, M. J. Tauc, J. Dilts, D. L. Dickensheets, J. A. Shaw, and W. Nakagawa, Electrical and Computer Engineering Dept., Montana State University. Work performed at Montana Microfabrication facility.

Funding support: NASA EPSCoR grant NNX14AN40A.

*National Research Priority: NAE/S Environmental Engineering Grand Challenge-
Curb Climate Change and Adapt to its Impacts*

Mineral precipitation in drops

The inverted confocal was used to image droplets containing ureolytic bacterial cells (detected by GFP, figure panel A). The drops also contain dissolved urea and calcium. The ureolytic bacteria hydrolyze the urea, leading to an increase in surrounding alkalinity and pH. This causes the dissolved calcium to precipitate out of solution as calcium carbonate (CaCO_3), a process called Microbially Induced Calcium carbonate Precipitation (MICP). The precipitates were detected by its strong reflection signal (figure panel B). The CaCO_3 crystals that formed in the drops also exhibited autofluorescence (figure panel C). This work allows the visualization of MICP at the single-cell level in real time and *in-situ*.



Multi-channel imaging on the confocal allowed for the detection of bacterial cells and microbially induced calcium carbonate precipitation in drops.

Neerja Zambare, Robin Gerlach, and Connie Chang, Dept. of Chemical and Biological Engineering, Montana State University. Work performed at MONT facility **Center for Biofilm Engineering**

Funding support: DOE DE-SC0010099; NSF CAREER DMR-1753352. *Frontiers in Microbiology*, 10, p.2112 (2019).

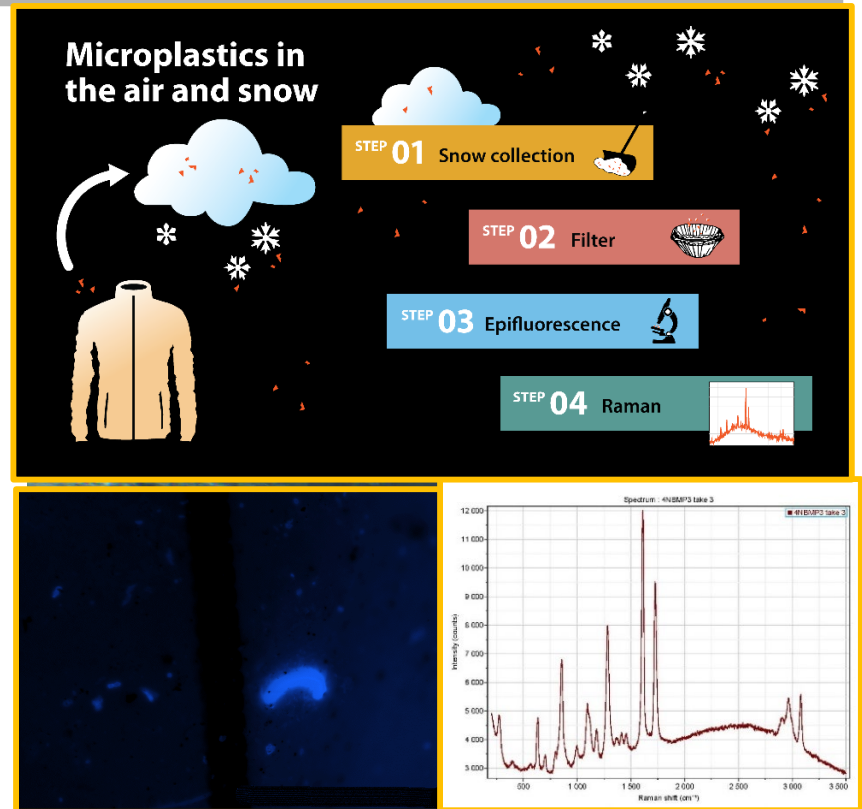
National Research Priority: NSF-Understanding the Rules of Life

Investigating microplastics in precipitation

Our modern lifestyle is consumed by plastic. A rapidly growing area of research is focused on microplastics, which are small plastic particles (< 5mm). Extensive research has been conducted on the characterization of marine microplastics, but less is known about freshwater systems and transport throughout the water cycle. Due to the ubiquitous nature of plastic, we hypothesized that there are microplastics in precipitation.

This research project aims to characterize microplastics in precipitation using epifluorescence microscopy and Raman spectroscopy to identify these particles.

Schematic overview of research, fluorescing microplastic particle and Raman identification.



Bekah Anderson, Markus Dierer and Christine Foreman, Montana State University, Dept. of Chemical & Biological Engineering. Work performed at Montana Nanotechnology Facility- Center for Biofilm Engineering.

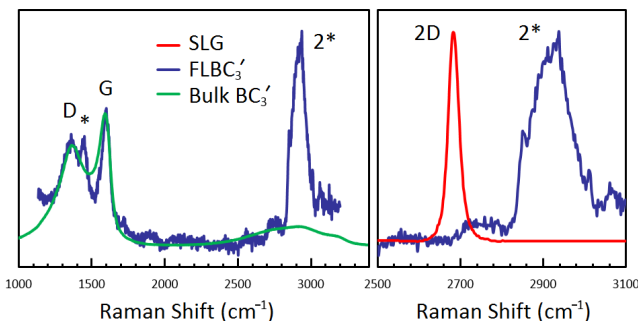
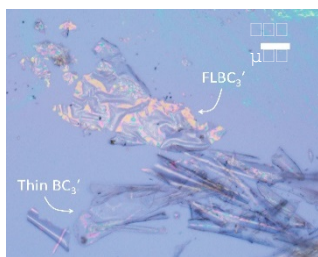
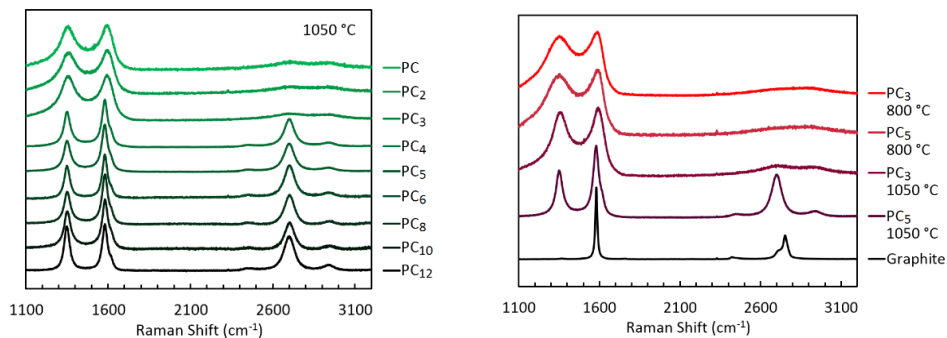
Funding source: MSU Undergraduate Scholars Program

National Research Priority: NSF-Growing Convergence Research

Raman Spectroscopy of Graphitic Carbon

Graphite is the state-of-the-art anode material for lithium-ion batteries. Our research concerns modifications to the graphitic network (chemical and physical) to assess their effects on battery metrics such as compatibility with new chemistries (e.g., sodium-ion batteries), energy density, rate capability, and cyclability.

Our most recent work concerns the chemical modification of disordered graphitic carbon materials using boron (BC_x) and phosphorus (PC_x). The studies shown at right investigate the dependence of both temperature and heteroatom content on the resulting graphitic structure, as probed by Raman spectroscopy.



Raman spectroscopy of boron- (BC_x) and phosphorus- (PC_x) doped graphitic carbon materials, and “few layer” exfoliated variants (e.g., FLBC₃).

Emanuel Billeter, Devin McGlamery, Jack Buckner, and Nicholas P. Stadie Work performed at Montana State University, MONT Facilities, Center for Biofilm Engineering and ICAL.

Funding provided by Montana State University start-up funding. *ACS Appl. Mater. Interfaces* 2019, 11, 39902–39909, *ACS Appl. Mater. Interfaces* 2019, 11, 17686–17696, *Chem. of Materials* 2018 30 (14), 4580-4589.

National Research Priority: NAE Grand Challenge-Make Solar Energy Economical

Sulfur Cycling in Deep Thermal Vents of Yellowstone Lake

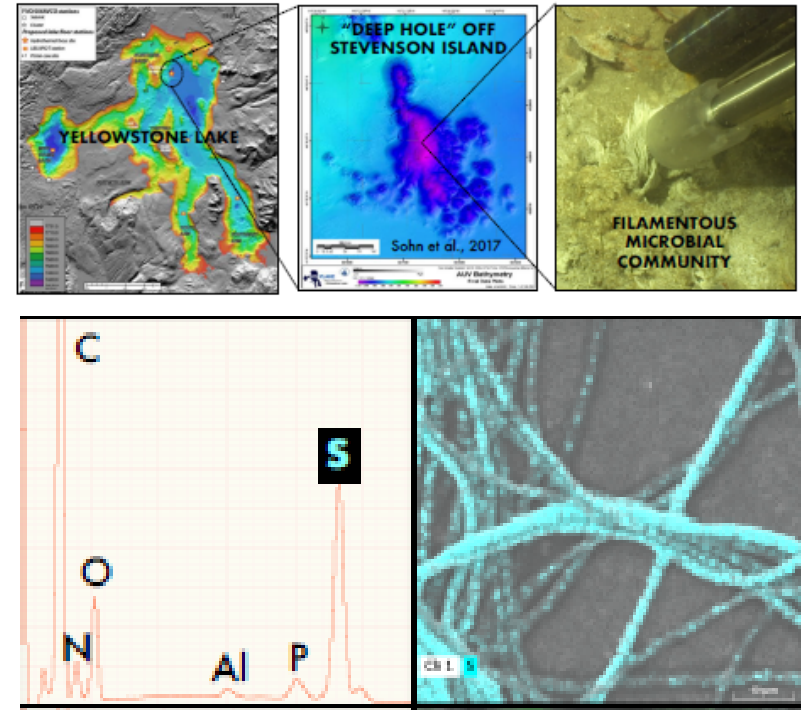
Geothermal activity is very significant on the floor of Yellowstone Lake, which is one of the most seismically active areas in Yellowstone National Park.

Numerous thermal vents rich in sulfur, hydrogen and methane were sampled in 2016-2018 east of Stevenson Island at depths of ~130 meters and maximum vent temperatures of ~ 130-140 °C.

Biomass samples were sequenced and reveal microbial populations capable of important steps within the S cycle.

Top: Location of Sulfur-rich Thermal Vents sampled in Yellowstone Lake.

Bottom: Elemental mapping using Integrated Auger Nanoprobe (ICAL, MSU) of microbial filaments showing S accumulation in S-oxidizing organisms.



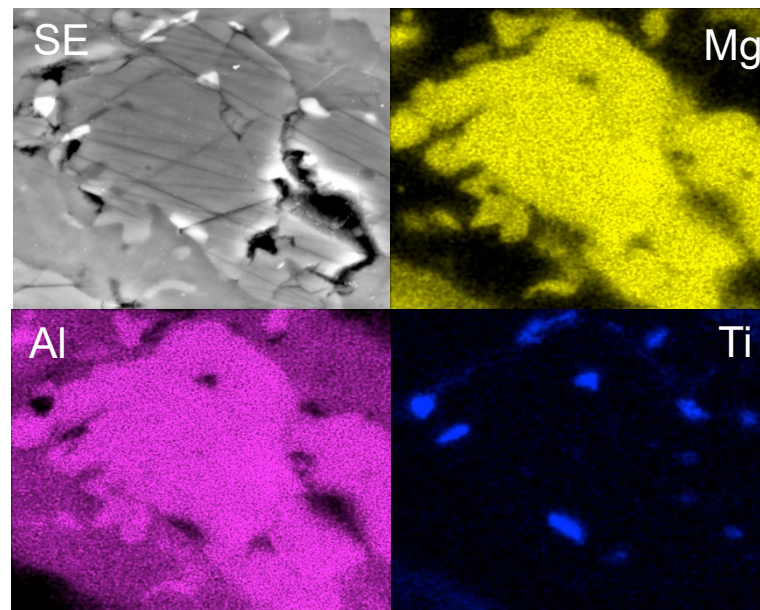
Luke McKay, William Inskeep, Dept. of Land Resources & Environ. Sci., Montana State University. Work performed at MONT facility ICAL.

This work was supported by NSF #1516316. Presented at AGU Fall Meeting 2019

National Research Priority: NSF-Understanding the Rules of Life

Auger N study: Efremovka chondrite

Calcium-aluminum-rich inclusions (CAIs) in primitive chondritic meteorites are likely the oldest materials produced in the Solar System. Samples from comet Wild 2 returned by the NASA Stardust spacecraft also contain CAIs. Within the Wild 2 CAIs refractory nm-scale TiV nitride inclusions have been observed. To determine whether the nitride inclusions also occur in chondrites and thus establish possible links between the Wild 2 CAI and chondritic meteorite source regions, an Auger study on the primitive CV3 chondrite Efremovka was begun. The principal goal of the Auger study was to determine whether the element N is present in the observed Ti-rich inclusions to verify the nitride minerals. However, difficulties in solving electron surface charging issues have prevented rigorous analyses to date and thus the study is currently ongoing.



10 keV secondary electron image and EDX Mg, Al and Ti element maps showing Ti inclusions in the mineral spinel in the primitive chondritic meteorite Efremovka. FOV for each image is approximately 8 μm .

David Joswiak, Department of Astronomy, University of Washington. Work performed at MONT facility ICAL

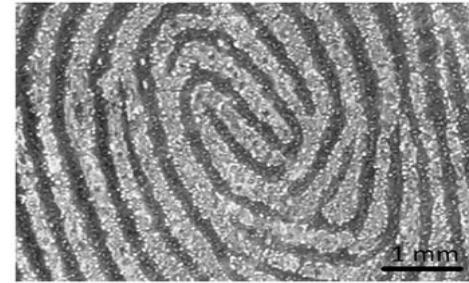
Supported by MONT/NNCI User Grant, NSF award #1542210

National Research Priority: NSF-Growing Convergence Research

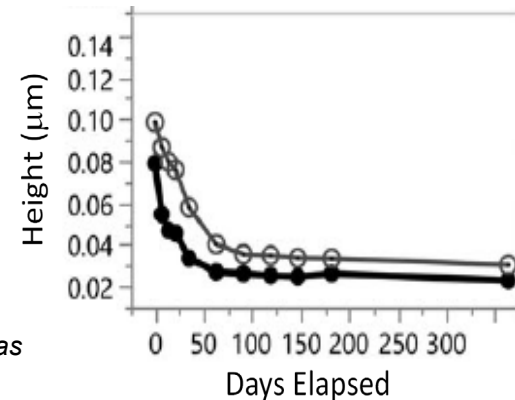
Nanotechnology Collaborative Infrastructure Southwest (NCI-SW)

Application of 3D Imaging Technology to Latent Fingerprint Aging Studies

In most latent fingerprint aging studies, two-dimensional (2D) features are obtained from photo images, scans, or inked impressions. However, some relevant information is possibly being missed because fingerprints are three-dimensional (3D) objects that age in all three dimensions. A feature that has not been carefully examined is how the height of ridges changes over time. In this report, a 3D imaging technology—called optical profilometry—is introduced as a tool for the visual examination of the aging process. Optical profilometry is a nondestructive technology that allows the visualization and data acquisition of unprocessed latent fingerprints. Detailed ridge images and spatiotemporal data were successively obtained on the x-, y- and z-axis, delivering 3D topographical information. OP was able to detect the loss of ridge heights over time. The feasibility of employing this technology to collect data on the aging process of ridges has been proven.



Fingerprint images powdered with TiO_2 powder after 1-year aging



Latent fingerprint ridge height as a function of days elapsed

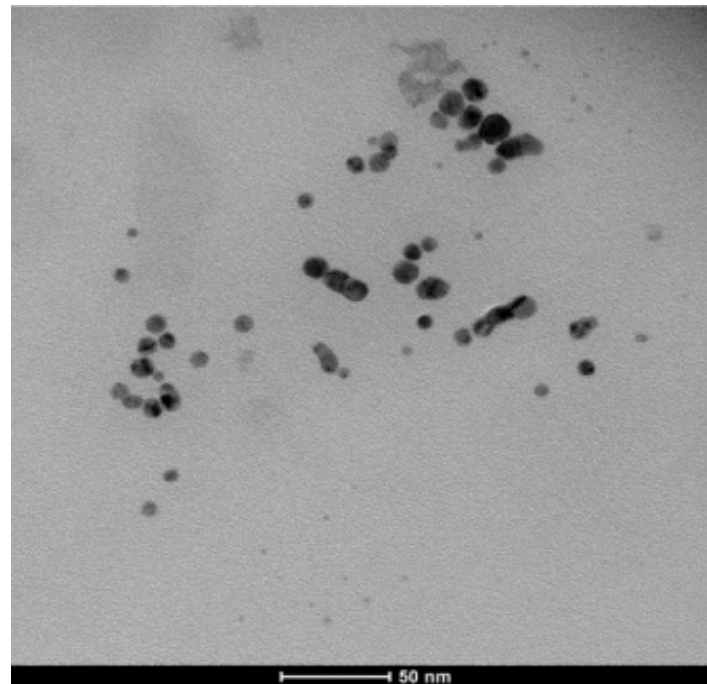
Josep De Alcaraz-Fossoul, College of Criminal Justice and Forensic Sciences, University of New Haven. Work performed at NCI-SW.

J. Forensic Sci., vol. 64, pp. 570 – 576, 2018.

National Research Priority: NSF-Growing Convergence Research

In vitro characterization of reactive oxygen species generation by Mesosilver™ dietary supplement

As silver nanoparticles (AgNPs) are frequently consumed as dietary supplements, it is important to understand the mechanism by which AgNPs might provide health benefits. In this study, we measure the *in vitro* dissolved Ag release and ROS (mainly H₂O₂ and hydroxyl radical) generation by a commercially available AgNPs supplement, Mesosilver™, over a range of pHs typical of the human gut. Both the dissolved Ag and ROS are implicated in the antibacterial behaviour of AgNPs and hence may also have an influence on the gut microbiome and eukaryotic cells. A kinetic model that describes the results obtained reasonably well has been developed and can be used to predict the dissolved Ag and ROS yield on dissolution of Mesosilver™ nanoparticles in the human digestive system.



TEM images of silver nanoparticles

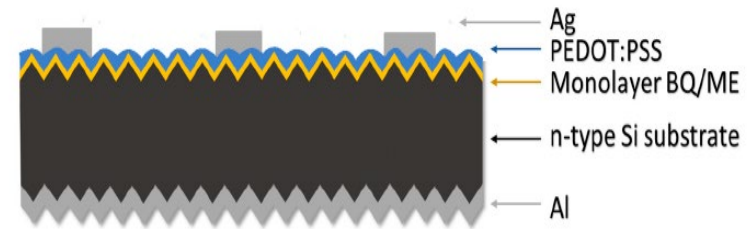
T. David Waite, School of Civil and Environmental Engineering, The University of New South Wales, Sydney, Australia.
Work performed at NCI-SW.

Environ. Sci.: Nano, vol. 5, pp. 2686 – 2698, 2018

National Research Priority: NSF-Understanding the Rules of Life

Effects of Co-Solvents on the Performance of PEDOT:PSS Films and Hybrid Photovoltaic Devices

Hybrid silicon solar cells have been fabricated by the spin coating of conductive polymer poly(3,4-ethylene-dioxythiophene):poly(styrenesulfonate) (PEDOT:PSS) as a p-type contact on textured n-type crystalline silicon wafers. The effect of adding co-solvents, ethylene glycol (EG) and dimethyl sulphoxide (DMSO), to PEDOT:PSS improves its conductivity which translates to the improved performance of solar cells. Transfer length measurements were conducted to realize optimal contact with minimal losses between the front silver contact and PEDOT:PSS. From the conductivity and device results, a 7% EG with 0.25 wt% Triton (surfactant) blend of PEDOT:PSS is found to be optimal for these cells. This current approach will pave the way for further improvement of PEDOT:PSS based hybrid silicon solar cells.



The schematic of the hybrid photovoltaic device architecture

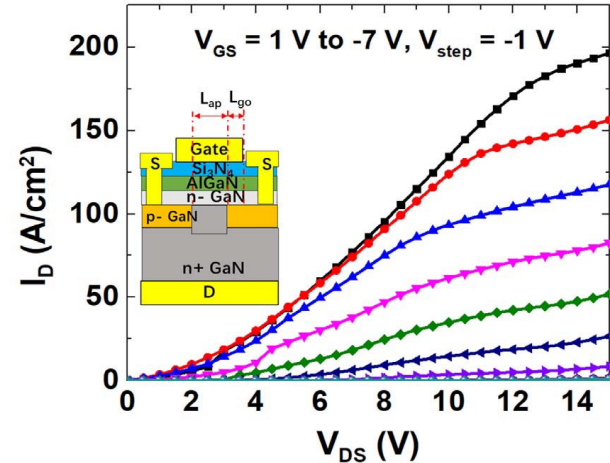
Abhishek Iyer and Robert Opila, Dept. of Electrical and Computer Engineering, University of Delaware. Work performed at NCI-SW.

This work was supported by NSF NNCI-1542160 and EEC-1041895. *Appl. Sci.* vol. 8, p. 2052, 2018.

National Research Priority: NAE Grand Challenge—Make Solar Energy Economical

Demonstration of GaN Current Aperture Vertical Electron Transistors

We have demonstrated current aperture vertical electron transistors (CAVETs) obtained by using a novel implantation-based compensation method to achieve a conductive aperture. This innovation leads to the first demonstration of “regrowth-free” CAVETs. An ion-implantation scheme using multiple-energy levels was designed to realize a 250-nm Si box profile with a total dose of $4.2 \times 10^{15} \text{ cm}^{-2}$, converting a 250-nm p-GaN layer to conductive (n-type) GaN. This novel fabrication method enables the use of Mg-doped CBLs without conventional etch and regrowth steps, leading to regrowth free CAVETs.



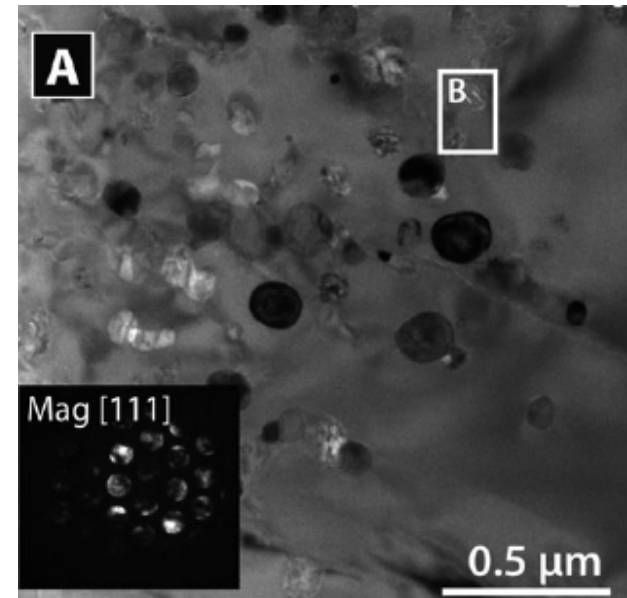
I_D - V_{DS} characteristics of a CAVET with gate-to-CBL overlap length $L_{go} = 3 \mu\text{m}$ and aperture length $L_{ap} = 32 \mu\text{m}$.

Srabanti Chowdhury, Department of Electrical and Computer Engineering, University of California-Davis. This work was performed at the NCI-SW.

IEEE Trans. Electron Devices, vol. 65, pp. 483 – 487, 2018.

Investigating the Response of Biotite to Impact Metamorphism

In this study, we investigate impact metamorphism recorded in crystalline basement rocks from the Steen River impact structure (SRIS), a 25 km diameter complex crater in NW Alberta, Canada. An array of advanced analytical techniques was used to characterize the breakdown of biotite in two distinct settings: along the margins of localized regions of shock melting and within granitic target rocks entrained as clasts in a breccia. The transformation of an inosilicate (pargasite) and a phyllosilicate (biotite) to form garnet, an easily identifiable, robust mineral, has been documented. We contend that in deeply eroded astroblemes, high-pressure minerals that form within or in the environs of shock veins may serve as one of the possibly few surviving indicators of impact metamorphism.



TEM bright-field images and SAED patterns of the biotite breakdown material along shock vein margins. The nanometer-sized dark inclusions in this image are Fe-rich

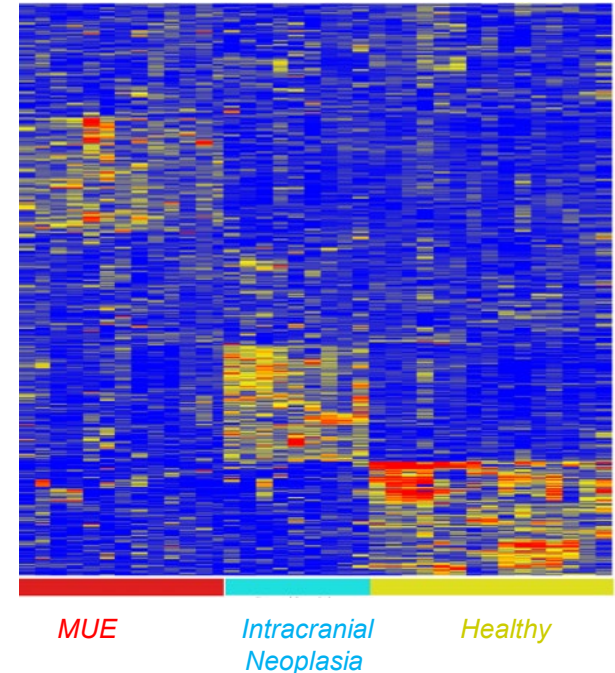
E. L. Walton, Department of Physical Sciences, MacEwan University, Edmonton, Alberta. This work was performed at NCI-SW.

Meteoritics & Planetary Science vol. 53, pp. 75–92

National Research Priority: NSF-Growing Convergence Research

Differentiation of Non-Infectious Diseases in Dogs using Peptide Microarrays

A variety of inflammatory conditions of unknown cause (meningoencephalomyelitis of unknown etiology—MUE) and neoplastic diseases can affect the central nervous system (CNS) of dogs. Immunosignaturing is a method by which an individual's antibody repertoire ($>10^8$ distinct antibodies) interacts with random-sequence peptides. The pattern of binding between serum antibodies and the 125,000 random peptides becomes the signature for that individual at that point in time. Peptide microarrays are manufactured using in-situ synthesis of 125,000 random-sequence peptides. The arrays are made from eight-inch silicon wafers that become the surface on which peptides are grown using standard synthesis techniques. This study evaluated the effectiveness of immunosignature profiles for distinguishing between three cohorts of dogs: healthy, intracranial neoplasia, and MUE. The results demonstrate that immunosignature profiles may help serve as a minimally invasive tool to distinguish between MUE and intracranial neoplasia in dogs



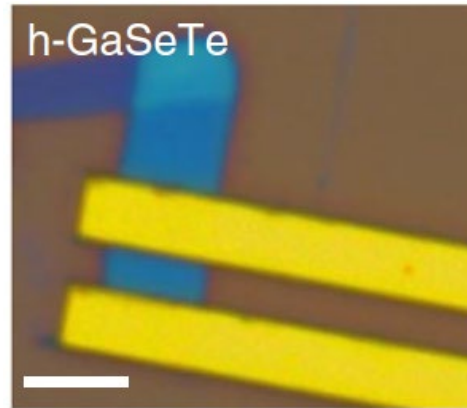
The immunosignature distinguishes healthy dogs, dogs with Intracranial neoplasia, and dogs with MUE.

Kurt L. Zimmerman, Department of Biomedical Sciences and Pathobiology, Virginia-Maryland College of Veterinary Medicine. This work was performed at the NCI-SW.

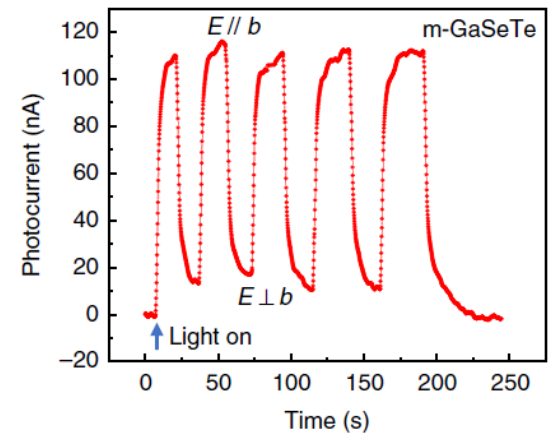
National Research Priority: NSF-Understanding the Rules of Life

GaSe_{1-x}Te_x nanomaterials for Photonic Devices

By stabilizing previously unobserved compositions and phases of GaSe_{1-x}Te_x at nanoscales on GaAs(111), we demonstrate abnormal band bowing effects and phase instability region when components crystallize in different phases. Results highlight potential applications in photonic and electronics.



2D GaSeTe photodetectors with strong polarization dependent photocurrents



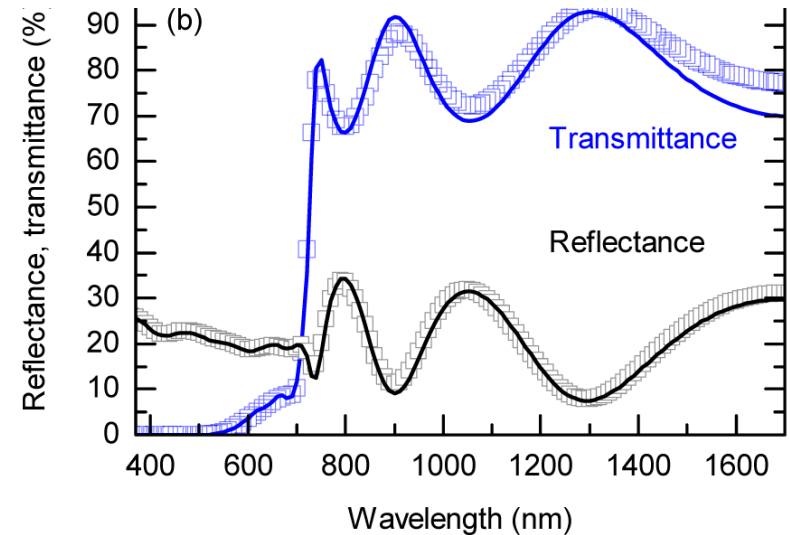
Sefaattin Tongay, School for Engineering of Matter, Transport and Energy, ASU. This work was performed at NCI-SW.

Nature Communications, vol. 9, Article 1927 (2018)

National Research Priority: NSF-Quantum Leap

Optical modeling of wide-bandgap perovskite and perovskite/silicon tandem solar cells

We report optical constants determined with ellipsometry and spectrophotometry for two new wide bandgap, cesium-formamidinium-based perovskites. We validate the optical constants by comparing simulated quantum efficiency and reflectance spectra with measured cell results for semi-transparent single-junction perovskite cells and find less than 0.3 mA/cm² error in the short-circuit current densities. Such simulations further reveal that reflection and parasitic absorption in the front ITO layer and electron contact are responsible for the biggest optical losses.



Simulated (line) and measured (symbol) reflectance and transmittance spectra of a wide bandgap CsBr perovskite

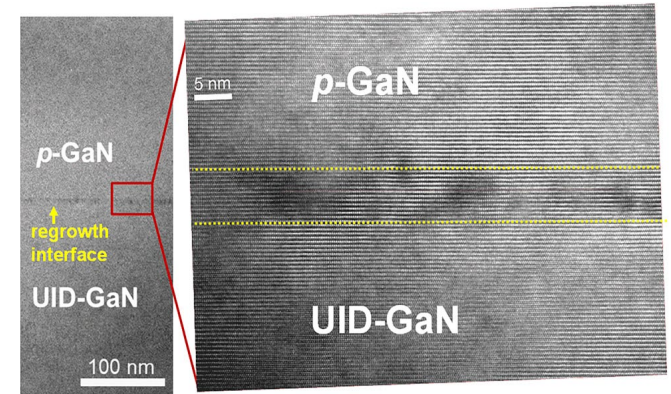
Zachary Homan, School for ECEE, ASU, and Michael McGehee, Stanford University. This work was performed at the NCI-SW.

Optics Express, vol. 26, pp. 27441 – 27460 (2018)

National Research Priority: NAE Grand Challenge—Make Solar Energy Economical

GaN vertical p-n diode with regrown p-GaN by metalorganic chemical vapor deposition

P-type GaN was regrown on an etched GaN surface on GaN substrates by metalorganic chemical vapor deposition. Vertical GaN-on-GaN p-n diodes were fabricated to investigate the effects of the etch-then-regrowth process on device performance. The crystal quality of the sample after each epitaxial step was characterized by X-ray diffraction, where the etch then-regrowth process led to a very slight increase in edge dislocations. The forward current density increased slightly with increasing temperature, while the reverse current density was almost temperature independent indicating tunneling as the reverse transport mechanism. This result is very similar to the reported Zener tunnel diode comprising a high doping profile at the junction interface. This work provides valuable information on p-GaN regrowth and regrown GaN p-n diodes, which can serve as an important reference for developing selective doping for advanced GaN power electronics for high voltage and high-power applications.



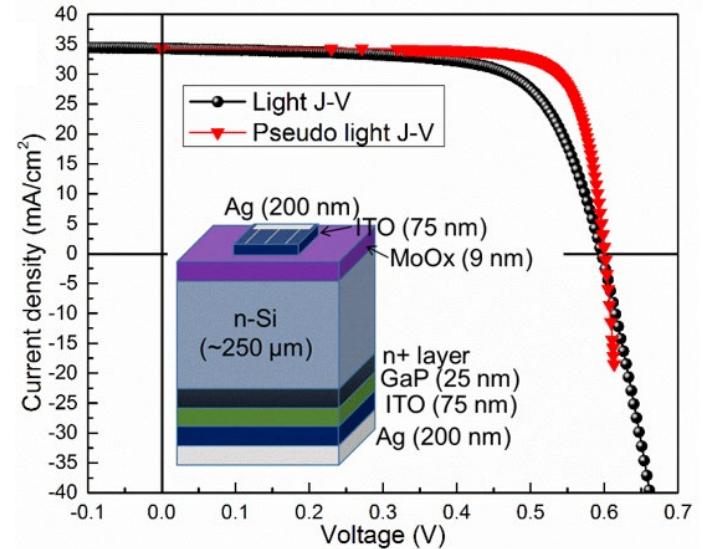
TEM images of the regrown p-n junction.

Yuji Zhao, School of Electrical, Computer and Energy Engineering, ASU. Work performed at NCI-SW.

This work was partially supported by NSF NNCI-1542160. *Appl. Phys. Letts.*, vol. 113, p. 233502-1 to 233502-4 (2018)

Developing High Performance GaP/Si Heterojunction Solar Cells

We present high performance GaP/Si heterojunction solar cells with a high Si minority-carrier lifetime and high crystal quality of epitaxial GaP layers. By applying phosphorus (P)-diffusion layers into the Si substrate and a SiNx layer, the Si minority-carrier lifetime is well-maintained during the GaP growth. The film quality is characterized by atomic force microscopy and high-resolution x-ray diffraction. In addition, MoOx was implemented as a hole-selective contact that led to a significant increase in the short-circuit current density. The achieved high device performance of the GaP/Si heterojunction solar cells establishes a path for further enhancement of the performance of Si-based photovoltaic devices.



Light J-V (black) and pseudo light J-V (red) of a MoOx/Si/GaP heterojunction solar cell

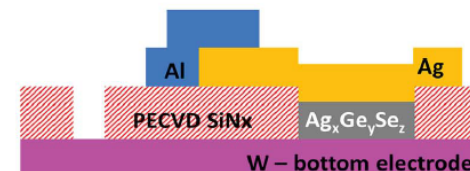
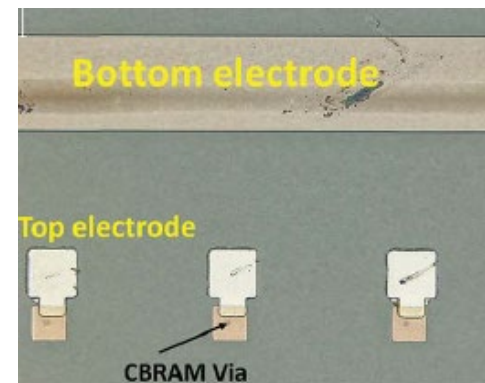
Chaomin Zhang, Ehsan Vadiee, Som Dahal, Richard R. King, and Christiana B. Honsberg, School of Electrical, Computer and Energy Engineering, ASU. This work was performed at the NCI-SW.

This work was partially supported by NSF ECCS-1542160. *Journal of Visualized Experiments*, vol. 141, p. e58292 (2018)

National Research Priority: NAE Grand Challenge—Make Solar Energy Economical

Impact of radiation induced crystallization on a programmable metallization cell

Chalcogenide-based, programmable metallization cells (PMC) cells have been characterized after exposure to increasing levels of absorbed dose (i.e., ionizing radiation exposure). We found, and show here for the first time, that total absorbed dose effects induce a slight modification of the switching phenomena with a moderate increase of the programmable low resistance state (LRS) of the PMCs after repeated switching depending on the processing conditions, while it does not impact the state programmed before exposure. We also show that an increase of the programmable high resistance state (HRS) occurs with irradiation.



Top view and cross-section of PMC devices with access to bottom electrode, top electrode bond pad, and PMC/CBRAM via

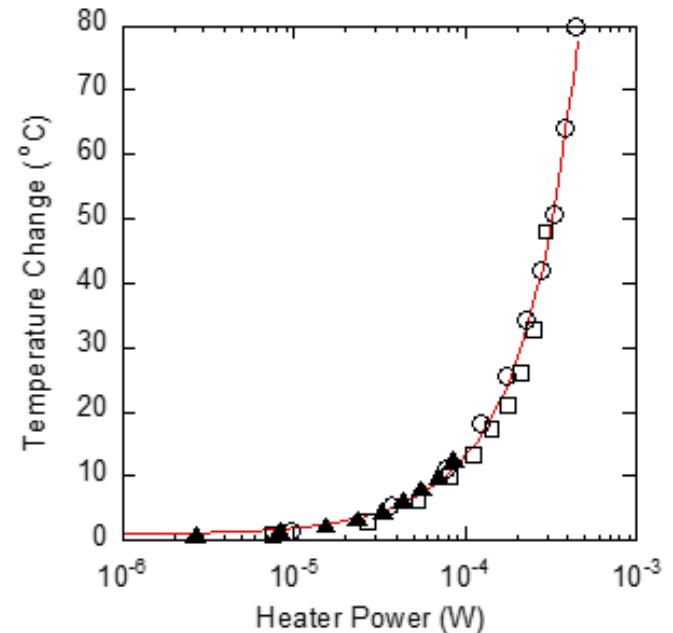
Y. Gonzalez-Velo, A. Patadia, H. J. Barnaby and M. N. Kozicki. This work was performed at NCI-SW.

This work was partially supported by NSF ECCS-1542160. *Faraday Discuss.*, vol. 213, pp. 53-66 (2019)

National Research Priority: NAE Grand Challenge—Prevent Nuclear Terror

Self-Heating in SOI MOSFETs at the 45nm Node

To understand the impact of self-heating in SOI CMOS technologies we have fabricated pairs of 40nm gate length n-channel MOSFETs that share a common source contact and the same active silicon region. One of the MOSFETs is turned on and heats the active silicon, while the other is biased into the sub-threshold regime and operates as a local thermometer. Preliminary results show that the MOSFET thermometer temperature increases approximately quadratically with the power dissipated in the MOSFET heater.



The temperature change in an NFET thermometer as a function of power dissipated in an adjacent NFET heater.

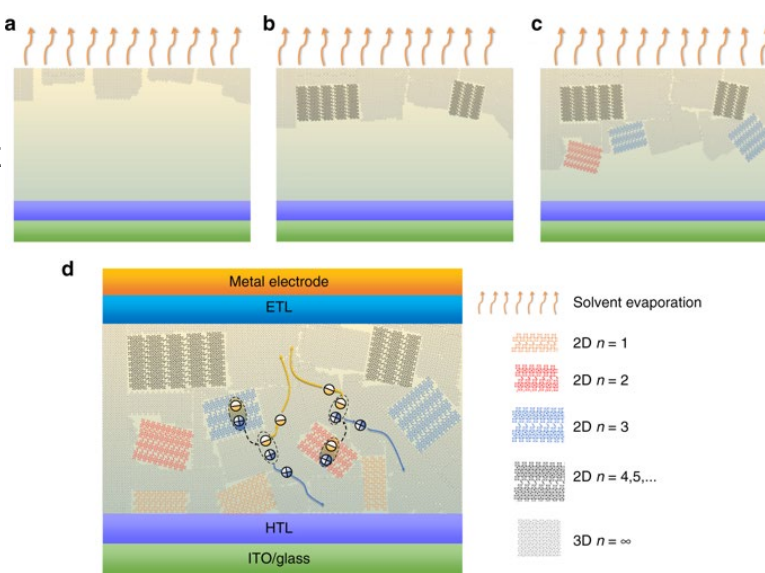
X. Zhang, P. H. Mehr, D. Vasileska, and T. J. Thornton. This work was performed at NCI-SW.

This work was partially supported by NSF ECCS-1542160. *Proceedings of the 13th IEEE Nanotechnology Materials and Devices Conference*, Portland, OR, 14-17 Oct. 2018

Nebraska Nanoscale Facility (NNF)

Unveiling the operation mechanism of layered perovskite solar cells

Layered perovskites have been shown to improve the stability of perovskite solar cells while their operation mechanism remains unclear. Yun Lin and coworkers used the NNF to investigate the process for the conversion of light to electrical current in high performance layered perovskite solar cells by examining its real morphology. The perovskite films in this study are found to be a mixture of layered and three dimensional (3D)-like phases with phase separations at micrometer and nanometer scale in both vertical and lateral directions. This phase separation is explained by the surface initiated crystallization process and the competition of the crystallization between 3D-like and layered perovskites. The authors proposed that the working mechanisms of the layered perovskite solar cells involve energy transfer from layered to 3D-like perovskite network. The impact of morphology on efficiency and stability of the hot-cast layered perovskite solar cells are also discussed to provide guidelines for the future improvement.



Growth kinetics, morphology and device operation mechanism model. **a–c** The growth kinetics and morphology model. **d** The device structure is indium tin oxide (ITO)/hole transport layer (HTL)/layered perovskite film/electron transport layer (ETL)/metal electrode

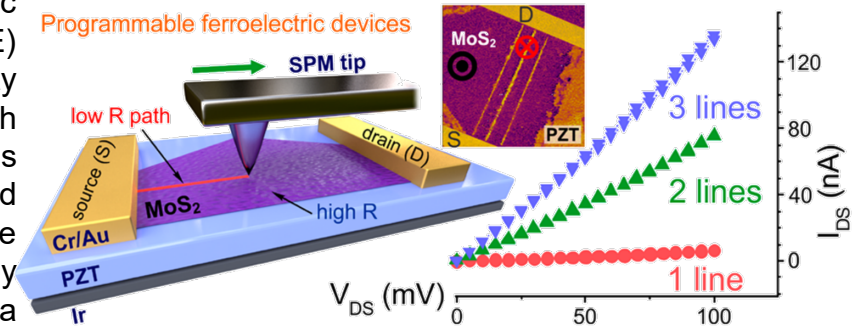
Yun Lin, Yanjun Fang, Jingjing Zhao, Yuchuan Shao, Samuel J. Stuard, Masrur Morshed Nahid, Harald Ade, Qi Wang, Jeffrey E. Shield, Ninghao Zhou, Andrew M. Moran & Jinsong Huang. Work performed in part at NNF and UNC-Chapel Hill.

This work was supported by NSF OIA-1538893 and DMR-1420645, Office of Naval Res. N00014-17-1-2727 and UNC. *Nature Communications* 10, 1008, 2019

National Research Priority: American Energy Dominance

Nanodomain Engineering for Programmable Ferroelectric Devices

This work introduces a concept of programmable ferroelectric devices composed of two-dimensional (2D) and ferroelectric (FE) materials. It enables precise modulation of the in-plane conductivity of a 2D channel material through nanoengineering FE domains with out-of-plane polarization. The functionality of these new devices has been demonstrated using field-effect transistors (FETs) fabricated with monolayer molybdenum disulfide (MoS_2) channels on the $\text{Pb}(\text{Zr},\text{Ti})\text{O}_3$ substrates. Using piezoresponse force microscopy (PFM), the authors show that local switching of FE polarization by a conductive probe can be used to tune the conductivity of the MoS_2 channel. Specifically, patterning of the nanoscale domains with downward polarization creates conductive paths in a resistive MoS_2 channel so that the conductivity of an FET is determined by the number and length of the paths connecting source and drain electrodes. In addition to the device programmability, they demonstrate the device ON/OFF cyclic endurance by successive writing and erasing of conductive paths in a MoS_2 channel. These findings may inspire the development of advanced energy-efficient programmable synaptic devices based on a combination of 2D and FE materials.



Scheme of a programmable FeFET where the in-plane conductivity is tuned by writing a conductive path (red line) in the MoS_2 channel through local polarization switching in the FE substrate. $I_{\text{DS}}-V_{\text{DS}}$ curves for different numbers of conductive paths.

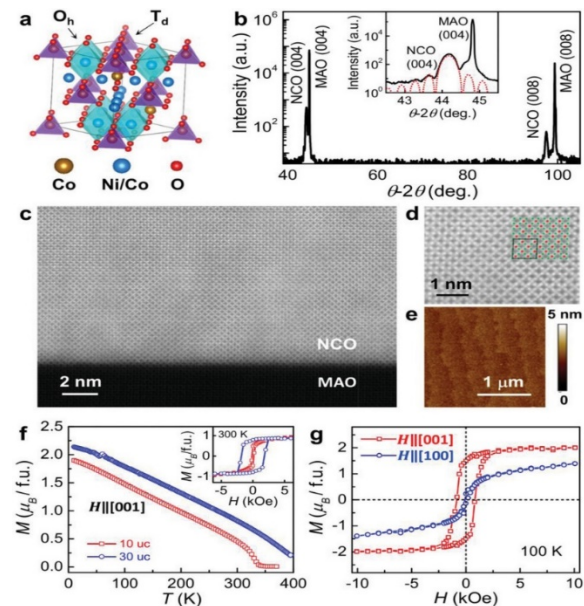
Alexey Lipatov, Tao Li, Nataliia S. Vorobeva, Alexander Sinitskii and Alexei Gruverman, Work performed in part at the Nebraska Nanoscale Facility.

This work was supported by NSF DMR-1420645. *Nano Letters* 19, 5, 3194, 2019.

National Research Priority: NSF-Harnessing the Data Revolution

Magnetotransport Anomaly in Room-Temperature Ferrimagnetic NiCo_2O_4 Thin Films

The inverse spinel ferrimagnetic NiCo_2O_4 presents a unique model system for studying the competing effects of crystalline fields, magnetic exchange, and various types of chemical and lattice disorder on the electronic and magnetic states. The NNF users Xuegang Chen and co-workers reported the magnetotransport anomalies in high-quality epitaxial NiCo_2O_4 thin films resulting from the complex energy landscape. A strong out-of-plane magnetic anisotropy, linear magnetoresistance, and robust anomalous Hall effect above 300 K are observed in 5–30 unit cell NiCo_2O_4 films. The anomalous Hall resistance exhibits a nonmonotonic temperature dependence that peaks around room temperature, and reverses its sign at low temperature in films thinner than 20 unit cells. The scaling relation between the anomalous Hall conductivity and longitudinal conductivity reveals the intricate interplay between the spin-dependent impurity scattering, band intrinsic Berry phase effect, and electron correlation. This study provides important insights into the functional design of NiCo_2O_4 for developing spinel-based spintronic applications.



Characterizations of NCO films. a) Schematic crystal structure of NCO. b) XRD θ - 2θ scan c) HAADF-STEM image d) a higher-magnification image e) AFM topography image. f) Out-of-plane M vs T for 10 and 30 uc films. Inset: M vs H at 300 K. g) M vs H in out-of-plane and in-plane magnetic fields for the 10 uc film at 100 K.

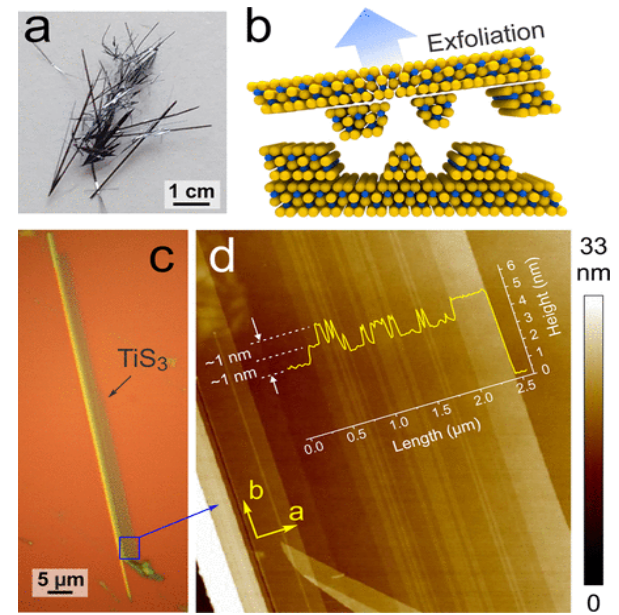
Xuegang Chen, Xiaozhe Zhang, Myung-Geun Han, Le Zhang, Yimei Zhu, Xiaoshan Xu, and Xia Hong. Work performed in part at the Nebraska Nanoscale Facility.

This work was supported by NSF DMR-1420645 and DMR-171046. *Advanced Materials* 31, 4, 1805260, 2019.

National Research Priority: NSF-Quantum Leap

Quasi-1D TiS_3 Nanoribbons: Mechanical Exfoliation and Thickness-Dependent Raman Spectroscopy

Quasi-1D materials enjoy growing interest due to their unusual physical properties and promise for miniature electronic devices. Sinitskii and co-workers used the NNF to investigate the micromechanical exfoliation of representative quasi-1D crystals, TiS_3 whiskers, and demonstrated that they typically split into narrow nanoribbons with very smooth, straight edges and clear signatures of 1D TiS_3 chains. Theoretical calculations show that the energies required for breaking weak interactions between the two-dimensional layers and between 1D chains within the layers are comparable and, in turn, are considerably lower than those required for breaking the covalent bonds within the chains. In the AFM experiments, it was possible to slide the 2D TiS_3 layers relative to each other as well as to remove selected 1D chains from the layers. They systematically studied the exfoliated TiS_3 crystals by Raman spectroscopy and identified the Raman peaks whose spectral positions were most dependent on the crystals' thickness. These results could be used to distinguish between TiS_3 crystals with thickness ranging from one to about seven monolayers. The possibility of exfoliation of TiS_3 into narrow crystals with smooth edges could be important for the future realization of miniature device channels with reduced edge scattering of charge carriers.



Visualization of one-dimensional chains in TiS_3 whiskers. (a) Optical photograph of TiS_3 whiskers. (b) Scheme of micromechanical exfoliation of TiS_3 . (c) Optical image of an exfoliated TiS_3 nanoribbon on Si/SiO_2 . (d) AFM image of a small area of the TiS_3 nanoribbon shown in (c). Overlaid over

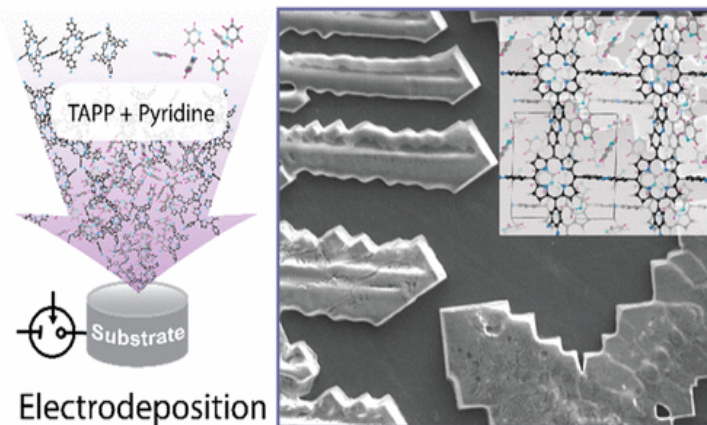
A. Lipatov, M.J. Loes, H. Lu, J. Dai, P. Patoka, N.S. Vorobeva, D.S. Muratov, G. Ulrich, B. Kästner, A. Hoehl, G. Ulm, X. C. Zeng, E. Rühl, A. Gruverman, P.A. Dowben, and A. Sinitskii. Work performed in part at the Nebraska Nanoscale Facility.

This work was supported by NSF ECCS-1740136 and ECCS-1508541, the nCORE (SRC), and NSF DMR-1420645. ACS NANO 12, 12, 12713, 2018

National Research Priority: NSF-Quantum Leap

In Situ Bottom-up Synthesis of Porphyrin-Based Covalent Organic Frameworks

Synthesis and processing of two- or three-dimensional covalent organic frameworks (COFs) have been limited by solvent intractability and sluggish condensation kinetics. Elham Tavakoli and co-workers used the NNF to report on the electrochemical deposition of poly(5,10,15,20-tetrakis(4-aminophenyl)porphyrin)-covalent organic frameworks (POR-COFs) via formation of phenazine linkages. By adjusting the synthetic parameters, they demonstrated the rapid and bottom-up synthesis of COF dendrites. Both experiment and density functional theory underline the prominent role of pyridine, not only as a polymerization promoter but as a stabilizing sublattice, cocrystallizing with the framework. The crucial role of pyridine in dictating the structural properties of such a cocrystal (Py-POR-COF) is discussed. Also, a structure-to-function relationship for this class of materials, governing their electrocatalytic activity for the oxygen reduction reaction in alkaline media, is reported.



Schematic representation of the in situ bottom-up synthesis of porphyrin based covalent organic frameworks.

Elham Tavakoli, Arvin Kakekhani, Shayan Kaviani, Peng Tan, Mahdi Mohammadi Ghaleni, Mohsen Asle Zaeem, Andrew M. Rappe, and Siamak Nejati. Work performed in part at the Nebraska Nanoscale Facility.

This work was supported by the DOE, Office of Basic Energy Sciences, DE-SC0019281. *JACS*, 2019, article in press.

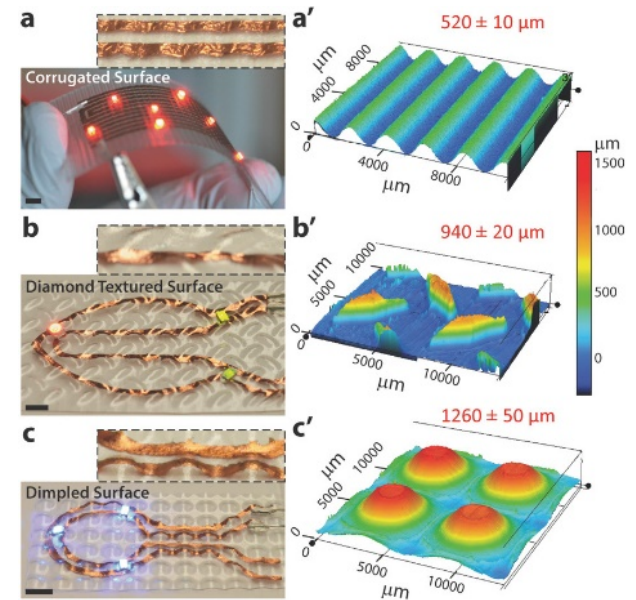
National Research Priority: American Energy Dominance

Soft Microreactors for the Deposition of Conductive Metallic Traces on Planar, Embossed, and Curved Surfaces

Advanced manufacturing strategies have enabled large-scale, economical, and efficient production of electronic components that are an integral part of various consumer products ranging from simple toys to intricate computing systems. However, the circuitry for these components is produced via top-down lithography and is thus limited to planar surfaces. Abhiteja Konda and co-workers used the NNF to demonstrate the use of reconfigurable soft microreactors for the patterned deposition of conductive copper traces on flat and embossed two-dimensional substrates as well as nonplanar substrates made from different commodity plastics. Using localized, flow-assisted, low-temperature, electroless copper deposition, conductive metallic traces are fabricated, which, when combined with various off-the-shelf electronic components, enabled the production of simple circuits and antennas with unique form factors. This solution-phase approach to the patterned deposition of functional inorganic materials selectively on different polymeric components will provide relatively simple, inexpensive processing opportunities for the fabrication of 2D/nonplanar devices when compared to complicated manufacturing methods such as laser-directed structuring.

A. Konda, A. Rau, M.A. Stoller, J.M. Taylor, A. Salam, G.A. Pribil, C. Argyropoulos, and S.A. Morin. Work performed in part at the Nebraska Nanoscale Facility.

This work was supported by the NSF Award No. 1555356. *Advanced Functional Materials*, 28, 40, 1803020, 2018.

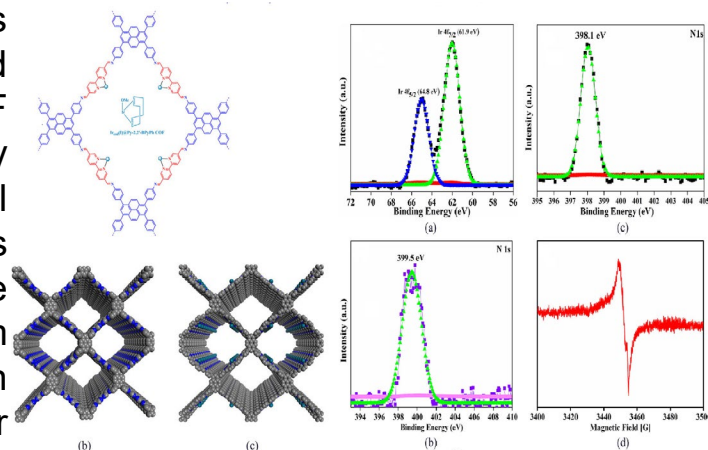


Deposition of conductive traces on embossed substrates using μ -DECD. The surfaces include: a) a corrugated surface ($520 \pm 10 \mu\text{m}$), b) a diamond textured surface ($940 \pm 20 \mu\text{m}$), and c) a dimpled surface ($1260 \pm 50 \mu\text{m}$). Surface mount LEDs were attached along the length of the traces. a'-c') Surface profiles of the substrates measured using confocal microscopy. Scale bars are 5 mm.

National Research Priority: NSF- Future of Work at the Human-Technology Frontier

Iridium complex immobilization on covalent organic framework for effective C—H borylation

The strong coordination between metal ions and binding moieties in functional porous materials is central to the design and advancement of heterogeneous catalysis. In this study, the NNF external user Harsh Vardhan and co-workers have successfully immobilized catalytically active iridium ions on a two-dimensional covalent organic framework (COF) having bipyridine moieties using a programmed synthetic procedure. They used XPS at the NNF to study the docking status of Iridium. The iridium immobilized framework, Ir_{cod}(I)@Py-2,2'-BPyPh COF, had high porosity, good stability, and exhibited excellent catalytic activity for C—H borylation, as compared with the pristine framework. Additionally, Ir_{cod}(I)@Py-2,2'-BPyPh COF was found to be an efficient catalyst for a series of electronically and sterically substituted substrates. The immobilized COF possessed excellent reusability, recyclability, and retention of crystallinity. This work highlights the role of porous materials as an ideal decorating platform for conducting a wide range of potent chemical conversions.



Schematic representation of Ir_{cod}(I)@Py-2,2'-BPyPh COF. (b left) Py-2,2'-BPyPh COF and (c left) Ir_{cod}(I)@Py-2,2'-BPyPh COF. (a-d right) XPS and EPR spectrum of (a) Ir_{cod}(I)@Py-2,2'-BPyPh COF (iridium); (b) Ir_{cod}(I)@Py-2,2'-BPyPh COF (nitrogen); (c) Py-2,2'-BPyPh COF (nitrogen); and (d) EPR spectra of Ir_{cod}(I)@Py-2,2'-BPyPh COF.

H. Vardhan, Y. Pan, Z. Yang, G. Verma, A. Nafady, T.M. Alotaibi, O.A. Almaghrabi, and S. Ma. Dept. of Chem., University of South Florida, Chem and Biochem Dept., North Dakota State University, Chem. Dept., King Saud University & University of Jeddah, Saudi Arabia, Chem. Dept., Sohag University, Egypt. Work performed in part at the Nebraska Nanoscale Facility.

APL Materials 7, 101111, 2019

National Research Priority: American Energy Dominance

NNCI Site @ Stanford (nano@stanford)

Bioinspired flexible organic artificial afferent nerve

The distributed network of receptors, neurons, and synapses in the somatosensory system efficiently processes complex tactile information. An international team of researchers from Stanford, South Korea and China used flexible organic electronics to mimic the functions of a sensory nerve. The artificial afferent nerve collects pressure information (1 to 80 kilopascals) from clusters of pressure sensors, converts the pressure information into action potentials (0 to 100 hertz) by using ring oscillators, and integrates the action potentials from multiple ring oscillators with a synaptic transistor. The system has potential applications in neurorobotics and neuroprosthetics.

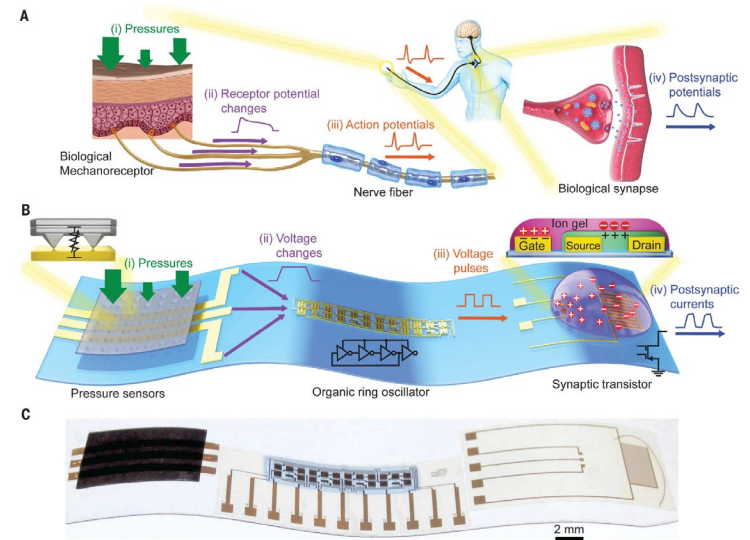


Figure: An artificial afferent nerve system in comparison with a biological one. (A) A biological afferent nerve that is stimulated by pressure. (B) An artificial afferent nerve made of pressure sensors, an organic ring oscillator, and a synaptic transistor. (C) A photograph of an artificial afferent nerve system.

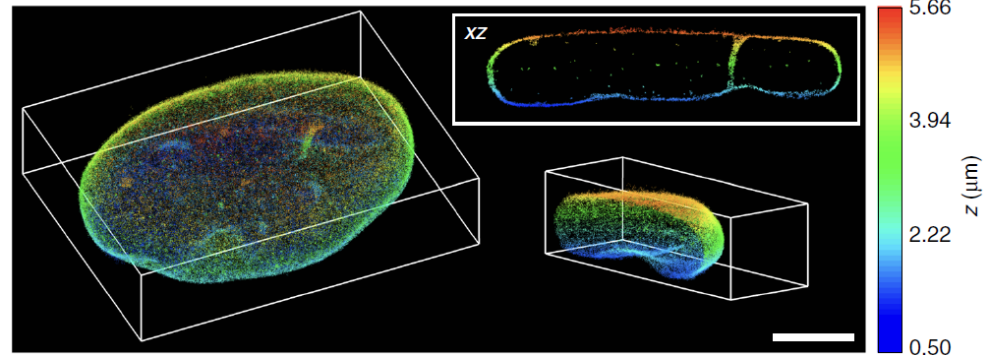
Kim, Chortos, Liu, Oh, Son, Kang, Foudeh, Zhu, Niu, Liu, Pfattner, Bao (Stanford), Xu, Lee, Lee (Seoul National University), Xu (Nankai University). Part of this work was performed at the nano@stanford site.

Work supported by National Research Foundation of Korea, Ministry of Science and ICT, Seoul National University, Agency for Science, Technology and Research (Singapore), Natural Sciences and Engineering Research Council (Canada), Marie Curie Cofund. *Science* 360 (2018)

National Research Priority: NSF-Understanding the Rules of Life

3D single-molecule super-resolution microscopy with a tilted light sheet

Tilted light sheet microscopy with 3D point spread functions (TILT3D) combines a novel, tilted light sheet illumination strategy with long axial range point spread functions (PSFs) for low-background, 3D super-localization of single molecules as well as 3D super-resolution imaging in thick cells. The group demonstrated simple and flexible 3D superresolution imaging with tens of nm localization precision throughout thick mammalian cells. The nano@stanford site was used to fabricate the dielectric phase masks used in the research.



Tilted light sheet imaging with long axial range point spread functions. 3D SR reconstruction of the entire nuclear lamina (lamin B1) in a HeLa cell. Scale bar: 5 μm

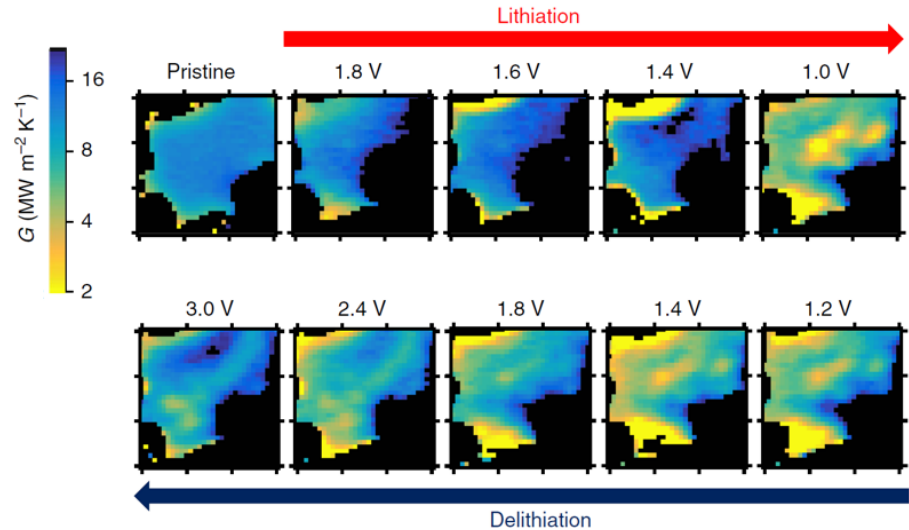
Gustavsson (Stanford, Karolinska Institutet (Stockholm, Sweden), Petrov, Lee, Moerner (Stanford), Shechtman (Stanford, Institute of Technology (Haifa, Israel)). Part of this work was performed at the nano@stanford site.

This work was supported by NIH National Institute of General Medical Sciences, National Institute of Biomedical Imaging and Bioengineering, Swedish Research Council, Foundation Blanceflor Boncompagni Ludovisi, National Science Scholarship (Singapore), Technion (Israel). *Nature Communications* 9 (2018)

National Research Priority: NSF-Understanding the Rules of Life

An Electrochemical Thermal Transistor

The ability to actively regulate heat flow at the nanoscale could be a game changer for applications in thermal management and energy harvesting. Such a breakthrough could also enable the control of heat flow using thermal circuits, in a manner analogous to electronic circuits. Researchers from Profs. Yi Cui, Eric Pop and Kenneth Goodson (Stanford), have demonstrated switchable thermal transistors with an order of magnitude thermal on/off ratio, based on reversible electrochemical lithium intercalation in MoS₂ thin films.



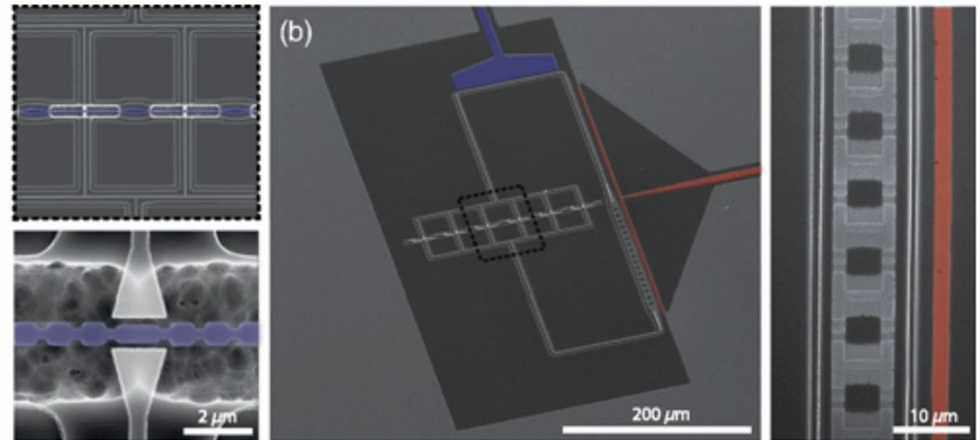
Operando scanning thermal conductance imaging. Maps of the inhomogeneous thermal conductance within the device taken at different stages of lithiation and delithiation over one electrochemical cycle.

Sood, Xiong, Wang, Zhang, McClellan, Sun, Cui, Pop, Goodson (Stanford) Chen (UC Davis) Selli (Max Planck Institute for Polymer Research (Germany), Donadio (UC Davis, Ikerbasque, Basque Foundation for Science (Spain). Part of this work was performed at the nano@Stanford site.

This work was supported by NSF EEC-1449548, NSF EFRI 2-DARE grant 1542883, AFOSR, Stanford University, DoE. *Nature Communication* 9 (2018)

Coupling a Superconducting Quantum Circuit to a Phononic Crystal Defect Cavity

Connecting nanoscale mechanical resonators to microwave quantum circuits opens new avenues for storing, processing, and transmitting quantum information. Researchers from Prof. Amir Safavi-Naeini's group demonstrated coupling a phononic crystal cavity to a tunable superconducting quantum circuit. The work has direct application to engineering hybrid quantum systems for microwave-to-optical conversion as well as emerging architectures for quantum information processing.



False-colored scanning-electron micrographs of the final device. The charge and flux lines are highlighted in blue and red, respectively. A close-up of the SQUID array clearly shows the Al/AlO_x/Al junctions and the trenching in the Si substrate on either side of the array, produced by a deliberate gap between the electron-beam and photolithography masks used to pattern the LiNbO₃ film, which results in the Si getting etched twice in those regions.

Arrangoiz-Arriola, Wollack, Pechal, Witmer, Hill Safavi-Naeini (Stanford). Part of this work was performed at the nano@stanford site.

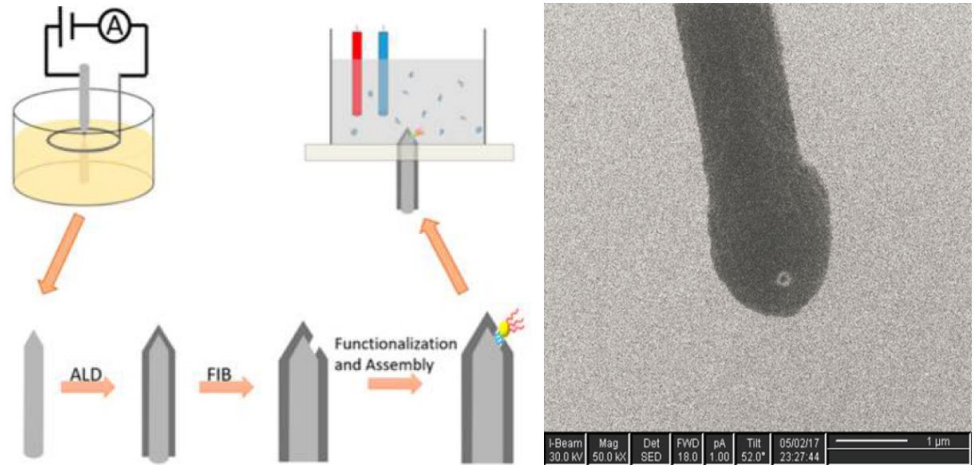
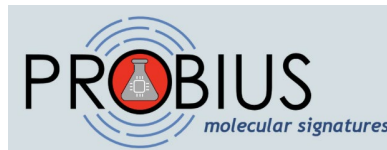
This work was supported by National Research Foundation of Korea, Ministry of Science and ICT, Seoul National University, Agency for Science, Technology and Research (Singapore), Natural Sciences and Engineering Research Council (Canada), Marie Curie Cofund. *Physical Review X* 8 (2018)

National Research Priority: NSF-Quantum Leap

ProbiusDX: Non-invasive Point of Care Diagnostic Technology

ProbiusDx aims to develop a non-invasive point of care diagnostic technology for detecting and monitoring blood concentrations of antimicrobial drugs. The ability to measure drug concentrations in a patient's blood provides valuable information for individualized optimal dosing, maximal efficacy and reduced potential for undesirable side effects.

The company was founded in 2015 and is a Stanford spin-off. Much of the initial prototyping and proof-of-concept sensor development and data generation were done by leveraging the nano@stanford facilities.



Electrochemical sharpening of the tip of the Pt-Ir wire, coating with an insulating HfO₂ film using atomic layer deposition (ALD), etching a small hole in the film using a focused ion beam (FIB), functionalization of the exposed Pt-Ir in the hole, and mounting in hole in PDMS membrane. Right: SEM image of sensor element (Pt-Ir wire) is coated with ALD HfO₂ and with a 50nm hole subsequently milled in the oxide with FIB.

Part of this work was performed at the nano@stanford site.

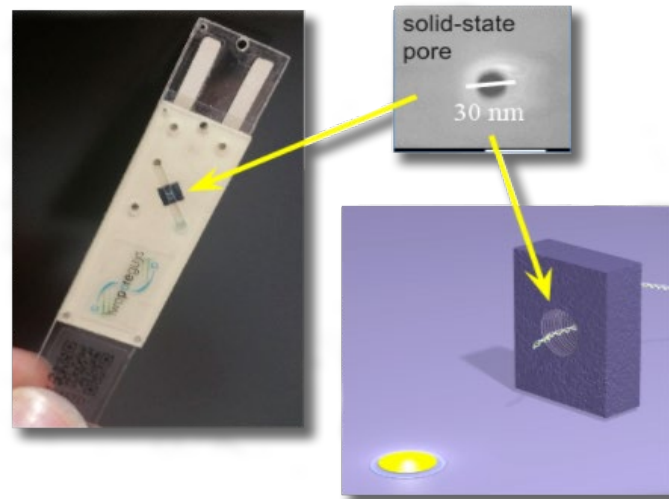
This work was supported by DoD SBIR Phase I, II

National Research Priority: NSF-Understanding the Rules of Life

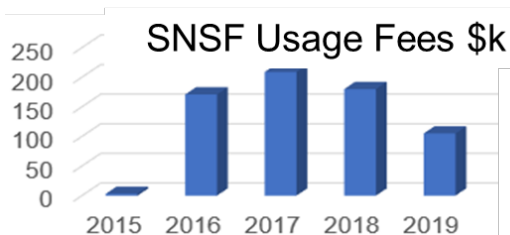
Ontera: Non-invasive Point of Care Diagnostic Technology

Ontera (formerly TwoPoreGuys) brings innovations in crop management technologies and catch devastating diseases early. Ontera's platforms use silicon nanopore chips and proprietary biochemistry to accurately detect and differentiate single molecules.

2011: Founded
2011: 2 employees
2013: \$150k SBIR
2015: joined [nano@stanford](#)
2016: ~40 employees
2016: \$475k SBIR
2016: \$5.2M Angel Round
2017: \$24.5M Series A
2017: ~60 employees
2018: \$2.8M Gates Foundation
2019: renamed to [Ontera](#)
2019: >100 employees



Ionic current change when DNA is driven through the pore



Access to [nano@stanford](#) facilities was especially crucial during the proof of concept phase for the company to develop their product, raise funding to sustain growth.

Part of this work was performed at the [nano@stanford](#) NNCI site.

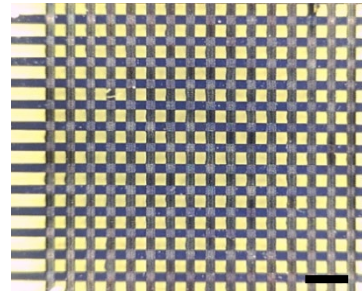
This work was supported by Department of Health and Human Services SBIR, Angel, VC, Gates Foundation

National Research Priority: NSF-Understanding the Rules of Life

Northwest Nanotechnology Infrastructure (NNI)

Perovskite Optoelectronics

Solution-processed metal halide perovskite materials are emerging as new optoelectronic materials with many appealing properties including high charge mobility, low defect densities, high optical absorption and emission efficiency. They also have unique features such as high color purity, tunable color emission, resistive and photo-memory effects. In the Lin Group at the University of Washington, we are pursuing perovskite LEDs with high brightness and perovskite lasers for integrated photonics. We are also investigating phototransistors, perovskite memristor arrays and photo-memory arrays for various applications.



Memristor array

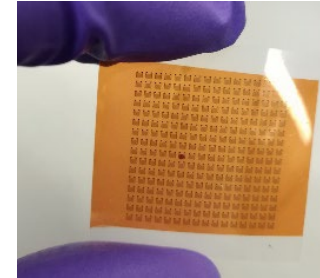
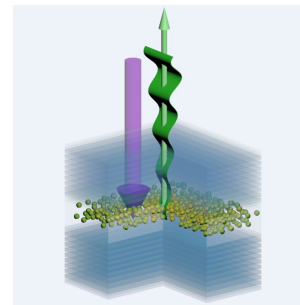
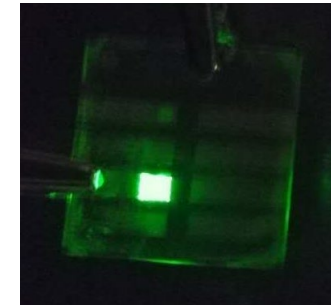


Photo-memory array



Laser



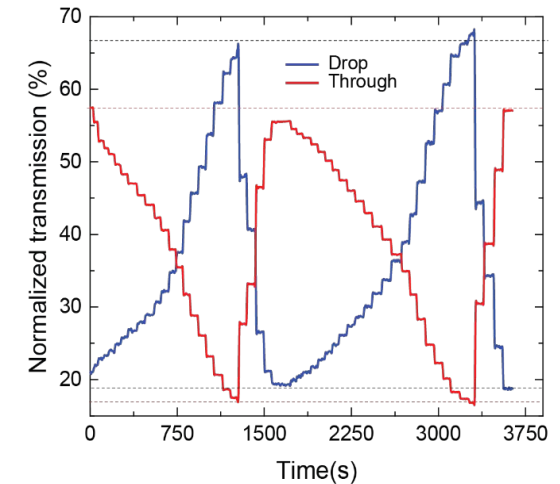
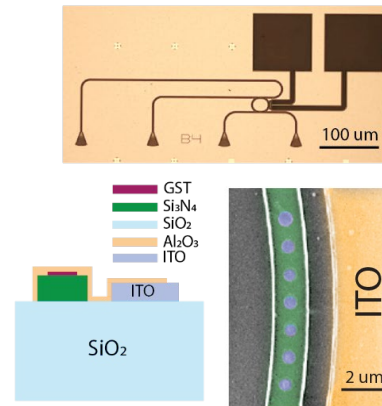
LED

Chen Zou, Cheng Chang, and Lih Y. Lin, Department of Electrical and Computer Engineering, University of Washington. Work performed at the Washington Nanofabrication Facility.

This work was supported by NSF Award # ECCS-1807397, IP Group and UW RRF. *Advanced Optical Materials* 6(14):180036 (2018), *Advanced Optical Materials* 7(18):1900558 (2019), *Physica Status Solidi RRL* 13(9):1900182 (2019).

Low-loss integrated photonic switch using sub-wavelength patterned phase change material

Efficient integrated photonic switches play a critical role in both interchip optical interconnects and data center networks that need to be dynamically reconfigured. The Mo Li Group at UW demonstrate a 1 x 2 switch using phase change material Ge-Sb-Te (GST) combined with a silicon nitride microring resonator. The switch operates by utilizing the dramatic difference in the optical refractive index and extinction coefficient between the crystalline and amorphous phases of GST. By patterning and encapsulating the GST into subwavelength structures, the device achieves a low insertion loss of less than 1 dB in both output ports and can be switched reliably both photothermally and electrothermally.



(Left) The image and Cross-sectional schematic of optical switch device. (Right) Realtime switching and resetting operation of the optical switch integrated with an ITO heater.

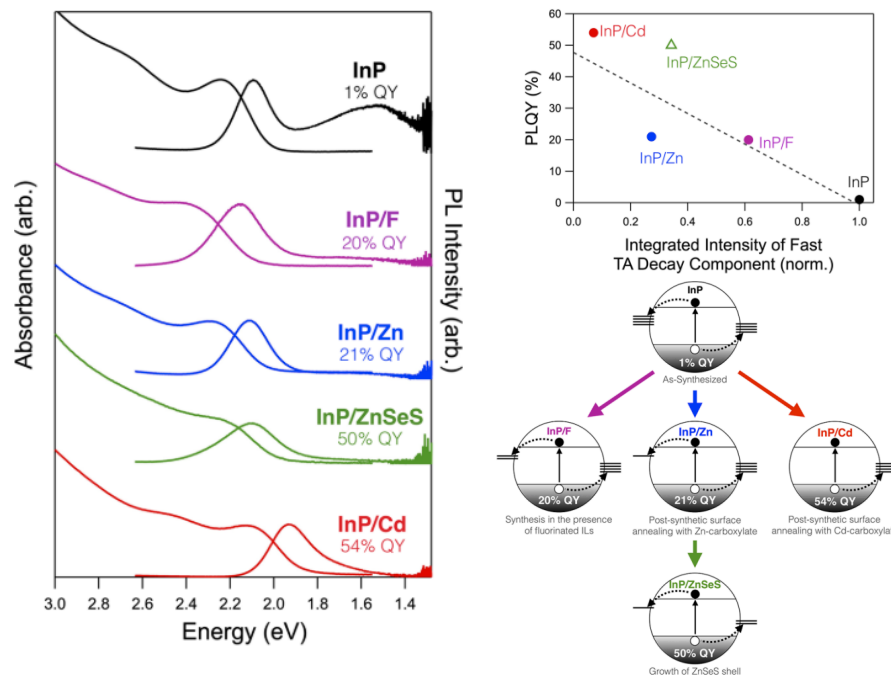
Changming Wu, Huan Li and Mo Li, Department of Electrical and Computer Engineering, University of Washington. Heshan Yu, Xiaohang Zhang and Ichiro Takeuchi, Department of Materials Science and Engineering, University of Maryland. Part of this work was performed at the Washington Nanofabrication Facility.

This work was supported by ONR MURI (N00014-17-1-2661). *ACS Photonics* (2018).

National Research Priority: NSF-Quantum Leap

Effects of Surface Chemistry on the Photoluminescence of Colloidal InP Nanocrystals

The Gamelin and the Cossairt groups are working to understand how the photoluminescent (PL) properties of indium phosphide nanocrystals is impacted by changes at the nanocrystal surface. Low PL is often the result of energetically accessible trap states which develop when ions at the surface are not well-passivated and stabilized. In this work, we synthesized a suite of InP nanocrystals with various surface modification and studied the resulting photophysical properties using ultrafast transient absorption and time resolved photoluminescent spectroscopies. This study revealed that the surface treatments are effective at passivating the electron traps, however the hole traps are not effectively addressed, indicating a limit on the PL enhancement that can be achieved through surface chemistry modification.



Left: Absorbance and PL spectra of surface-modified InP nanocrystals. Top: exciton PL quantum yields plotted as a function of the normalized integrated fast transient absorption bleach recovery. Bottom: effect of different surface chemistries on electron and hole trapping.

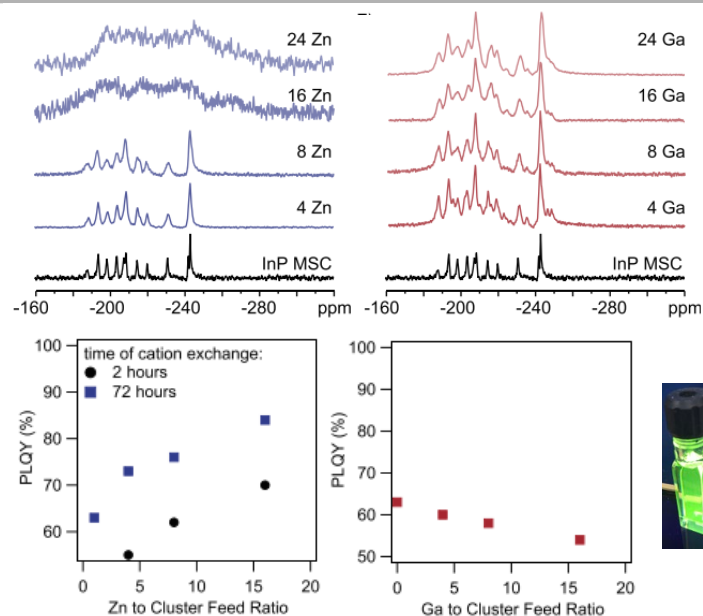
Kira E. Hughes, Jennifer L. Stein, Max R. Friedfeld, Brandi M. Cossairt, Daniel R. Gamelin, Department of Chemistry, University of Washington. Work performed at the Washington Molecular Analysis Facility.

This work was supported by NSF #NNCI-1542101 and #DMR-1719797. *ACS Nano*, 2019, doi: 10.1021/acsnano.9b07027.

National Research Priority: NSF-Quantum Leap

Effects of Zn^{2+} and Ga^{3+} doping on the quantum yield of cluster-derived InP quantum dots

The Cossairt lab is developing new synthetic methods to make highly photoluminescent indium phosphide nanomaterials. Molecular InP clusters are ideal single-source precursors and they can serve as tunable platforms to introduce cation dopants that can improve the resultant material properties. We have developed techniques to dope the clusters with Zn^{2+} ions, and these modified clusters are effective precursors to make highly luminescent core-shell quantum dots. Cation doping with Ga^{3+} ions is less effective at achieving highly luminescent materials. The difference in these two doping processes likely results from the aliovalency between Zn^{2+} and In^{3+} which enables high doping concentrations.



Top: ^{31}P NMR spectra for Zn^{2+} - and Ga^{3+} -doped InP clusters. Bottom: photoluminescent quantum yield of resulting nanomaterials, and a picture of a luminescent sample under UV irradiation.

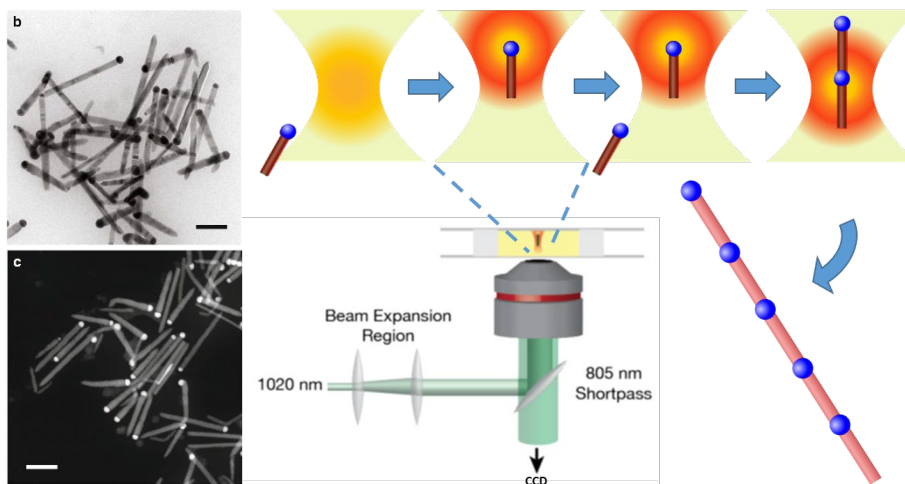
Max Friedfeld, Jennifer Stein, Dane Johnson, Nayon Park, Nicholas Henry, Michael Enright, Brandi Cossairt, Department of Chemistry, University of Washington. David Mocatta, Nanomaterials Group, Performance Materials, Merck Group. Work performed at the University of Washington, Molecular Analysis Facility.

This work was supported by NSF Award #NNCI-1542101 and #DMR-1719797. *J. Chem. Phys.* 2019, 151, 194702.

National Research Priority: NSF-Quantum Leap

Focused Laser Light Used to Manipulate and Assemble Colloidal Nanostructures in Solution

In 2018, single-beam laser tweezers were awarded the Nobel Prize in Physics due to their extraordinary ability to manipulate and control the position of materials in three dimensions using a focused beam of light. In the past year, the Pauzauskie and Holmberg groups at UW demonstrated the use of laser tweezers for the assembly of individual nanoscale building blocks into complex structures that cannot be made through conventional semiconductor growth methods. In particular, they used laser tweezers to organize semiconductor nanowires (NWs) into a linear chain connected by metallic soldering junctions. The metallic catalyst particles used to grow the NWs were also used to solder the NWs together into novel linear chains that have potential applications in sensors, energy conversion, and quantum information devices.



Focused laser light is used to generate an optical “tractor beam” that is used to manipulate and orient semiconductor nanorods (red) with metal tips (blue) in solution. The energy from the laser is then used to heat the metal tip on the end of the trapped nanorod, allowing the semiconductor nanorods to be aligned and welded together in a solution-based “nanosoldering” process.

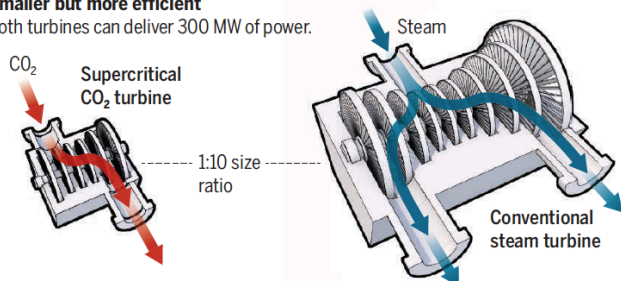
Matthew J. Crane, Elena P. Pandres, E. James Davis, Vincent C. Holmberg, and Peter J. Pauzauskie, Departments of Chemical Engineering and Materials Science and Engineering, University of Washington. Imaging work performed at the University of Washington Molecular Analysis Facility.

This work was supported by NSF ECCS-1506473 and DMR-1719797. *Nature Communications* 10, 4942 (2019).

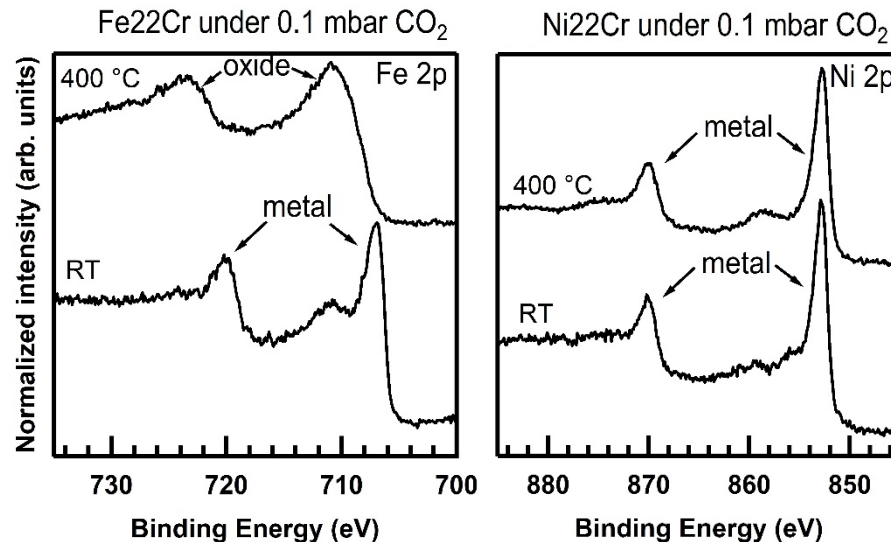
Revealing Alloy Corrosion Mechanisms in High-Temp. CO₂

- Next-generation power plants require structural alloys resistant to corrosion in high-temperature CO₂.
- Ambient-pressure X-ray photoelectron spectroscopy provides fundamental understanding of the reactive surface species beginning at the very initial stages of oxidation and allows development of corrosion-resistant and economical alloys.

Smaller but more efficient
Both turbines can deliver 300 MW of power.



L. Irwin, Y.L. Moullec, Science 356, 805 (2017)



AP-XPS spectra of model Fe-based and Ni-based alloys containing 22 wt% Cr during exposure to CO₂ at room temperature and 400 °C. The Fe-based alloy undergoes significant oxidation whereas the Ni-based alloy is completely unchanged at this temperature.

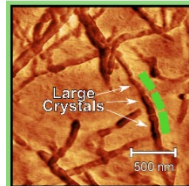
Richard P. Oleksak, National Energy Technology Laboratory. Work performed at Oregon State University Ambient Pressure Surface Characterization Laboratory.

National Research Priority: NSF-Growing Convergence Research

Morphological Insights into π -Conjugated Polymer Crystalline Domain Formation

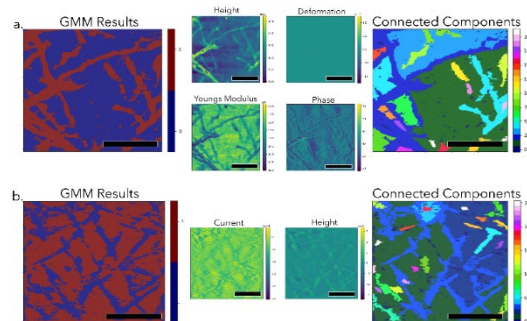
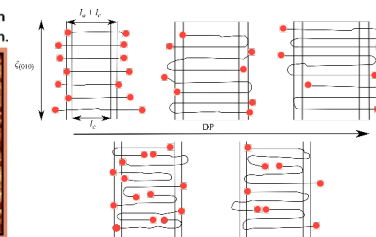
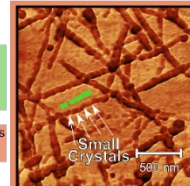
The performance of next-generation electronic materials is inextricably linked to their morphology, which describes the crystallinity, structure, and other physical descriptions of the material from the nanoscale to bulk material. The Luscombe group uses the poly(3-hexylthiophene) (P3HT) to probe the intrinsic properties of one such next-generation material, π -conjugated polymers. Synthesizing series of P3HT polymers with precisely distributed defects and allowing them to self-assemble into nanowires allows us to examine their crystalline state free of amorphous polymer. We determined nanowire dimensions and observed differences in crystalline domain sizes using Quantitative Nanomechanical Mapping (QNM). The electronic and viscoelastic properties were also mapped out using conductive atomic force microscopy (C-AFM) and amplitude-modulated, frequency-modulated bimodal AFM (AMFM).

Low-defect P3HT nanowires with "harmonic" (left) and "non-harmonic" (right) chain lengths. Chain length is used to tune end-group inclusion, frustrating crystal growth.



Chemical Defects:

- Are readily incorporated into the crystal lattice
- Aromatic end-groups promote short-range order
- Slow crystal growth kinetics
- Disrupt short-range order



(Top Left) QNM visualized effects of end-group incorporation on crystal growth (Top Right) P3HT folding and stacking structures expected from QNM and bulk characterization. (Bottom) P3HT Nanowires visualized with AMFM and C-AFM (top and bottom rows, respectively), and their image segmentation results. The plotted domain maps can also be used to rapidly analyze different morphological characteristics.

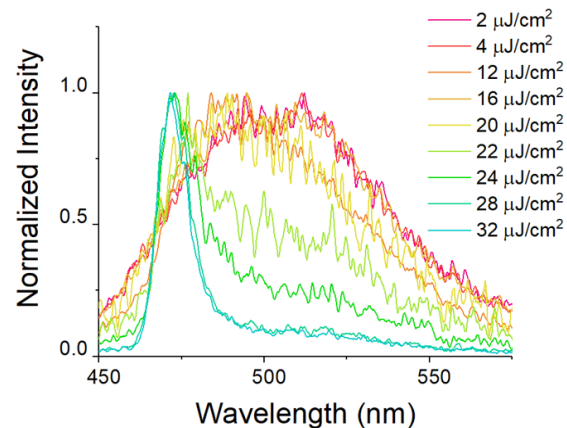
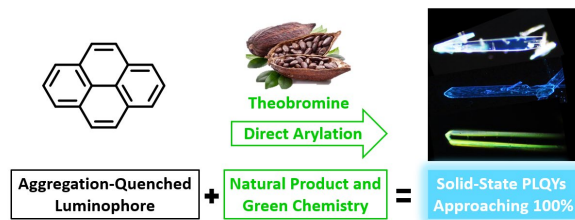
Wesley Tatum, Lucas Q Flagg, Anton Resing, David S Ginger, Christine K Luscombe, Depts. of Materials Science and Engineering, Chemistry, Molecular Science and Engineering, University of Washington. Work performed and the Molecular Analysis Facility.

This work was supported by NSF ECCS-1542101, DMR-1708317, DMR-1607242. *ACS Appl. Polym. Mater.* 2019, 1, 1466–1475.

National Research Priority: NSF-Harnessing the Data Revolution and Growing Convergence Research

Theobromine and direct arylation: a sustainable and scalable solution to minimize aggregation caused quenching

The Luscombe Group in UW focuses on developing sustainable synthesis methodologies for organic semiconductors. In this project, we utilized green chemistry (direct arylation) and natural products (theobromine and caffeine) to synthesize novel organic semiconductors with minimized aggregation caused quenching, to further enhance the luminescence performance of final devices. We used the ultrafast pulse laser in Molecular Analysis Facility to investigate the excited state kinetics of these new materials. This experiment allowed us to determine the amplified spontaneous emission (ASE) threshold of these materials and explore their potentials in organic lasers. An optimal threshold of $20 \mu\text{J cm}^{-2}$ was obtained, verifying the efficacy of this novel synthesis.



(Top) Graphic illustration of this project. (Bottom) Determination of ASE threshold with assistance of an ultrafast laser. ASE threshold is indicated by the sudden narrowing of the emission spectrum, which occurs at $20 \mu\text{J cm}^{-2}$ for this system.

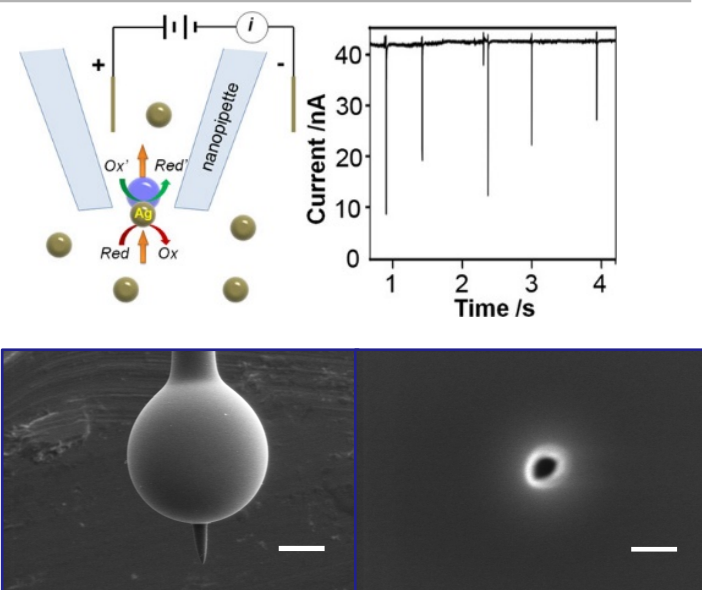
Yunping Huang and Christine K. Luscombe, Materials Science and Engineering, Univ. of Washington. Yun Liu, Parker J. W. Somerville, Werner Kaminsky and David S. Ginger, Chemistry, Univ. of Washington. Work performed at the Molecular Analysis Facility.

This work was supported by NSF CHE-1700982, DMR-1719797, DGE-1633216 and ONR #N00014-17-1-2201. *Green Chem.*, 2019,

National Research Priority: NSF-Growing Convergence Research

Observing Transient Bipolar Electrochemical Coupling on Single Nanoparticles Translocating through a Nanopore

We have observed transient bipolar electrochemical coupling on freely moving 40 nm silver nanoparticles translocating through both pulled nanopipettes and nanopores milled with a focused ion beam (FIB) in blown glass microbulbs (pictured at right). The use of an asymmetric nanoelectrochemical environment at the nanopore orifice, for example, an acid inside the pipette and halide ions in the bulk, enabled us to observe unusually large current blockages of single Ag nanoparticles. We attribute these current blockages to the formation of H_2 nanobubbles on the surface of Ag nanoparticles due to the coupled faradaic reactions, in which the reduction of protons and water is coupled to the oxidation of Ag and water under potentials higher than 1 V. The appearance of large current blockages was strongly dependent on the applied voltage and the choice of anions in the bulk solution. The correlation between large current blockages with the oxidation of Ag nanoparticles and their nanopore translocation was further supported by simultaneous fluorescence and electric recordings. This study demonstrates that transient bipolar electrochemistry can take place on small metal nanoparticles below 50 nm when they pass through nanopores where the electric field is highly localized. The use of a nanopore and the resistive-pulse sensing method to study transient bipolar electrochemistry of nanoparticles may be extended to future studies in ultrafast electrochemistry, nanocatalyst screening, and gas nucleation on nanoparticles.



(Top Left) Schematic of bipolar coupling occurring on a translocating Ag nanoparticle. (Top Right) Representative *i-t* trace of several current blockage events. (Bottom) A blown glass microbulb (Left) and FIB-milled nanopore (Right).

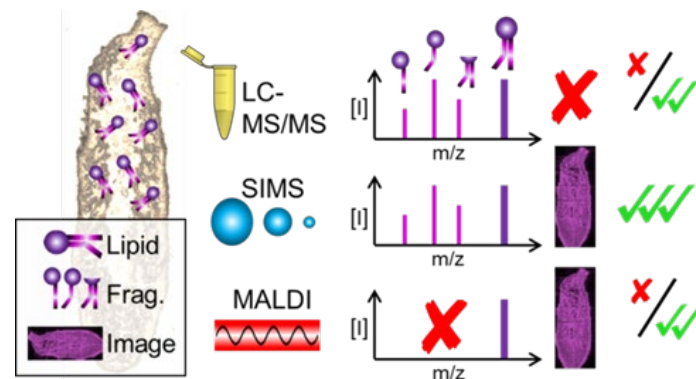
Chu Han, Rui Hao, Yunshan Fan, Martin A. Edwards, Hongfang Gao, and Bo Zhang. Parts of this work were carried out at the Molecular Analysis Facility.

This work was supported by NSF ECCS-1506473 and AFOSR MURI (FA9550-14-1-0003). *Langmuir* 2019, 35, 7180-7190.

National Research Priority: NSF-Growing Convergence Research

Exploiting the semi-destructive nature of GCIB-ToF-SIMS imaging for simultaneous localization and confident lipid annotations

Lipids have been recognized as key players in cell signaling and disease. Information on their location and distribution within a biological system, under varying conditions, is necessary to understand the contributions of different lipid species to an altered phenotype. The lack of location specific and lipid specific analysis methods makes interpreting lipid function difficult. Using planarian flatworms as a model system, in our recent article we demonstrate that imaging gas cluster ion beam (GCIB)-ToF-SIMS has the unique capability to simultaneously structurally identify and image detectable lipid species with sub-cellular resolution in a sample within one experiment. This was accomplished by correlating intact lipids and associated fragments in SIMS-images. The lipid assignments, respective fragment identities, and locations gathered from ToF-SIMS data were confirmed via LC-MS/MS on lipid extracts and ultra-high mass resolution MALDI-MS imaging. Together, these data show that the semi-destructive nature of ToF-SIMS can be utilized advantageously to enable both confident molecular annotations and to determine the locations of species within a biological sample.



Scheme displaying the depth of information provided by different techniques for lipid analysis.

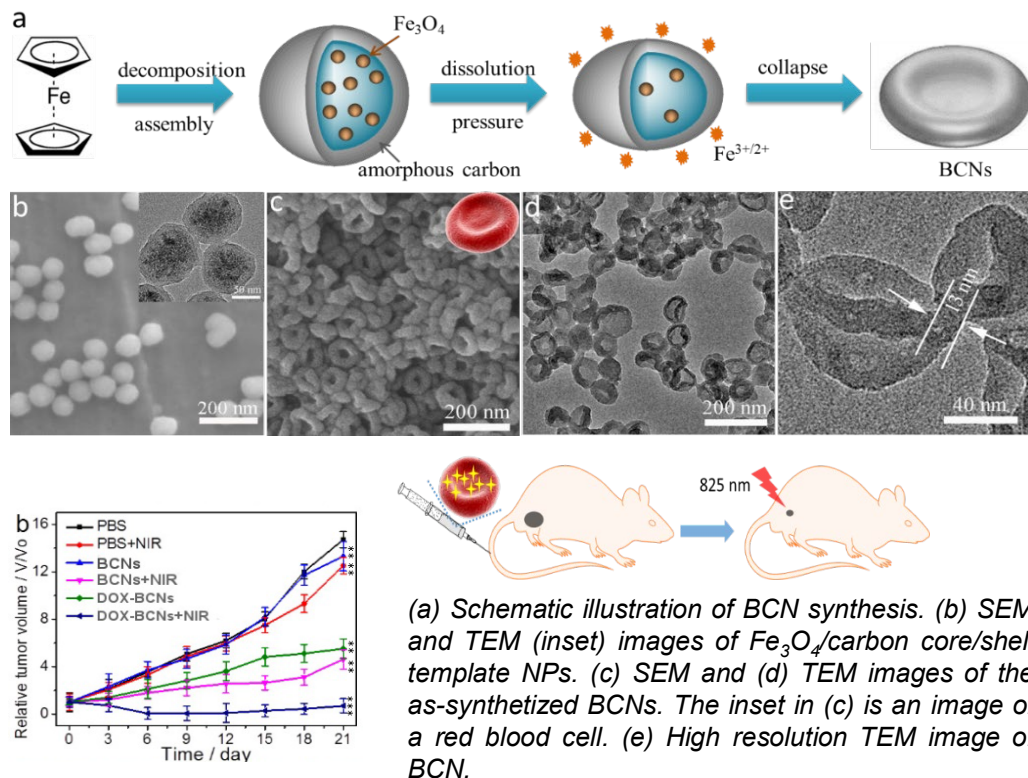
Tina B. Angerer, Dusan Velickovic, Carrie D. Nicora, Jennifer E. Kyle, Daniel J. Graham, Christopher Anderton, Lara J. Gamble, NESACBIO, Univ. of Washington, Dept. of Bioengineering, Univ. of Washington, Earth and Biological Sciences Directorate, Pacific Northwest National Laboratory. This work was performed at the NNI.

This work was supported by NSF NNCI-1542101 and NESACBIO NIH P41 (EB002027). *Analytical Chemistry*, DOI:10.1021/acs.analchem.9b03763(2019).

National Research Priority: NSF-Understanding the Rules of Life

Biconcave Carbon Nanodisk for Enhanced Drug Accumulation and Chemo-photothermal Tumor Therapy

The Zhang group at UW has developed a biconcave carbon nanodisk (BCN) as a versatile platform that can provide fluorescent imaging, near-infrared (NIR)- and pH-responsive drug release, as well as combined photothermal- and chemo-therapy. BCNs show a greater accumulation in tumors in mice than its carbon nanosphere (CNS) counterpart. Furthermore, BCNs absorb and convert NIR light to heat, which enables NIR-responsive drug release and photothermal- and chemo-therapy. Significantly, systemic administration of DOX-loaded BCNs combined with NIR irradiation demonstrates a complete suppression of tumor growth in a mouse model of triple-negative breast cancer tumor.



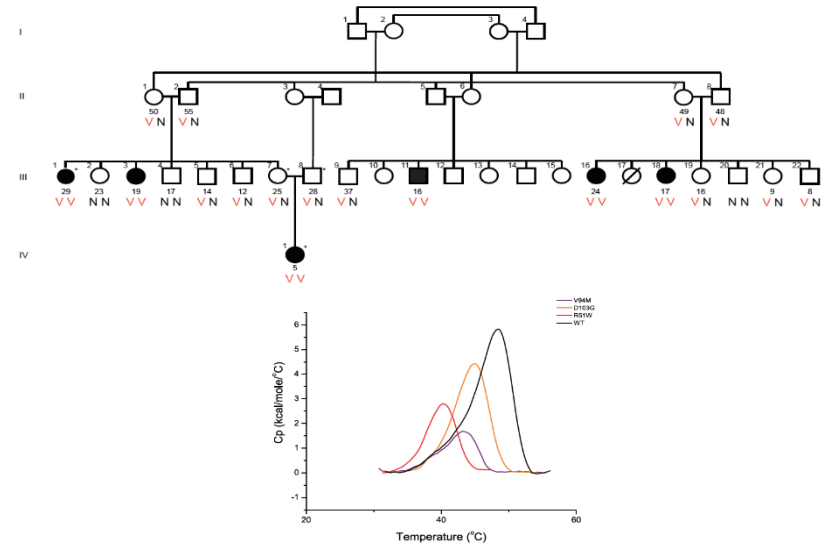
Qingxin Mu, Hui Wang, Xinyu Gu, Zachary R. Stephen, Charles Yen, Fei-Chien Chang, Christopher, J. Dayringer, and Miqin Zhang. This work was performed at University of Washington.

This work was supported by NIH (R01CA161953 and R01EB026890), and NSF (NNCI-1542101). *Advanced Healthcare Materials*, in press (2019).

National Research Priority: NSF-Understanding the Rules of Life

Inherited Thrombocytopenia Associated with Mutation of UDP-Galactose-4-Epimerase (GALE)

Severe thrombocytopenia, characterized by dysplastic megakaryocytes and intracranial bleeding, was diagnosed in six individuals from a large kindred. Whole genome sequencing revealed one candidate mutation segregating with thrombocytopenia under a recessive model: GALE Arg51Trp. This mutation is extremely rare worldwide and the likelihood of the observed co-segregation occurring by chance is 1.2×10^{-06} . GALE encodes UDP-galactose-4-epimerase, an enzyme of galactose metabolism and glycosylation responsible for interconversion of UDP-galactose with UDP-glucose, and of UDP-N-acetylgalactosamine with UDP-N-acetylglucosamine. Mutations in GALE have not previously been associated with thrombocytopenia. GALE Arg51Trp alters an amino acid residue that is conserved from yeast to humans. GALE Arg51Trp has significantly reduced enzymatic activity for both interconversion reactions. Differential scanning calorimetry revealed highly significant thermal instability of the mutant protein ($P = 4.8 \times 10^{-9}$). Proper glycosylation is critical to normal hematopoiesis, in particular to megakaryocyte and platelet development. Our results suggest that GALE Arg51Trp is inadequate for normal glycosylation and therefore that GALE may play a critical role in hematopoiesis.



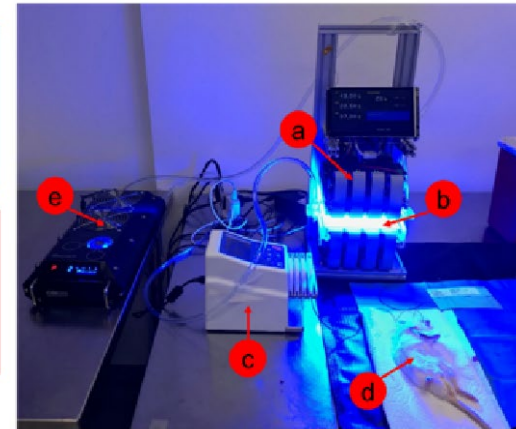
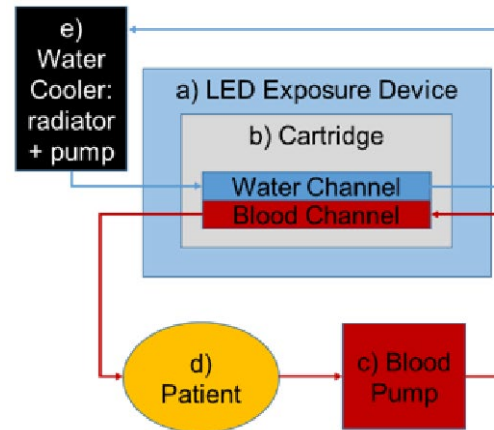
(Top) Extended family with severe thrombocytopenia (filled symbols). V represents the variant allele GALE Arg51Trp; N represents the normal GALE allele. (Bottom) Endotherm plots for GALE Arg51Trp (red) and two GALE alleles (purple and orange) known to cause other severe disorders of glycosylation. Thermal instability is most severe for GALE Arg51Trp. Endotherm data was normalized for protein concentration, with intrascan baseline correction.

Aaron Seo and Mary-Claire King, Dept. of Medicine, University of Washington. Work partially performed at the UW Molecular Analysis Facility.

This work was supported by NIH R24DK099808, R35CA197458, F30DK103462, and T32HD007183, and NSF ECCS-1506473. *Human Molecular Genetics* 28,133-142 (2019)

Microfluidic Photoreactor for Treatment of Hyperbilirubinemia

Over half of newborns suffer from jaundice, a condition characterized by high levels of bilirubin in the blood that can have devastating consequences including brain damage, seizures and death. Whole-body phototherapy is currently used for light-catalyzed conversion of bilirubin to nontoxic products, but this process is limited by light penetration into the skin and is too slow to prevent brain damage in extreme cases of jaundice. This project focuses on the development of a microfluidic photoreactor for extracorporeal treatment of blood to safely and rapidly reduce bilirubin levels.



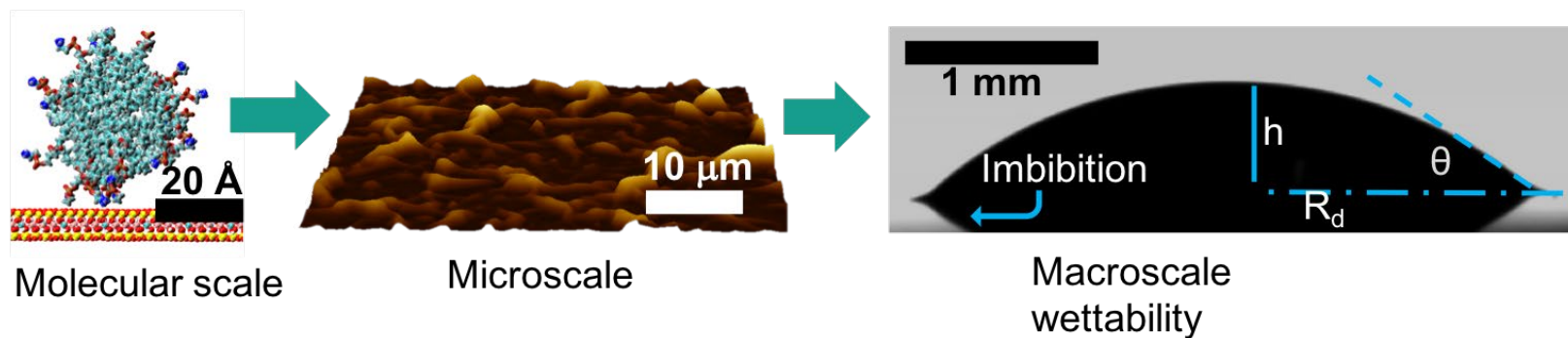
Schematic view and corresponding experimental setup for rat treatment. The LED exposure device (a) consists of a top and bottom array of LED lights.

Joe Baio, Adam Higgins and Kate Schilke. School of Chemical, Biological and Environmental Engineering, Oregon State University. Work performed at OSU NNCI site.

This work was supported by NIH Award # 5R21HD096301.

Finding the causes of soil water repellency in simple model systems

While it is known that soil water repellency is induced by organic matter, the exact mechanisms controlling soil hydrophobicity remain largely a mystery. Our work demonstrates that the distribution of lipids in a model film is the primary control on water imbibition into the film. The chemistry of the lipids themselves also has a large effect on water flow: lipids which bind to the mineral surface, are solid at room temperature, and evenly spread through the sample cause the largest changes in wettability.



Brenda L. Kessenich, Nihit Pokhrel, Elias Nakouzi, Christina J. Newcomb, Markus Flury, Lutz Maibaum, James J. De Yoreo, Depts. of Chemistry and Materials Science, Univ. of Washington, PNNL Physical Sciences Division, and Washington State Univ., Dept. of Crop and Soil Sciences. Work performed at NNI.

This work was supported by NSF ECCS-1506473, NSF Graduate Research Fellowship Program DGE-1762114, and BES Chemical Sciences, Geosciences, and Biosciences Division. *JCIS* 2019.

National Research Priority: NSF-Growing Convergence Research

Research Triangle Nanotechnology Network (RTNN)

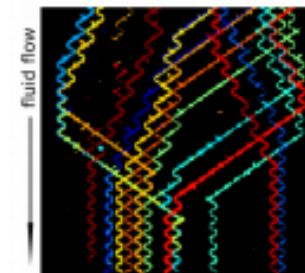
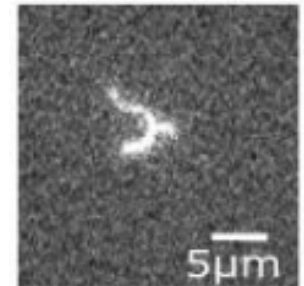
Nanoplumbing with 2D Materials

- Development of nanofluidic devices with distributed network of channel junctions, a 2D material, that enable complex manipulation of DNA. Useful for genetic mapping applications and interrogation of DNA-protein interactions.
- Controlled flow speed through device such that molecules traveled along intersecting but quasi-ballistic paths
- Generated model of DNA dynamics at a nanochannel junction that can be used in the design and optimization of future devices for specific applications
- System design may enable on-chip DNA preparation and modification by controlling DNA and liquid buffer transport through device



A junction of two nanochannels induces folded configurations of DNA molecule

A fluorescence micrograph of a DNA molecule at a nanochannel junction



Overlaid collection of multiple DNA molecules' transport through large-area device

Saroj Dangi and Robert Riehn, Department of Physics, NC State University. Work performed at the NCSU Nanofabrication Facility and Analytical Instrumentation Facility & Georgia Tech Institute for Electronics and Nanotechnology.

Work supported by the NSF (DBI-1353897) and NIH (R01GM107559). *Small*, 15 (2019).

National Research Priority: NSF-Understanding the Rules of Life

Platelet-inspired nanocells (PINCs) for targeted heart repair

- PINCs designed to address limitations of stem cell therapy: poor cell retention and targeting ability
- PINC core: cardiac stromal cell-secreted factors (e.g. growth factors) encapsulated in poly(lactic-co-glycolic acid)
- PINC shell: platelet membrane decorated with prostaglandin E2 (PGE₂)
 - Targets damaged blood vessels and heart muscle
 - Facilitates tissue repair through PGE₂/EP receptor signaling
- In mouse heart attack model, PINC therapy restored heart's pumping function by promoting growth of cardiac cells and vasculature and activating endogenous stem/progenitor cells

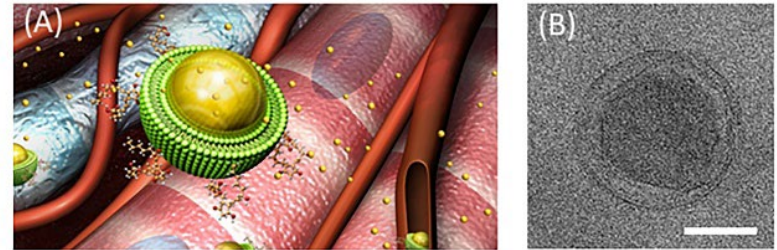
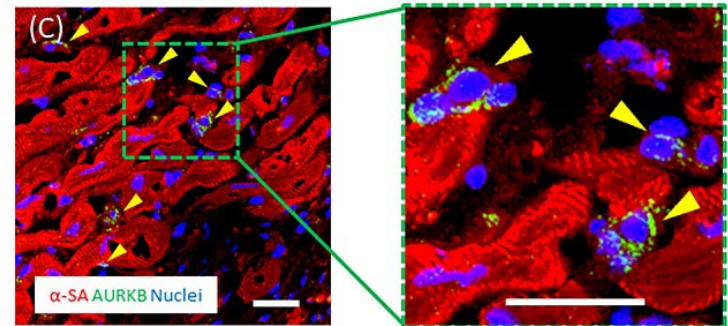


Illustration (A) and transmission electron micrograph (B) showing PINC structure. Scale bar: 100 nm



Fluorescent micrographs of cardiac muscle cells stained for cytokinesis marker (AURKB) in damaged regions of PINC-recipient mouse hearts 4 weeks post-treatment. Scale bar: 20 μ m

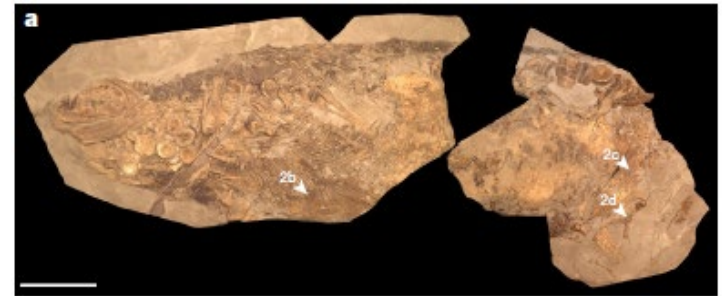
Teng Su, Ke Huang, Hong Ma, Frances Ligler, & Ke Cheng, Joint Department of Biomedical Engineering, UNC-Chapel Hill and NC State University. Work performed at NCSU Analytical Instrumentation Facility.

Work supported by NIH (R01 HL123920 and HL137093) and American Heart Association (18TPA34230092). *Adv. Funct. Mater.*, 29 (2019).

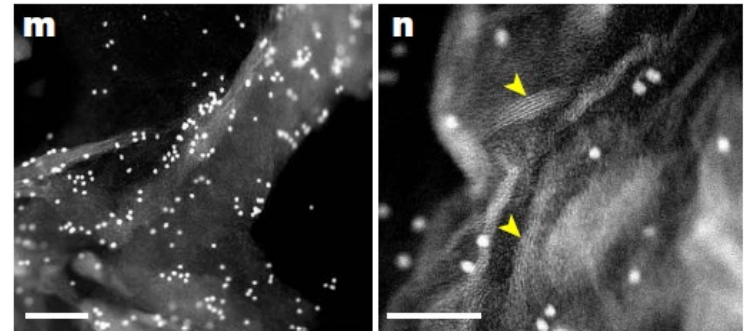
National Research Priority: NSF-Understanding the Rules of Life, NAE Grand Challenge-Engineer Better

Soft-tissue evidence for homeothermy and crypsis in a Jurassic ichthyosaur

- Nanoscale chemical and structural evaluation of a well-preserved specimen of the Early Jurassic ichthyosaur *Stenopterygius*
 - Ichthyosaurs resemble dolphins but more closely related to lizards
- Investigated skin at cellular and molecular level and identified features characteristic of modern warm-blooded marine mammals
 - e.g. structure of skin: epidermal and dermal layers underlain with blubber
- Led to better understanding of evolution in this group of animals and how other animals made the transition from terrestrial habitats to marine environments at the molecular level



Photograph of *Stenopterygius* specimen



Low-magnification (m) and high-magnification (n) immunogold labeling of keratin in ichthyosaur skin fibers. Scale bars: 100 nm (n), 200 nm (m)

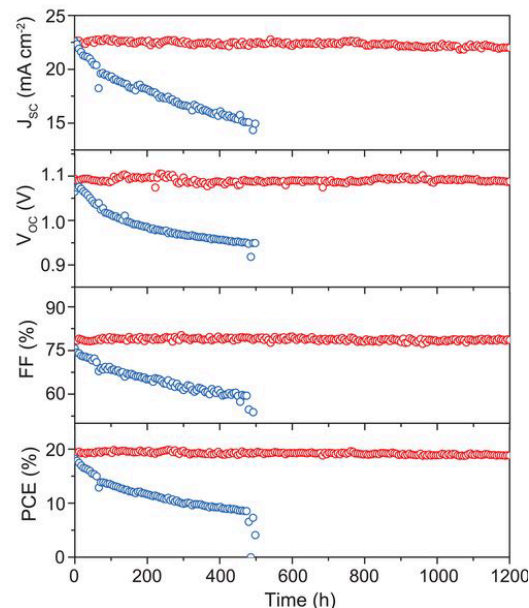
Wenxia Zheng and Mary Schweitzer, Department of Biological Sciences, NC State University; Johan Lindgren, Department of Geology, Lund University. Work performed at NCSU Analytical Instrumentation Facility.

Work supported by NSF INSPIRE grant (EAR-1344198). *Nature*, 564 (2018).

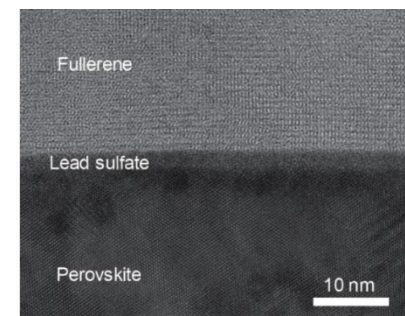
National Research Priority: NSF-Understanding the Rules of Life

Stabilizing perovskite surfaces of solar cells

- Perovskite solar cells face long-term instability issues under operating conditions
- Conversion of surfaces from lead halide perovskite to water-insoluble lead (II) oxysalt can stabilize surface and bulk material
- Oxysalt thin layers
 - Enhance water resistance and reduce defect density
 - Boost (by 21%) and maintain efficiency of solar cells



Stability test of encapsulated solar cell devices based on **control** and **sulfate-treated** perovskite active layers



Cross-section HR-TEM image of perovskite device

Shuang Yang, Shangshang Chen, and Jinsong Huang, Department of Applied Physical Sciences, UNC-Chapel Hill. Work performed at the Chapel Hill Analytical and Nanofabrication Laboratory.

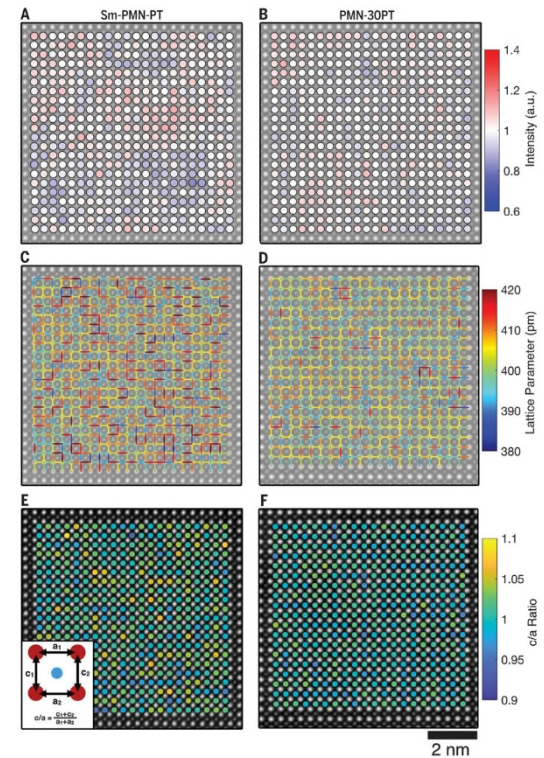
Work supported by the NSF (CBET-1437656), ONR (N00014-17-1-2727), and AFOSR (A9550-16-1-0299). *Science*, 365 (2019).

National Research Priority: NAE Grand Challenge-Make Solar Energy Economical

Giant piezoelectricity of Sm-doped $Pb(Mg_{1/3}Nb_{2/3})O_3$ - $PbTiO_3$ single crystals

- High-performance piezoelectrics benefit transducers and sensors in a variety of applications but progress toward improving piezoelectric responses has been slow
- New process used to grow Sm-doped $Pb(Mg_{1/3}Nb_{2/3})O_3$ - $PbTiO_3$ (Sm-doped PMN-PT) single crystals
- Resulting crystals had high piezoelectric coefficients (3400 to 4100 picocoulombs per newton, double that of undoped PMN-PT) and exhibited good property uniformity
- Strategy enlarged the usable portion of the crystals, which can improve reliability for piezoelectric devices requiring large crystal wafers with minimal variation in properties

Image: Atomic-resolution HAADF-STEM images for Sm-doped PMN-PT and PMN-30PT crystals recorded along the [010] crystallographic direction.



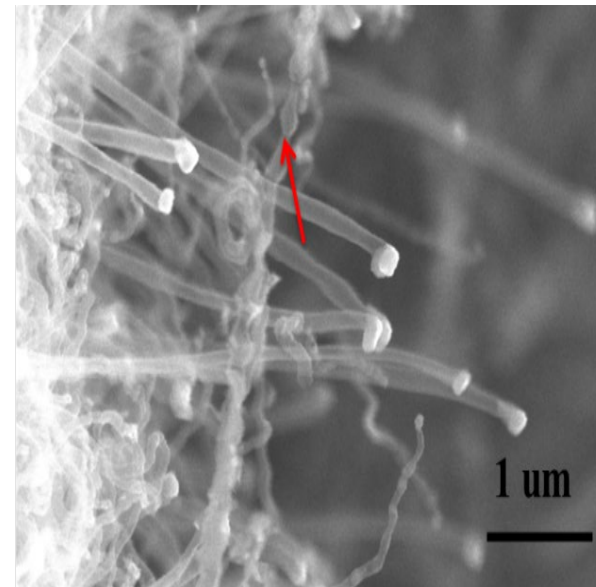
Matt Cabral, Elizabeth Dickey, and Jim LeBeau, Department of Materials Science and Engineering, NC State University. Work performed at NCSU Analytical Instrumentation Facility.

Work supported by the NSF (DGE-1633587, IIP-1361571, IIP-1361503). *Science*, 364 (2019).

*National Research Priority: NSF-Future of Work at the Human-Technology Frontier
And NAE Grand Challenge-Advance Health Informatics*

Melamine as a single source for fabrication of mesoscopic 3D composites of N-doped carbon nanotubes on graphene

- Integration of two-dimensional graphene and one-dimensional carbon nanotubes (CNTs) to create potentially useful 3D mesoscopic carbon structures
- Use simple chemical vapor deposition (CVD) methods to fabricate bead-like nitrogen-doped CNT/graphene composites (NCNT/G) via a simple pyrolysis of the N-rich melamine in the presence of graphene oxide (GO) as a substrate using a Mn–Ni–Co ternary catalyst
- These bead-like N-doped CNTs (red arrow in figure) are vertically organized on the GO nanoplates yielding a 3D structure.
- Three dimensional NCNT/G hybrids have unique network structures, moderate graphitization, high specific surface area, good mesoporosity, and N doping, which makes them promising materials for applications in energy storage and



SEM image of NCNT-G (the red arrow refers to the bead-like NCNT)

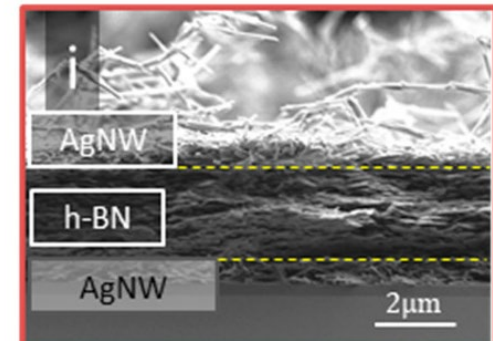
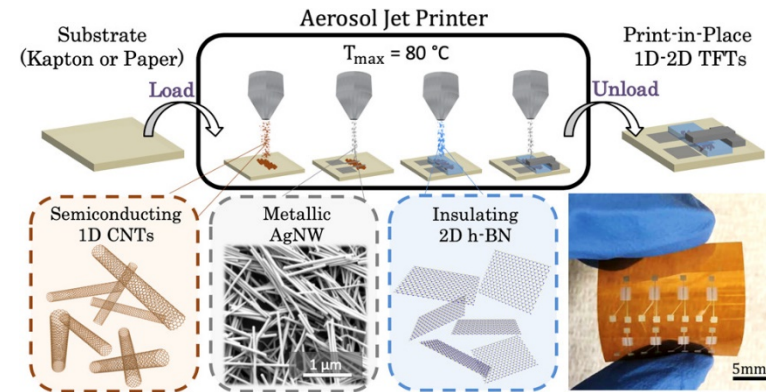
Xiao-Ling Yan, School of Resources Environmental & Chemical Engineering, Nanchang University; Gui-Ping Dai and K. Vinodgopal, Department of Chemistry and Biochemistry, North Carolina Central University. Work performed at the Chapel Hill Analytical and Nanofabrication Laboratory.

Work supported by the NSF (HRD-0833184, DMR-1523617). *RSC Adv*, 8 (2018).

National Research Priority: White House FY 2021 Administration Research and Development Budget Priorities

Flexible, Print-in-Place 1D–2D Thin-Film Transistors Using Aerosol Jet Printing

- Semiconducting carbon nanotubes (CNTs) printed into thin films offer high electrical performance, significant mechanical stability, and compatibility with low-temperature processing but implementation has been hindered by high process temperature requirements imposed by other device layers
- Can overcome temperature constraints and demonstrate 1D–2D thin-film transistors (1D–2D TFTs) in a full print-in-place process using an aerosol jet printer
 - Semiconducting 1D CNT channels used with a 2D hexagonal boron nitride (h-BN) gate dielectric and silver nanowires as conductive electrodes
- 1D–2D TFTs exhibit mechanical stability under bending, with minimal changes in performance after 1000 bending test cycles at 2.1% strain



Top: Overview of printing process
Bottom: SEM cross-sectional image of AgNW/h-BN/AgNW stack

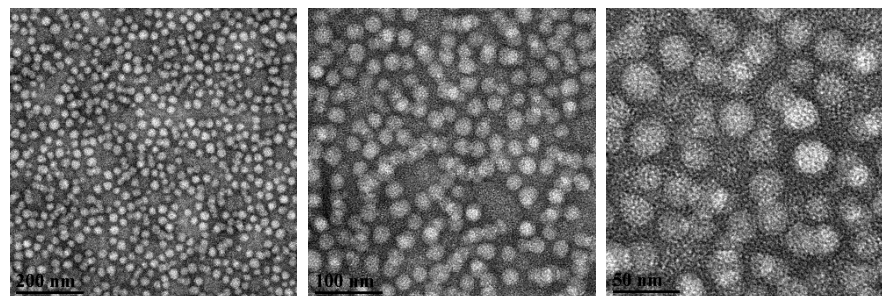
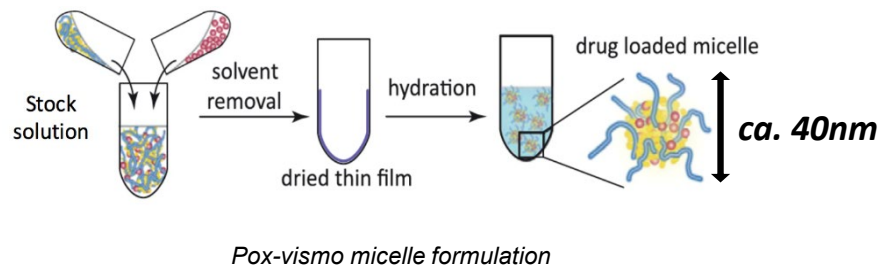
Shiheng Lu, Jorge Cardenas, and Aaron Franklin. Department of Electrical and Computer Engineering, Duke University. Work performed at Duke's Shared Materials Instrumentation Facility.

Work supported by the US Army (W81XWH-17-2-0045) and NIH (1R01HL146849). *ACS Nano*, 13 (2019).

National Research Priority: NNI Signature Initiative-Sensors and NAE Grand Challenge-Advance Health Informatics

Poly(2-oxazoline) micelles as personalized drug carriers for brain tumors

- Polymeric micelles based on amphiphilic poly(2-oxazoline) block copolymers can help in delivery of poorly soluble uncharged drugs
- Used thin film method to prepare mixture of the chemotherapeutic vismodegib and dehydrated polymer in aqueous medium to spontaneously form nano-sized polymeric micelles (POx-vismo)
- Nanoparticle formulation allows high drug loading capacity, sustained drug release, enhanced drug stability, and enhanced drug exposure *in vivo* with improved therapeutic outcome of the drug



TEM micrographs of POx-vismo. (Scale: 200 nm (left), 100 nm (middle), 50 nm (right))

Duhyeong Hwang, Alexander Kabanov, and Marina Sokolsky, Eshelman School of Pharmacy, UNC-Chapel Hill. Work performed at the Chapel Hill Analytical and Nanofabrication Laboratory.

Work supported by NCI (U54CA198999) and NINDS (R01NS088219, R01NS102627). *Neuro-Oncology*, 21 (2019).

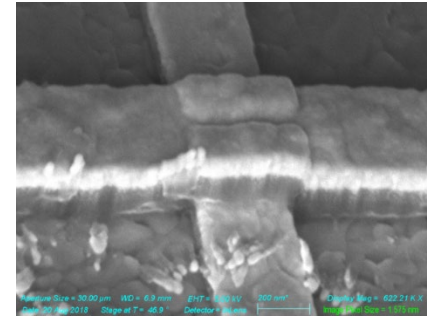
National Research Priority: NAE Grand Challenge-Engineer Better Medicines

San Diego Nanotechnology Infrastructure (SDNI)

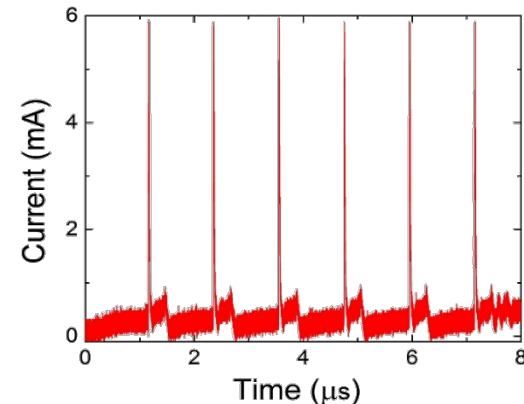
Quantum Materials for Energy Efficient Neuromorphic Computing

The development of a machine that works like the brain is one of the great challenges presented recently to science and technology. This requires the development of **energy-efficient quantum-materials based devices which emulate biological devices** such as neurons, synapses, axons and dendrites. We have developed recently a so called “neuristor” i.e. a solid state device that emulates a spiking neuron. This allows the use of the internal degrees of freedom of **strongly correlated quantum materials to emulate the complex behavior of biological neurons**, which will be the basis of an Energy Efficient Neuromorphic Computer.

Quantum materials



Spiking in a VO_2 nano “neuristor”



Javier del Valle, Pavel Salev, Federico Tesler, Nicolás M. Vargas, Yoav Kalcheim, Paul Wang, Juan Trastoy, Min-Han Lee, George Kassabian, Juan Gabriel Ramírez, Marcelo J. Rozenberg and Ivan K. Schulle. Work performed at SDNI.

This work was supported by NSF ECCS-1542148, DOE, Office of Science, Basic Energy Sciences DE-SC0019273. *Nature*, 569, 388–392, 2019.

National Research Priority: NSF-Growing Convergence Research, Quantum Leap

Fabrication of Starshade Mask for Detection of Earth-Like Planet by NASA

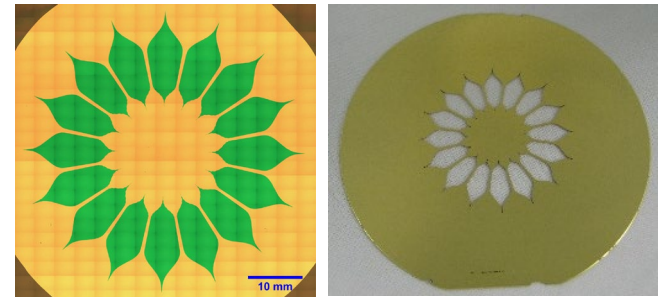
Starshade (or External Occulter) is a starlight suppression technology proposed by NASA for high contrast imaging of exoplanets within the habitable zones, the regions where liquid water can be sustained on the planets' surfaces.

Before manufacture and launch of a full-sized starshade into space, theoretical modeling and experimental validation with small-scale starshade masks are critical for a successful mission.

SDNI was chosen by JPL/NASA to fabricate small-scale starshade masks to be used at Princeton Starshade Testbed because SDNI's unique capability of manufacturing SOI wafers with PECVD stress-free SiO₂ and thick (>1 μ m) amorphous Si films has shortened the prototyping development time and most importantly, **provided JPL/NASA a unique opportunity to quantify and reduce polarization effects.**



Starshade blocking starlight from a nearby planetary system



Starshade masks to be used at Princeton Starshade Testbed. Device was designed by Jet Propulsion Laboratory and fabricated by SDNI staff engineers.

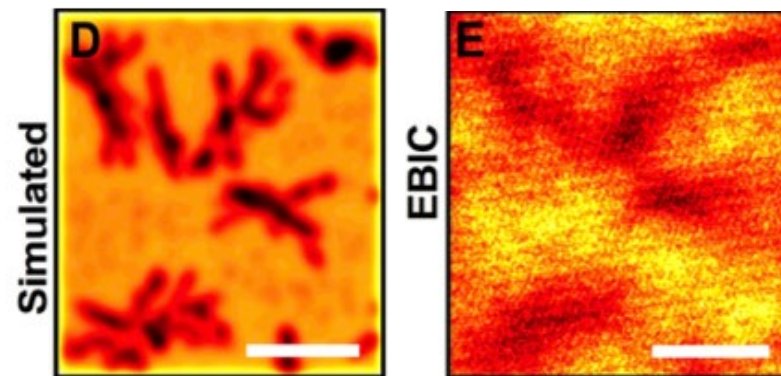
This work was supported by Jet Propulsion Laboratory/NASA

National Research Priority: NSF-Windows on the Universe, NSF 2026

Discoveries in Organic-Inorganic Perovskite Materials

The hybrid perovskite materials offer disruptive potential to replace existing solar cell, lighting, and display technology at lower cost. The research by Prof. Fenning uncovered the mechanisms of material degradation and proposed techniques as promising solutions.

The typical perovskite absorber adopts the ABX₃ crystal structure, but mixing on the A- and X-sites creates a challenge in producing a homogeneous high-optoelectronic quality film. It was discovered that through incorporation of additional alkali salts such as CsI and RbI, we can homogenize the halide sublattice in the perovskite film, yielding spatially-uniform fast carrier dynamics, longer lived charge carriers, and ultimately higher solar cell efficiencies and likely the improved stability.



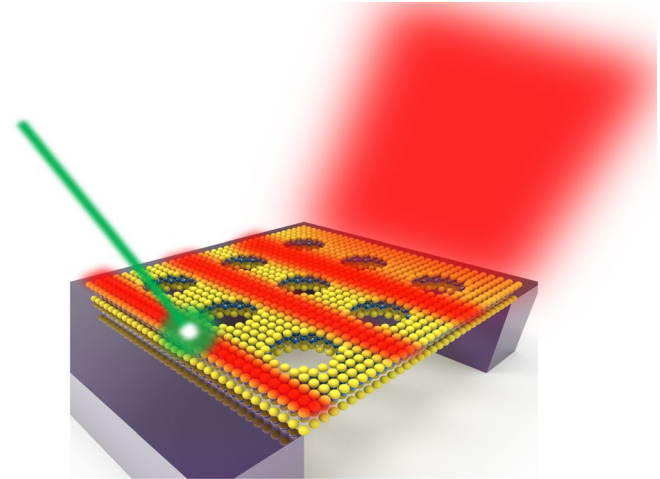
Simulated and experimental plan-view E-beam induced current (EBIC) measurement reveal that the Rb-rich clusters are recombination active.

This work was supported by NSF DMR-1507803, GRFP 1122374, CHE-1338173, DOE DE-AC02-06CH11357, DOE DE-SC0001088,. *Science* 363, 627 (2019)

National Research Priority: NSF-Quantum Leap

Light Guiding in Atomically Thin Semiconductor

Optical waveguides are vital components of data communication system technologies, but their scaling down to the nanoscale has remained challenging despite advances in nano-optics and nanomaterials. Recently, it was theoretically predicted that the ultimate limit of visible photon guiding can be achieved in monolayer-thick transition metal dichalcogenides. Here, we present an experimental **demonstration of light guiding in an atomically thick tungsten disulfide membrane patterned as a photonic crystal structure**. Two-dimensional WS_2 excitonic photoluminescence couples into quasi-guided photonic crystal modes known as resonant-type Wood's anomalies. These modes propagate via total internal reflection with only a small portion of the light diffracted to the far field. Such light guiding miniaturizes optoelectronic devices and tests fundamental physical concepts.



Visible light guiding was demonstrated in a three-atoms thick waveguide.

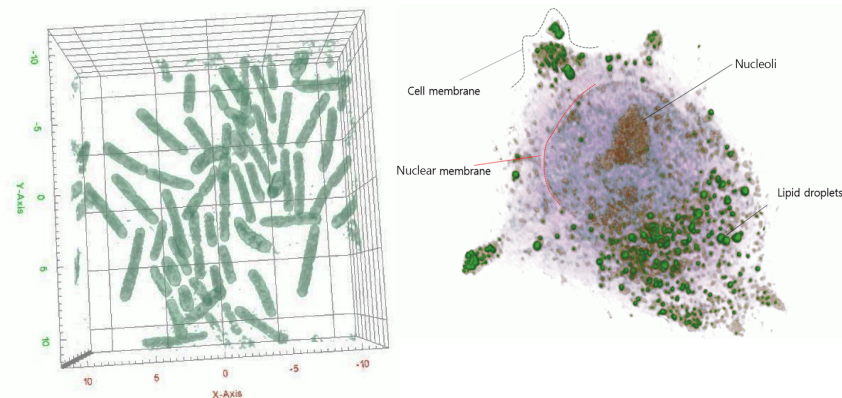
Suspended monolayer WS_2 patterned with array of nanoholes enables probing of guided light in the far field.

This work was supported by NSF 2-DARE Program (EFMA-1542879 and EFMA-1542863) and DMR-1709996. *Nat. Nanotechnol.* 2019, 14(9), 844–850.

National Research Priority: NSF-Quantum Leap

Live Cells Characterized Using High-Speed and Label-Free Optical Diffraction Tomography

As an optical analogy to X-ray computed tomography, digital holographic technology named Holotomography produces 3D holographic, quantitative imaging of live biological samples and is the world's first and only microscopy that **enables visualization of 3D refractive index (RI) tomography and 3D fluorescence imaging of live cells and tissues**. HT provides new means for researchers to investigate live cells and to analyze morphological, biophysical, and biomechanical properties of the cells. The systems enable researchers and clinicians to break into new frontiers of understanding, diagnosing and treating diseases.



*3D holography system showing bacterial (*B. subtilis*) growth and hepatocyte detail captured by Tomocube Inc.'s HT-1 holographic microscope*

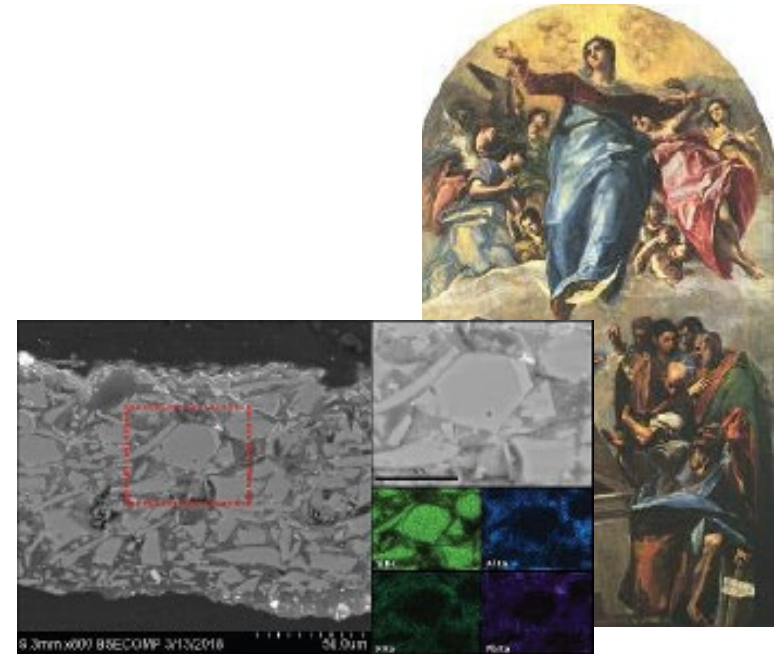
This work was supported by Tomocube, a startup company carrying out research in SDNI. *Cells*, 8(11), p.1368, 2019.

National Research Priority: NSF-Understanding the Rules of Life

Soft and Hybrid Nanotechnology Experimental (SHyNE) Resource

Analysis of El Greco painting, the Assumption of the Virgin

The sample pictured is a cross-section (a small fragment of paint embedded in polyester resin and polished) from an area of purple-colored paint in the robe of one of the figures that appeared dark and discolored. The large, irregular particles are smalt, a pigment made from blue-colored glass that was popular in El Greco's time. However, it is prone to degradation and often loses its blue color and appears dark in old paintings. The EDS maps show that the particles are rich in silicon (characteristic of glass) and depleted in potassium, which is sometimes observed in degraded smalt in which elements such as potassium have leached out of the pigment and into the paint matrix. This finding helps us to understand the intended appearance of this part of the painting.



El Greco "Assumption of a Virgin" painting with backscatter electron image and EDS maps of paint to determine pigment sources.

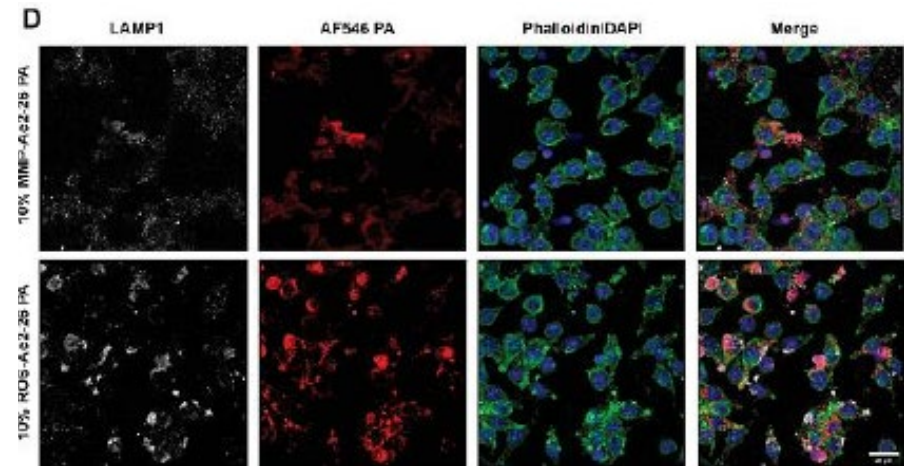
Kenneth Sutherland, Art Institute of Chicago. This work was performed in NUANCE Center at Northwestern University.

This work was supported through NU-ACCESS by Andrew W. Mellon Foundation.

National Research Priority: NSF-Growing Convergence Research

Atheroma Niche-Responsive Nanocarriers for Immunotherapeutic Delivery

SHyNE facilities were utilized by the **Kibbe** lab at the **University of North Carolina** for the design and synthesis of peptide amphiphiles (PAs) used in this study. PAs were designed to have environmentally responsive cleavage points when exposed to either high reactive oxygen species or matrix metalloproteinases, which would then release a therapeutic peptide sequence Ac-2-26 that is known to resolve inflammation in atherosclerotic lesions. The PA nanocarrier system also contained a peptide sequence that could target it to areas of atherosclerotic plaques. This initial study showed Ac-2-26 peptide release and bioactivity when tested in vitro and in cellular assays with macrophages. Future work will explore this system in more kinetic detail and in animal models.



Cellular uptake of therapeutic nanocarrier PAs in macrophages. Merged image shows co-localization of PA nanocarrier in macrophages.

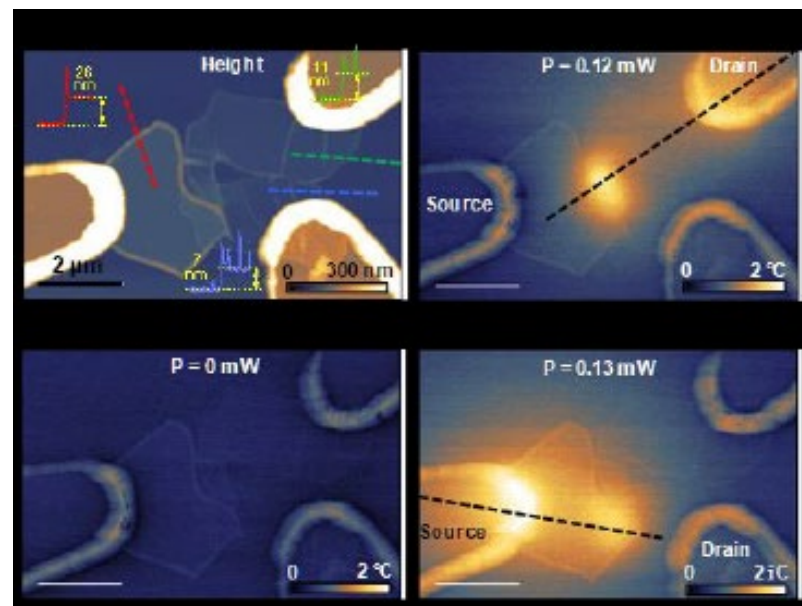
Stupp (Chemistry, Materials Science, Medicine, SQI, Northwestern), Peters (Surgery, UNC-Chapel Hill), et al. Work performed in Simpson Querrey Institute at Northwestern University.

This work was supported by NIH (1R01HL116577-01). *Advanced Healthcare Materials* (2019)

National Research Priority: NSF-Understanding the Rules of Life

Mapping Hot-Spots at Heterogeneities of Few-Layer Ti_3C_2 MXene Sheets using SThM

Scanning thermal microscopy (SThM) was developed to spatially map the temperature rise across various defects and heterogeneities of titanium carbide ($Ti_3C_2T_x$; T stands for surface terminations) MXene nanostructures under high electrical bias with sub-50 mK temperature resolution and sub-100 nm spatial resolution. High-resolution temperature rise maps allow us to identify localized hot spots and to quantify the non-uniformity of the temperature fields across various morphological features. The results show that the local heating is most severe in vertical junctions of MXene flakes and is highly affected by non-uniform conduction due to the presence of line defects GBs and its vicinity. The results suggest that the atomic structure at the interface plays a crucial role in enabling efficient charge transport without inducing localized heating.



SThM characterization of vertical interfaces of $Ti_3C_2T_x$ flakes. (a) Topography maps and height profiles of three $Ti_3C_2T_x$ MXene flakes. (b) Temperature map of the device before applying any current. (c-d) Temperature maps of the device under electrical biasing applied to different electrodes.

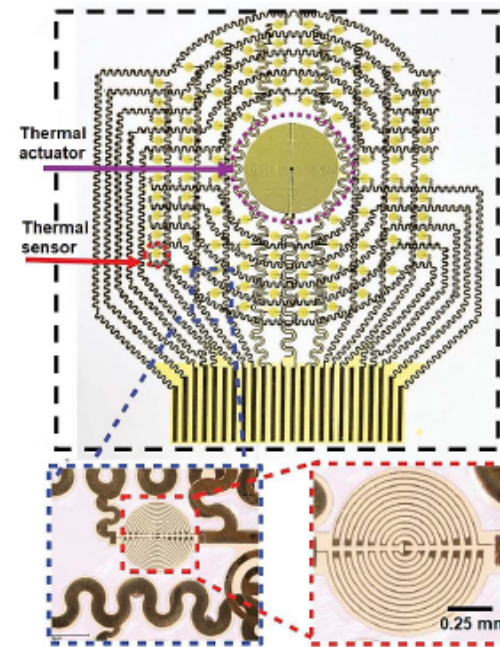
Shekhawat (Materials Science Department), Yasaei, et al. collaborated with APPNano, Inc. Work performed in the NUANCE Center at Northwestern University.

This work was supported by NSF IDBR-1256188, AFRL Grant FA8650-15-2-5518. *ACS Nano* (2019)

National Research Priority: NSF-Growing Convergence Research and Quantum Leap

Epidermal electronics for ventricular shunt function assessment in patients with hydrocephalus

The **Rogers group** at Northwestern University utilized SHyNE facilities for the development of epidermal electronics for ventricular shunt function assessment in patients with hydrocephalus. This noninvasive, skin-mounted, wearable measurement platform incorporates arrays of thermal sensors and actuators for precise, continuous, and intermittent measurement of flow through subdermal shunts, without the drawbacks of other methods such as CT and MRI. Systematic theoretical and experimental benchtop studies have demonstrated the high performance across a range of practical operating conditions. The advanced electronics design allows wireless embodiment for continuous monitoring based on rechargeable batteries and data transmission using Bluetooth protocols.



Optical micrograph of epidermal electronic device with enlarged images showing stretchable interconnects (blue dashed line) and individual temperature sensors (red dashed line).

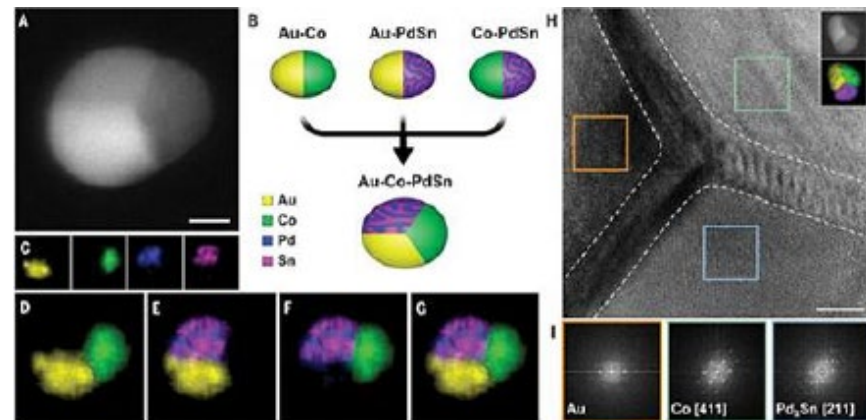
Rogers (Materials Science, Medicine, Chemistry), Krishnan, et al. Work performed in the NUANCE Center at Northwestern University.

This work was supported by NSF DMR-1720139NSF (also 1400169, 1534120, 1635443). *Science Translational Medicine* (2018).

National Research Priority: NSF-Future of Work at the Human-Technology Frontier

Interface and heterostructure design in polyelemental nanoparticles

Complex, multielement nanoparticles have broad applications in the fields of catalysis, optoelectronics, transistors, bio-imaging and energy storage. Development of the thermodynamically stable metal nanoparticles composed of multiple elements allows researchers to explore the structure and composition of alloy (i.e., Pd-Sn) nanoparticles formed with up to five other elements. For the triphase nanoparticles, two or three interfaces are architecture. For the tetraphase nanoparticles, up to six interfaces can be designed. The balance between surface and interfacial energies influence the observed phases and interface structure. The transmission electron microscopy observations were carried out in SHyNE facilities.



Heterostructured Au-Co-PdSn triphase nano-particle with three interconnected interfaces. (Science 2019)

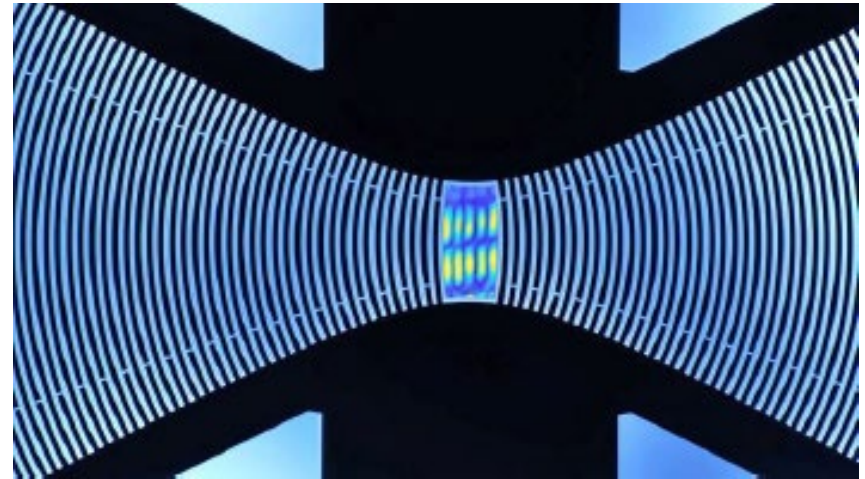
Mirkin (IIN, Chemistry, Materials Science), Dravid (Materials Science), Wolverton (Materials Science), et al. Work performed in the NUANCE Center at Northwestern University.

This work was supported by AFOSR FA9550-17-1-0348, Navy N00014-15-1-0043, Vannevar Bush; *Science* (2019)

National Research Priority: NSF-Growing Convergence Research

Spin-phonon interactions in silicon carbide addressed by Gaussian acoustics

Hybrid spin-mechanical systems provide a platform for integrating quantum registers and transducers.. Point defects in silicon carbide (SiC) offer long-lived, optically addressable spin registers in a wafer-scale material with low acoustic losses, making them natural candidates for integration with high-quality-factor mechanical resonators. Gaussian focusing of a surface acoustic wave in SiC, We demonstrate all-optical detection of acoustic paramagnetic resonance without microwave magnetic fields, relevant for sensing applications. Finally, we show mechanically driven Autler-Townes splittings and magnetically forbidden Rabi oscillations. These results offer a basis for full strain control of three-level spin systems.



SEM micrograph of resonant microstructure with integrated resistors for thermal excitation and piezoresistive detection of in-plane oscillations.

Whitely (Physics, UChicago), Awschalom (Pritzker Inst. for Molecular Engineering), Ma (PIME, Chemistry, UChicago), Wolfowicz (AIMR, Japan), et al. Work performed in the **Pritzker Nanofabrication Facility** at University of Chicago.

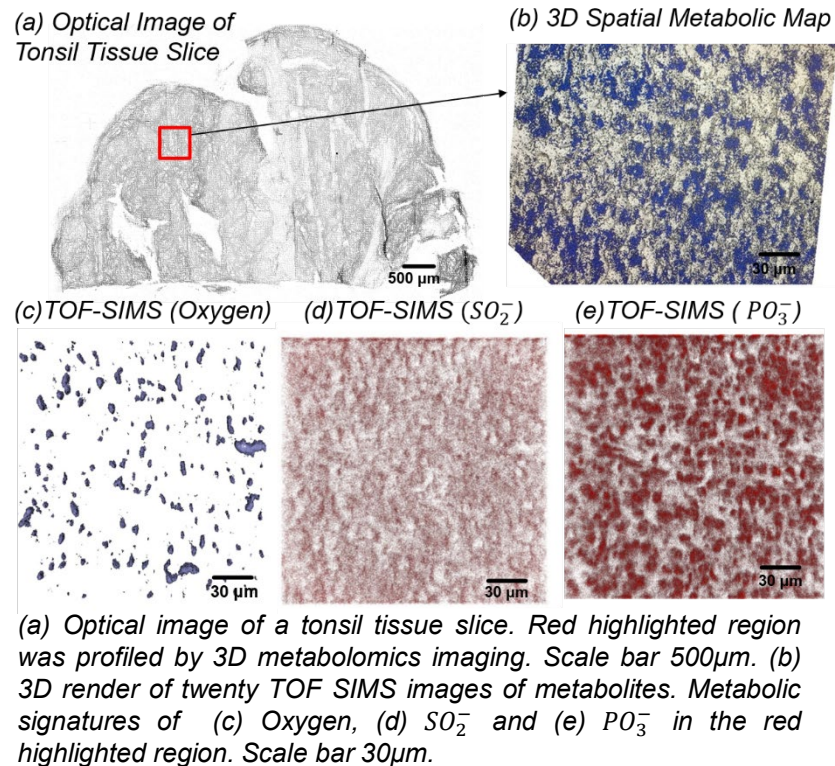
This work supported by NSF DMR-1420709, AFOSR, DOE, DOD, Argonne DE-AC02-06CH11357; *Nature Physics* (2019)

National Research Priority: NSF-Quantum Leap

Southeastern Nanotechnology Infrastructure Corridor (SENIC)

Spatially resolved 3D metabolomic profiling of immune cells by subcellular volumetric analysis

This project profiles human tonsil tissues by analyzing the spatial distribution of antibodies and immune cells such as T cells and B-cells, using three dimensional (3D) molecular analysis framework. Time-of-Flight Secondary Ion Mass Spectrometry (TOF-SIMS) instrument was used to obtain 3D metabolic profiles of chemical fingerprints such as phosphorous, sulphur, and lipid signatures from the immune cells in the tonsil tissue. To analyze these 3D metabolic channels in the immune cells, metabolic data dimensionality reduction techniques such as Principal Component Analysis (PCA) was initially carried out. To quantify 3D spatial metabolic distribution, unsupervised clustering algorithms such as K-means clustering was implemented based on the metrics such as density, means, and correlations. Thus, the presented 3D metabolic analysis pipeline will be useful for quantifying engineered immune cells in health and disease.



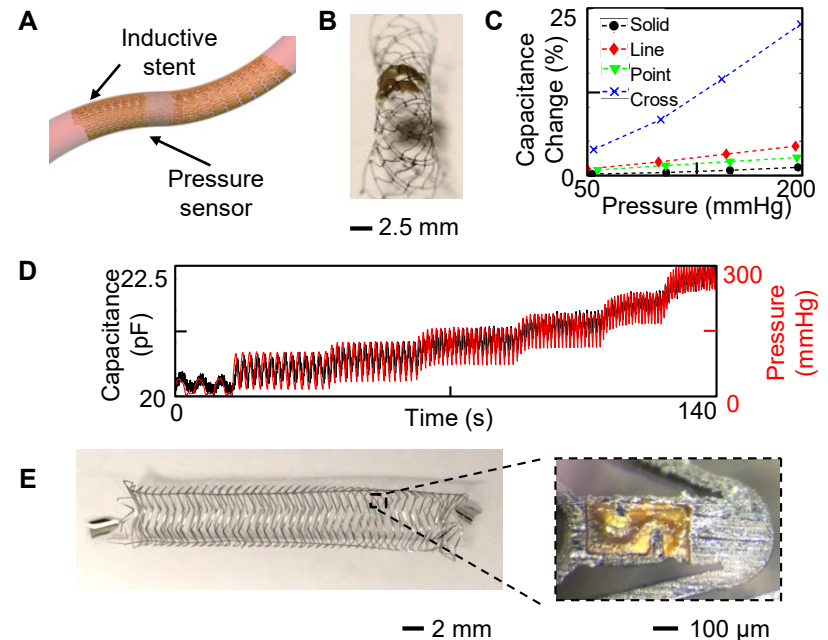
Shambavi Ganesh, Eric Woods, Mayar Allam, Shuangyi Cai, Walter E. Henderson, and Ahmet F. Coskun, Biomedical Engineering, Electrical and Computer Engineering, Biological Sciences, Institute for Electronics and Nanotechnology, Georgia Tech and Emory University. Work performed at Georgia Tech Materials Characterization Facility.

This work was supported by BWF-CASI # 1015739.02, NIH # K25AI140783, and Georgia Tech & Emory start-up funds.

National Research Priority: NSF-Understanding the Rules of Life

Fully Wireless, Nanostructured, Hemodynamic Sensor System for Continuous Monitoring of Blood Pressure and Flow Rate

- Hemodynamic conditions are used as indications for cardiovascular diseases, which account for over 30% of deaths worldwide
- Focused on developing an implantable smart stent with two nanostructured, soft pressure sensors for wireless monitoring of blood pressure and flow rate
- Stent is balloon expandable and employs a solenoid-like shape with polymer support links to maintain mechanical integrity and a high inductance ($1.4 \mu\text{H}$)
- Fully printed, low-profile capacitive pressure sensors use a microstructured PDMS dielectric layer to achieve high sensitivity (3.8 fF/mmHg).
- Future work will include wireless testing and in vivo demonstration



A) Illustration of implantable smart stent and sensor. B) Low-profile pressure sensor integrated on stent. C) Pressure sensitivity comparison of PDMS microstructures. D) Pressure sensor response to pulsatile flow in model blood vessel. E) Smart stent after balloon expansion with enlarged view of polyimide support link.

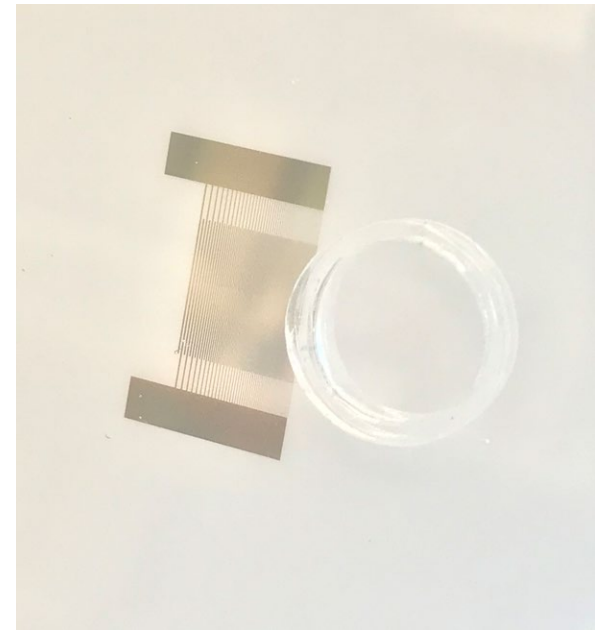
Robert Herbert and Woon-Hong Yeo, Mechanical and Biomedical Engineering, Georgia Tech. Work performed at Georgia Tech's Institute for Electronics and Nanotechnology.

This work was supported by an IEN Facility Seed Grant (funded by NSF ECCS-1542174).

National Research Priority: NSF-Growing Convergence Research

Physics of Acoustic-Neuro Interaction

The goal of this project is to study how ultrasonic waves of different frequencies alter the electrophysiology of neurons in vitro. A chromium and gold interdigitated transducer is deposited on a piezoelectric lithium niobate substrate. The spacing between digits on the transducer is varied to accommodate frequencies ranging from 10 to 60 MHz. A PDMS ring is positioned adjacent to the transducer and serves as a neural cell culture dish directly on the substrate. Directly growing the cells on the piezoelectric substrate allows for the ultrasonic waves to interact with the neurons with minimal attenuation. This device is suited to fit under a patching rig for patch clamping measurements or an optical interferometry stage to observe cell movement.



PDMS ring is plasma bonded to the lithium niobate wafer directly adjacent to the interdigitated transducer (IDT)

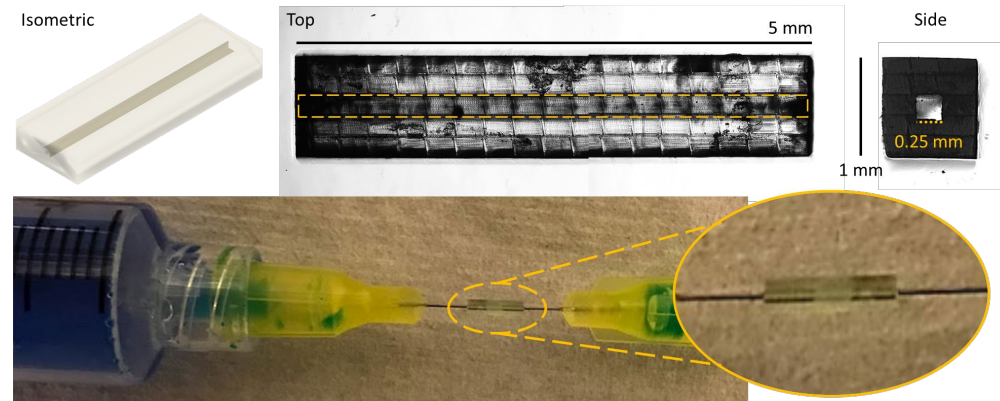
Phoebe J. Welch and Chengzhi Shi, Mechanical Engineering, Georgia Tech. Work performed at Georgia Tech's Institute for Electronics and Nanotechnology.

This work was supported by an IEN Facility Seed Grant (funded by NSF ECCS-1542174).

National Research Priority: NSF-Growing Convergence Research

3D Bioprinted Endothelialized Vascular Tissues for Investigating Cardiovascular Diseases

This work targets a 3D printed platform for tissue engineering human microvasculatures. This work simultaneously investigates the endothelialization process and structural patterning of vasculatures to fabricate biomimetic channel systems in our tissue engineered constructs. A single channel construct with dimensions of 1x1x5 mm externally and 0.25x0.25x5 mm internally was developed and able to be perfused. From this construct, we successfully fabricated an arteriolar conduit model based on diameter (100-300 μm). With the channel suspended on all sides by cured photoresist, this avoids the need for a glass sample slide to enclose the channel. This is significant because printing with future biocompatible resists can be fully seeded and remodeled by cells for longer, more complex tissue cultures.



An isometric view and brightfield images (top and side views, 4x) of the 3D printed construct are shown highlighting the channel in yellow. The physical construct was perfused via 32 gauge needles with no leakage when sealed.

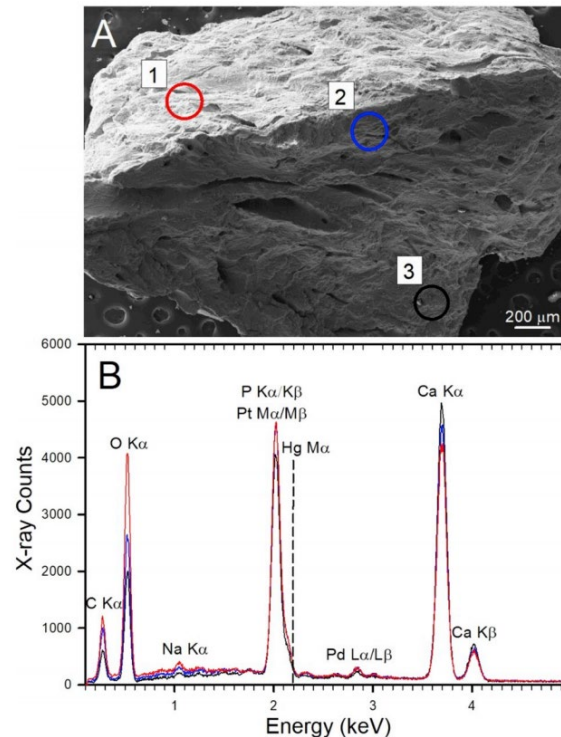
Alexander Cetnar and Vahid Serpooshan, Biomedical Engineering, Georgia Tech and Emory University. Work performed at Georgia Tech's Institute for Electronics and Nanotechnology.

This work was supported by an IEN Facility Seed Grant (funded by NSF ECCS-1542174).

National Research Priority: NSF-Growing Convergence Research

Mercury in archaeological human bone: biogenic or diagenetic?

In this work, mercury (Hg) levels in human bone from archaeological sites in the Iberian Peninsula were investigated. Previous analyses have shown high levels of total mercury (THg) in human bone at numerous Neolithic and Chalcolithic sites in this region, but the question remains if this mercury entered the bones via diagenetic processes in the soil, especially where cinnabar powder and paint was found associated with the burials, or if it entered the bone via biogenic pathways from exposure to mercury from using cinnabar in life. The pattern of Hg deposition in skeletal material from different sites and ages strongly suggests a biogenic origin for the mercury



EDS spectroscopy of human bone sample UE-112 from Montelirio tholos known to have high THg concentrations (> 273 ppm).

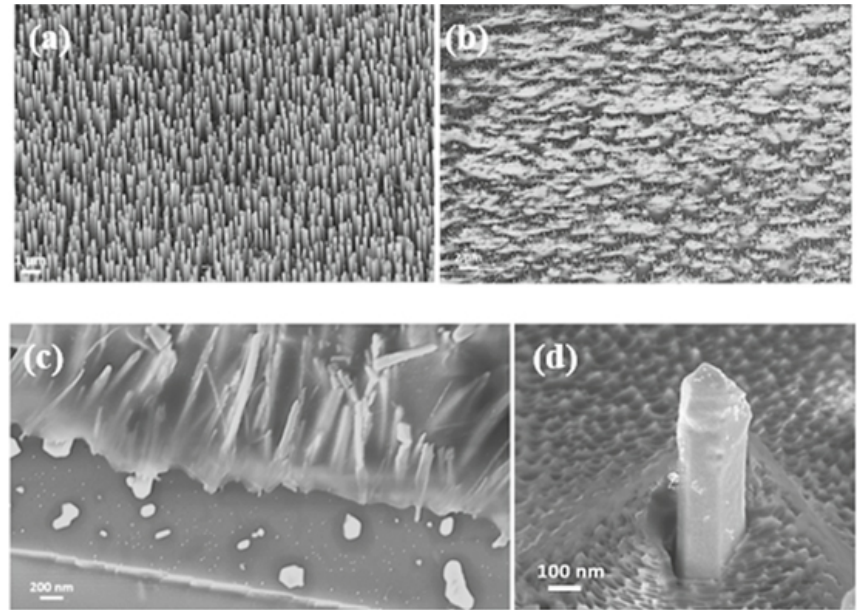
Steven D. Emslie, Alison R. Taylor et al., Department of Biology and Marine Biology, University of North Carolina Wilmington. Work performed at Joint School of Nanoscience and Nanoengineering.

Journal of Archaeological Science, 108 (2019) 104969.

National Research Priority: NSF-Understanding the Rules of Life

Space charge limited conduction mechanism in GaAsSb nanowires

In this work, the first observation of the space charge limited conduction mechanism (SCLC) in GaAsSb nanowires (NWs) grown by Ga-assisted molecular beam epitaxial technique, and the effect of ultra-high vacuum in situ annealing have been investigated. The low onset voltage of the SCLC in the NW configuration has been advantageously exploited to extract trap density and trap distribution in the bandgap of this material system, using simple temperature dependent current–voltage measurements in both the ensemble and single nanowires. In situ annealing in ultra-high vacuum revealed significant reduction in the trap density from 10^{16} cm^{-3} in as-grown NWs to a low level of $7 \times 10^{14} \text{ cm}^{-3}$ and confining wider trap distribution to a single trap depth at 0.12 eV.



(a) GaAsSb NWs on Si (111), (b) top view of GaAsSb NW ensemble coated with PMMA, (c) tilted view of NW ensemble and (d) NW tip exposed above PMMA.

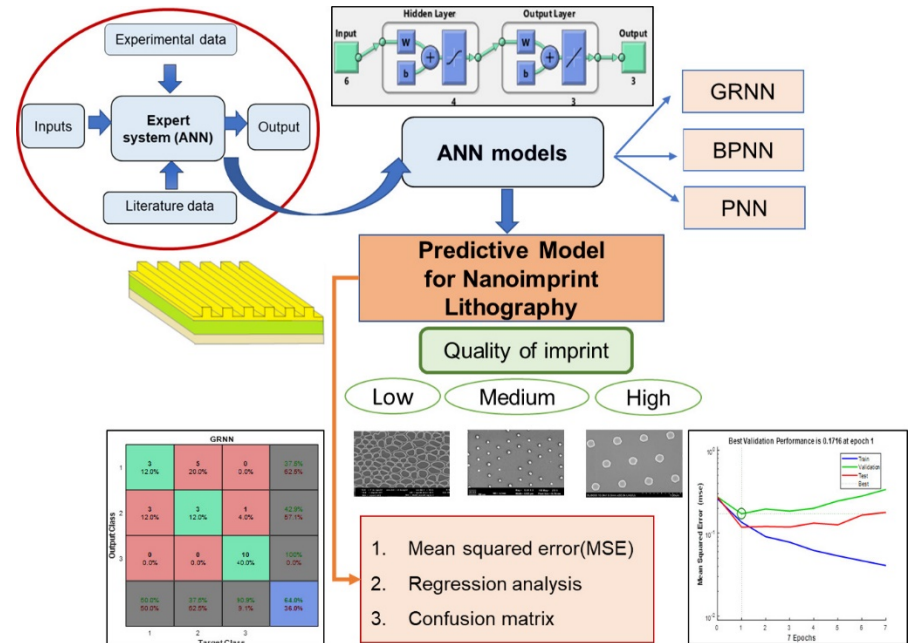
Mehul Parakh and Shanthi Iyer, Dept. of Nanoengineering, North Carolina A&T State University. Work performed at Joint School of Nanoscience and Nanoengineering.

This work was supported by NSF# ECCS-1832117. *Nanotechnology* 31, no. 2 (2019): 025205.

National Research Priority: NSF-Quantum Leap

Developing a predictive model for nanoimprint lithography using artificial neural networks

Nanoimprint lithography (NIL) is a high-throughput and cost-effective technique for fabricating nanoscale features. However, the fine tuning of NIL process parameters is critical in achieving defect-free imprints. Currently, there exists no unified material and process design guidelines to deal with the complex set of process parameters. In this research, an artificial neural network (ANN) algorithm was developed to predict the imprint quality based on a set of input factors collected from experiments and literature. The prediction of the model was validated with experimental results confirming the accurate classification of all the outputs. This research lays the foundation for the development of an expert system for nanoimprint lithography.



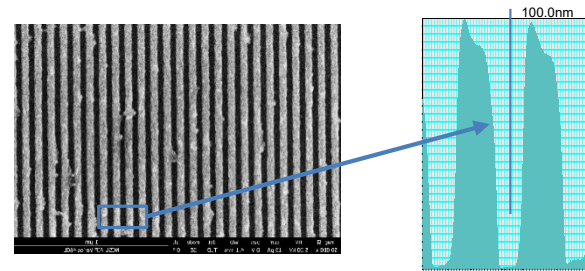
Tahmina Akter and Salil Desai, Dept. of Industrial & Systems Engineering, North Carolina A&T State University. Work performed at Joint School of Nanoscience and Nanoengineering.

This work was supported by NSF CMMI-1663128. *Materials & Design* 160 (2018): 836-848.

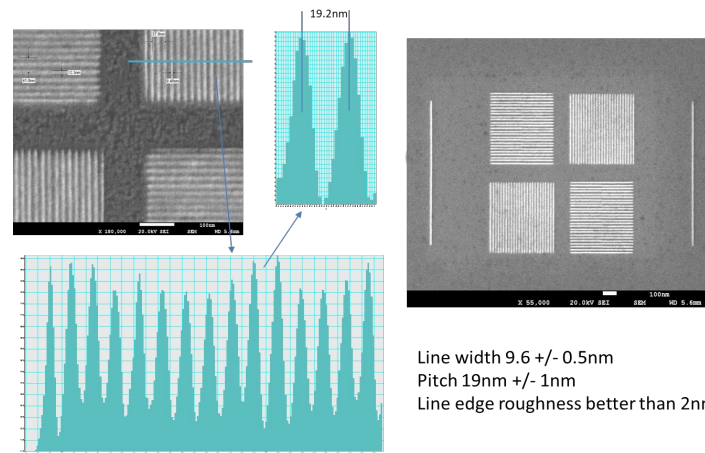
National Research Priority: NSF-Growing Convergence Research

Development of a Sub-20nm Pitch Critical Dimension Standard Using Electron Beam Lithography

The objective of this project is to produce a critical dimension standard applicable to the calibration needs of the ultra-high-resolution field emission scanning electron microscopy community as well as electron microscope suppliers. The intent is to develop electron beam lithography (EBL) techniques to enable fabrication of a critical dimension standard with a pitch of 20 nm or less. The main goal is to obtain fiducial lines with a high Z contrast material relative to silicon such as gold, rather than the low Z contrast lines obtained from previous work using Hydrogen Silsesquioxane (HSQ) as the EBL resist. Following successful completion of this project, measurements of this novel metrology standard will be undertaken in collaboration with the NIST Semiconductor and Dimensional Metrology Division.



SEM micrograph of recent ~50nm half pitch Cr-Au metal lift-off lines obtained from a test sample produced at Georgia Tech IEN



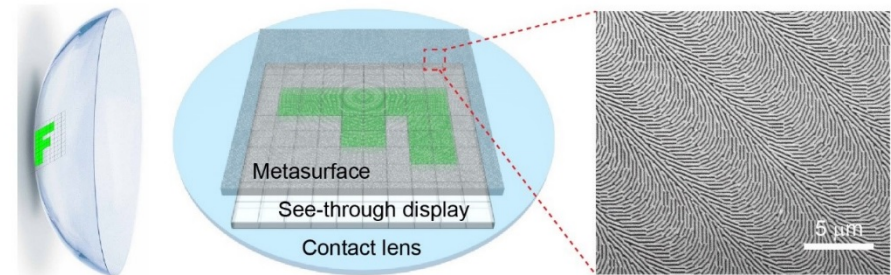
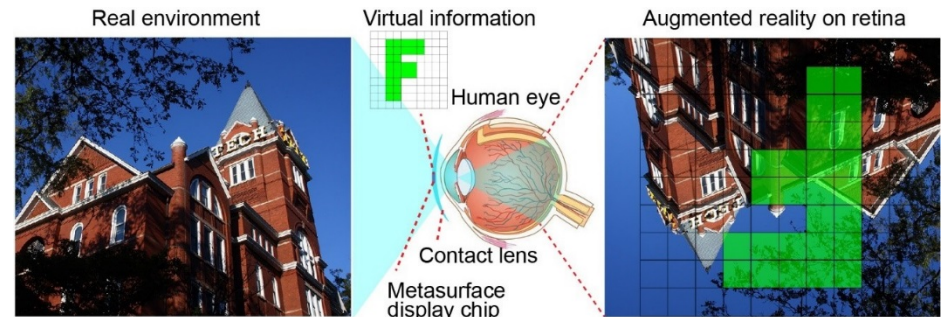
SEM of previously obtained EBL patterns using HSQ EBL resist.

Dudley S. Finch, AIStthesis Products, Inc. Work performed at Georgia Tech's Institute for Electronics and Nanotechnology.

National Research Priority: NAE Grand Challenge-Engineer the Tools of Scientific Discovery

Metasurfaces for Near-Eye Augmented Reality

This work proposes and experimentally demonstrates a holographic display technology that casts virtual information directly to the retina so that the eye sees it while maintaining the visualization of the real-world intact. The key to our design is to introduce metasurfaces to create a phase distribution that projects virtual information in a pixel-by-pixel manner. Unlike conventional holographic techniques, our metasurface-based technique, based on Pancharatnam-Berry phase elements made of silicon, is able to display arbitrary patterns using a single passive hologram. With a small form-factor, the designed metasurface empowers near-eye AR, excluding the need for extra optical elements, such as a spatial light modulator, for dynamic image control.



Schematic of metasurface enable device. The lower-right image is the SEM micrograph of a small portion of the metasurface comprises the predesigned distribution of silicon nanobeams.

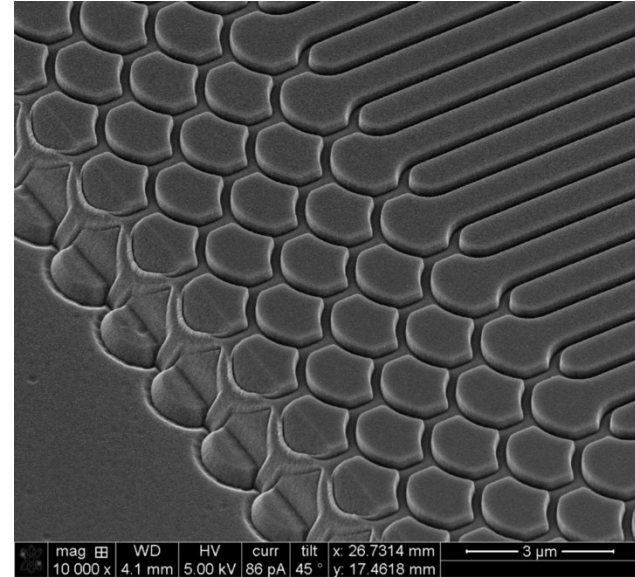
Shoufeng Lan, Xueyue Zhang, Mohammad Taghinejad, Sean Rodrigues, Kyu-Tae Lee, Zhaocheng Liu, and Wenshan Cai, Electrical and Computer Engineering, Georgia Tech. Work performed at Georgia Tech's Institute for Electronics and Nanotechnology.

This work was supported by NSF Award # ECCS-1542174. *ACS Photonics* 2019, 6, 864–870

National Research Priority: NSF-Future of Work at the Human-Technology Frontier

Continuous Flow Nanofluidic Devices for Whole Genome Optical Mapping

This work focuses on the development of nanofluidic devices for the real-time restriction site mapping of whole genomes. Devices are fabricated with nanochannels through which single molecules of genomic DNA are electrokinetically driven. Molecules are digested during transit using restriction endonucleases to produce an ordered map sensitive to structural variation in the genome. Electron beam lithography with proximity error correction produces devices capable of generating high-resolution optical maps. In combination with sequencing data, such maps promise to illuminate the full spectrum of genomic variation impacting human health.



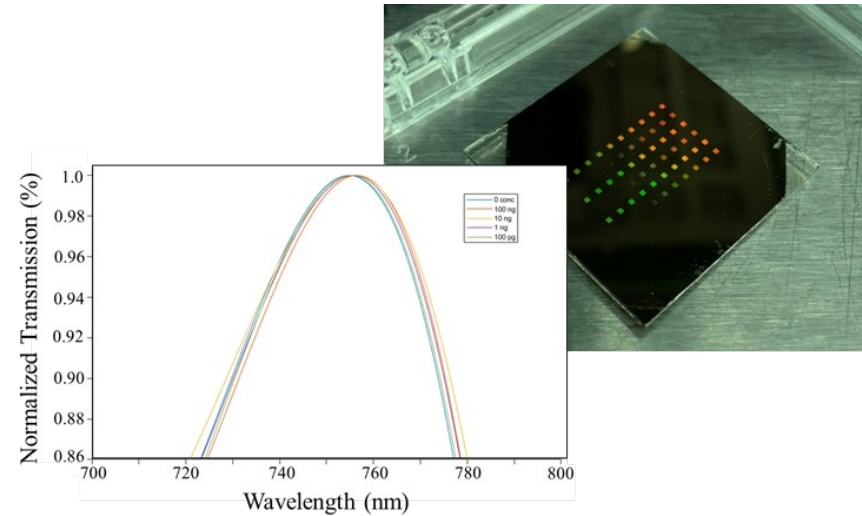
SEM micrograph of the entry of a nanochannel array used for generating high-resolution human genome maps.

Varshni Singh and Laurent D. Menard, Genturi Inc. Work performed at Georgia Tech's Institute for Electronics and Nanotechnology.

National Research Priority: NSF-Growing Convergence Research and Understanding the Rules of Life

Nanoslit Arrays for Plasmonic Sensing of Cardiac Biomarker

This work targets large scale nanoslit arrays (0.5x0.5 mm) fabricated in gold film coated on a quartz substrate. A series of nanoslit arrays with different slit width (around 100 nm) were obtained and demonstrates optical characteristics (showing different color under nature white light) due to plasmonic resonance within the nanoslit array. The extraordinary optical transmission (EOT) of the array has peak shift to red as a response to biological binding at the gold surface of the nanoslit area which is used for biomarker detection due to the refractive index changes before and after the binding reaction.



An image of the nanoslits arrays generated on gold film on a quartz substrate.

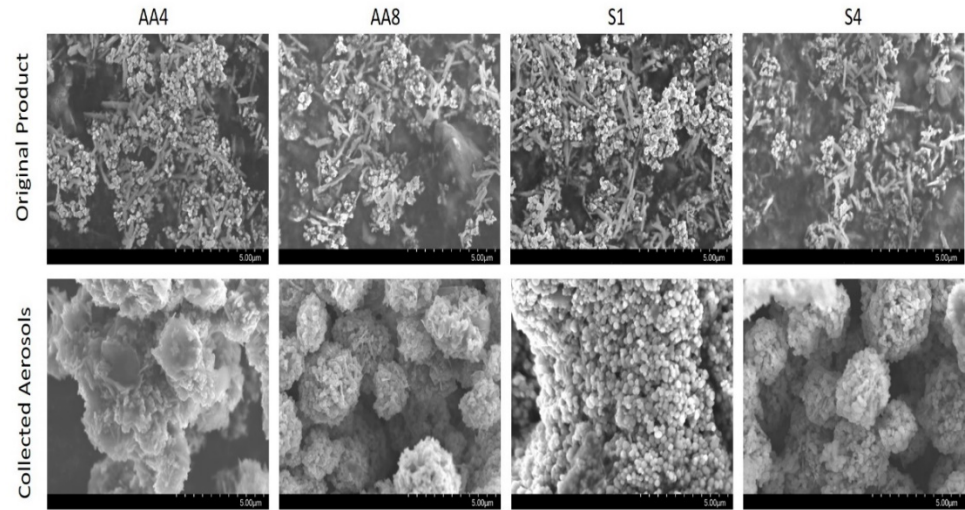
Jianjun Wei, Bhawna Bagra, Dept. of Nanoscience, Joint School of Nanoscience and Nanoengineering, UNC Greensboro. This work was partially performed at Georgia Tech's Institute for Electronics and Nanotechnology.

This work was supported by North Carolina Biotechnology Center (NCBC), NCBC Grant #2019-TEG-1501.

National Research Priority: NAE Grand Challenge-Engineer the Tools of Scientific Discovery

Characterization of particles emitted from aerosolized consumer products

This work focuses on understanding potential inhalation risks and hazards during the use of common aerosolized consumer products. Four de-identified consumer aerosolized cosmetic aerosols (AA4, AA8, S1, and S4) were assessed. Aerosols were generated, monitored and sampled using a novel aerosol generation system complete with aerosol monitoring instrumentation and animal exposure pods for in vivo toxicological evaluations. Aerosols were sampled onto aluminum substrates and evaluated using transmission electron microscopy coupled with energy dispersive X-ray spectroscopy (TEM-EDX)(Figure 1). Aerosols were multimodal consisting of micro-sized particles decorated with nanoparticles containing primarily titanium and iron.



TEM micrograph consumer product aerosols emitted from aerosolized nano-enabled cosmetics.

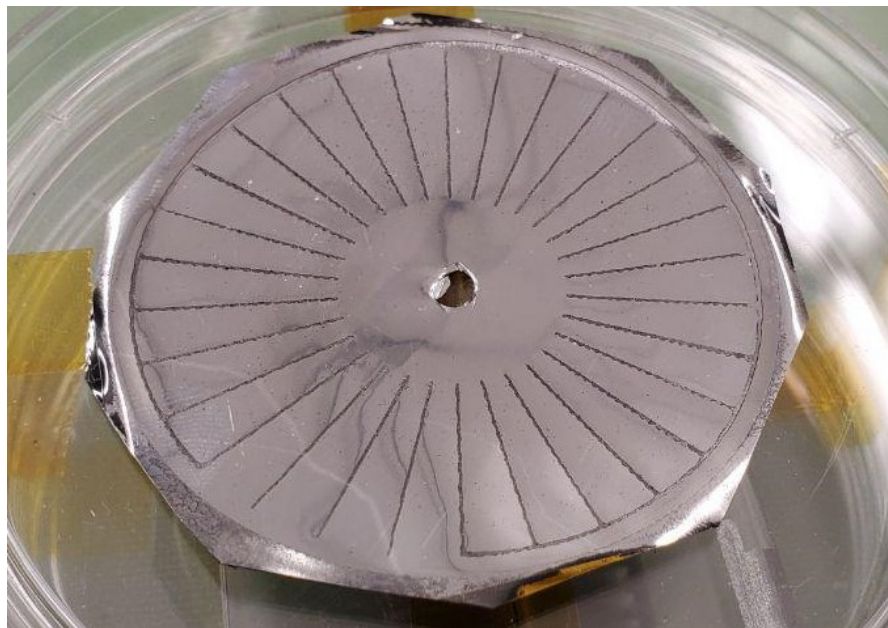
K.M. Pearce, W.T. Goldsmith, R. Greenwald, C. Yang, G. Mainelis, & C. Wright, Dept. of Population Health Sciences, School of Public Health, Georgia State University, IES techno, Morgantown, WV, Institute for Electronics and Nanotechnology, Georgia Tech, Dept. of Environmental Sciences, Rutgers University. TEM-EDX work completed at Georgia Tech IEN.

Inhalation Toxicology, DOI: 10.1080/08958378.2019.1685613 (2019)

National Research Priority: NSF-Growing Convergence Research

Subsurface pressure profiling: computing colony pressures on substrate during fungal infections

Colony expansion is an essential feature of fungal infections. Although mechanisms that regulate hyphal forces on the substrate during expansion have been reported previously, there is a critical need of a methodology that can compute the pressure profiles exerted by fungi on substrates during expansion. This will facilitate the validation of therapeutic efficacy of novel antifungals. Here, we are trying to introduce an experimental method based on Biot's incremental stress model, which was used to map the pressure distribution from an expanding mycelium of a popular plant pathogen, *Aspergillus parasiticus*.



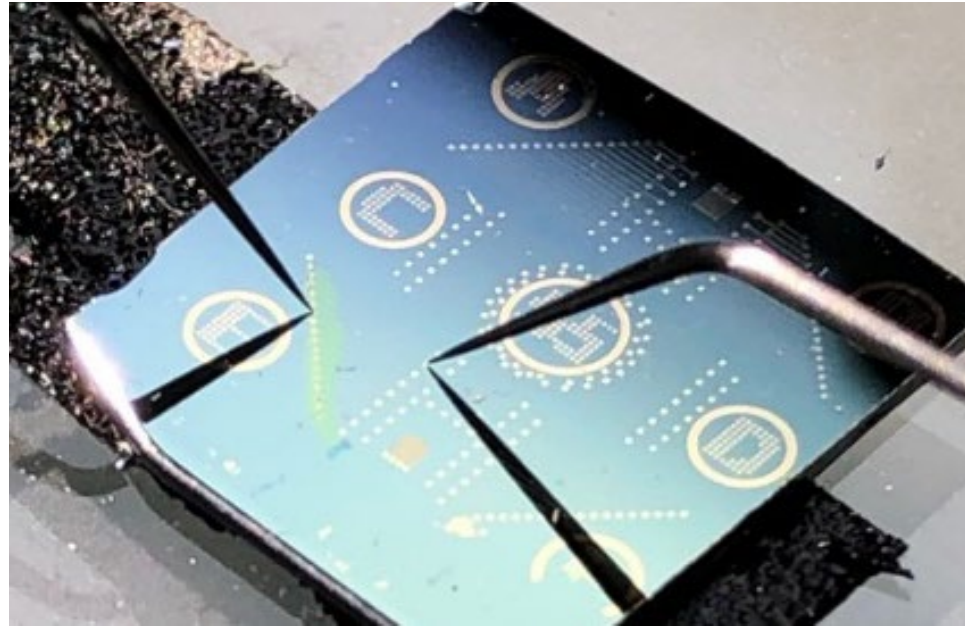
Using Denton Explorer - E-beam Evaporator to deposit the Chromium electrodes on both sides of PVDF membrane

Sourav Banerjee and Mohammadsadegh Saadatzi, Dept. of Mechanical Engineering, University of South Carolina. Work performed at Georgia Tech's Institute for Electronics and Nanotechnology.

National Research Priority: NAE Grand Challenge-Engineer the Tools of Scientific Discovery

On-chip energy harvesting using the movement of highly flexible suspended graphene

This work targets the extreme flexibility of suspended graphene as a source of vibrational energy. During this phase of the project we etched a pattern into silicon dioxide to form trench, well, and tip structures. Next, we re-patterned the surface and coated this with gold. Afterward, graphene was suspended over the well/tip structures to form a capacitor. Graphene can be seen in the photograph over the array of electrodes in section E to the right (under left probe). As the graphene moves up and down, the capacitance of the tip-graphene junction also fluctuates and this produces an alternating current. This technology is an on-chip power source.



Optical photograph of graphene suspended over a previously etched silicon tip, well, and trench structures.

Paul Thibado, Millicent Gikunda, et al. Department of Physics, University of Arkansas-Fayetteville. High-resolution lithography work was performed at the Georgia Tech's Institute for Electronics and Nanotechnology.

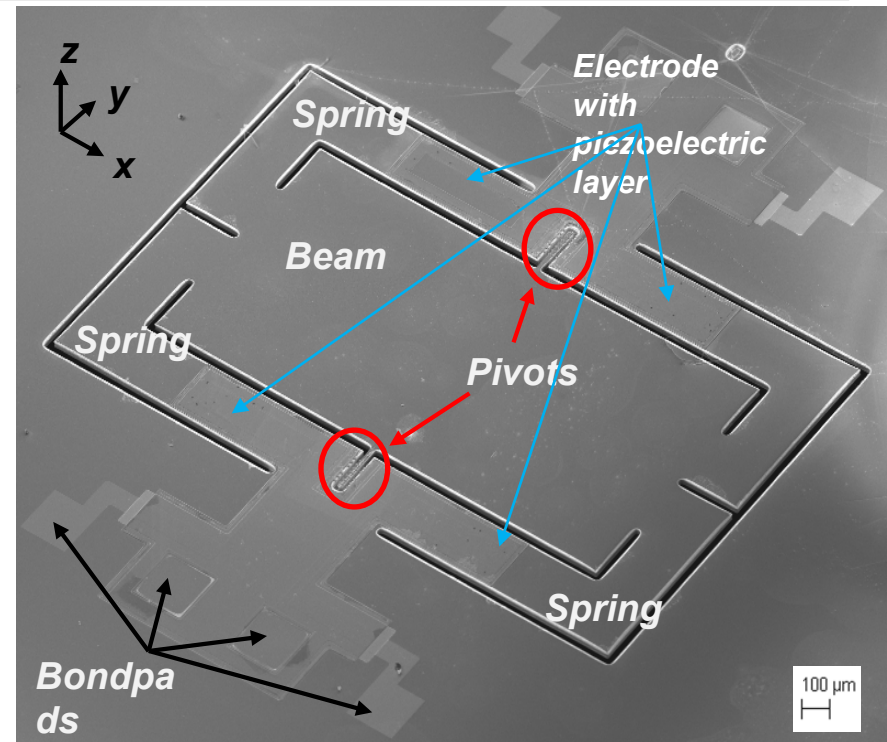
This work was supported by Walton Family Foundation Charitable Trusts.

National Research Priority: DOE-Microelectronics

Texas Nanofabrication Facility (TNF)

New Acoustic MEMS Based on a Fly's Acute Hearing for Hearing Aids and Military

Silicon Audio has developed a tiny prototype device that mimics a parasitic fly's hearing mechanism, which may be useful for a new generation of hypersensitive hearing aids. The 2-millimeter-wide device uses piezoelectric materials, which turn mechanical strain into electric signals. The use of these materials means that the device requires very little power. Humans and other mammals have the ability to pinpoint sound sources because of the finite speed of sound combined with the separation between our ears. The fly has evolved an unusual physiological mechanism to make the most of that tiny difference in time. The fly's ear has a structure that resembles a tiny teeter-totter seesaw about 1.5 mm long. Teeter-totters, by their very nature, vibrate such that opposing ends have 180-degree phase difference, so even very small phase differences in incident pressure waves force a mechanical motion that is 180 degrees out of phase with the other end. This effectively amplifies the four-millionths of a second time delay.



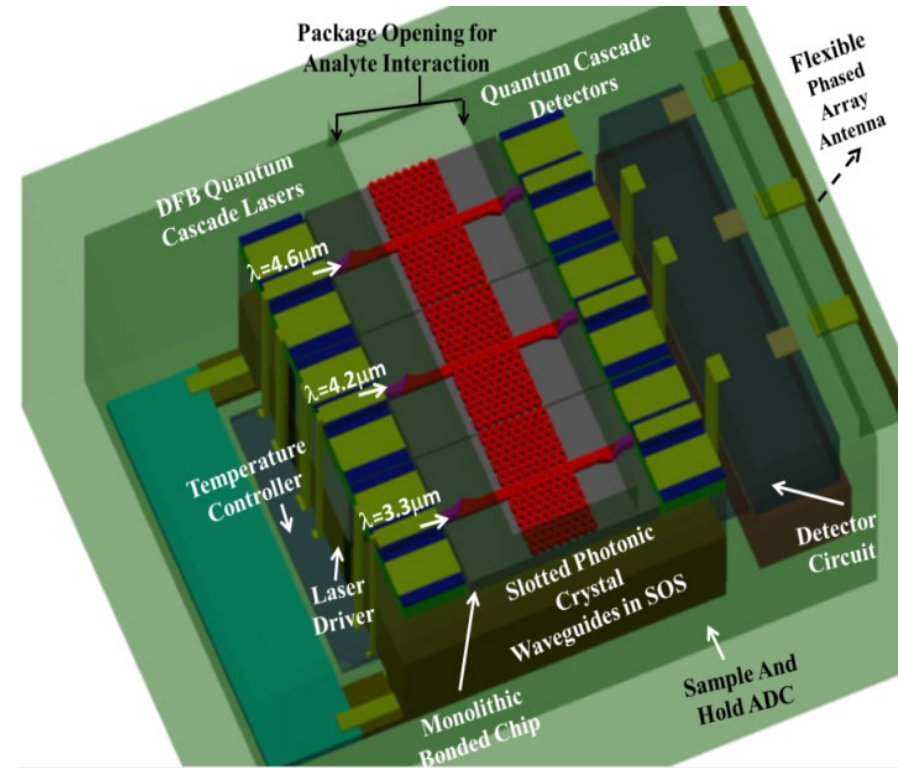
N Hall, Silicon Audio. Work performed at TNF.

Funded by DARPA.

National Research Priority: NSF-Quantum Leap

PPB CO Sensing in Silicon-on-Sapphire Mid-Infrared Photonic Crystal Waveguides

With recent advances in optoelectronics and photonics, optical sensors have flourished. Optical sensors are typically built of three parts: a light source and detector, a photonic crystal substrate, and an analyte flow mechanism made of microfluidic channels. Experimentally demonstrated mid-IR slotted photonic crystal waveguides at $\lambda=4.55$ micron in silicon-on-sapphire. Experimentally detected 3ppm CO with mid-IR absorbance signatures. Feasibility of parts per billion sensing was shown. Experiments in progress to validate ppb- sensitivity.



Swapnajit Chakravarty, Omega Optics. Work performed at TNF.

Supported by NASA SBIR Contract #: NNX17CA44P, NSF Grant #:1711824

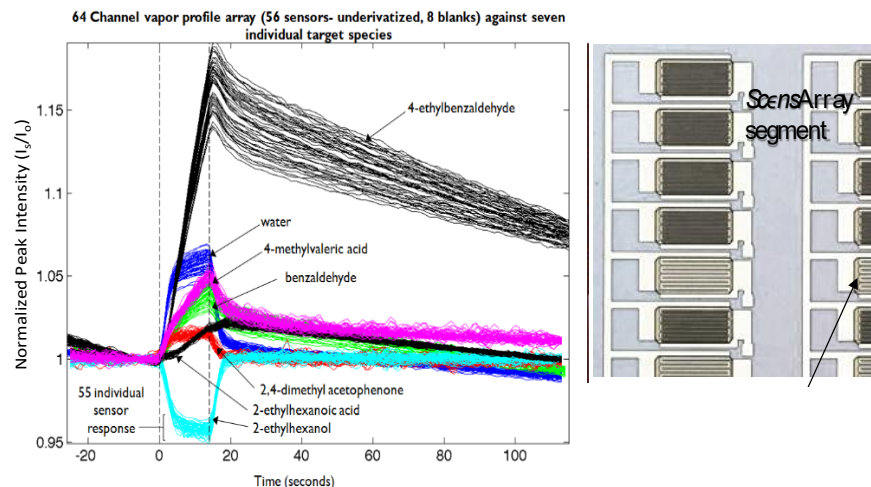
National Research Priority: NSF-Quantum Leap

Multiplexed Metal-Oxide Gas and Fluid Sensor Arrays

Bioassays employed to evaluate the diverse range of biomarkers associated with organ injury are time-consuming, costly and require multiple instruments/testing formats to reach a diagnosis (i.e. fluorescence-based capture, ELISAs, PCR, etc.). Individually, these platforms are incapable of predicting the onset of irreversible organ tissue injury (e.g. kidney, liver, heart and lung). One barrier to transitioning microarray technology into multiplex medicinal diagnostics has been the limitations imposed by fluorescence/optical-based labeling and endpoint detection. To overcome these limitations, Nanohmics Inc., developed the SnO₂ nanowire chemiresistive sensor array. The diverse surface derivitizations across array elements allows for incident gas/ion species identification. The platforms are room temperature operable and provide fast response in gas applications.

Steve Savoy, Nanohmics. Work performed at TNF.

Funded by DHP Phase II SBIR Program and NIH Phase I SBIR Program.

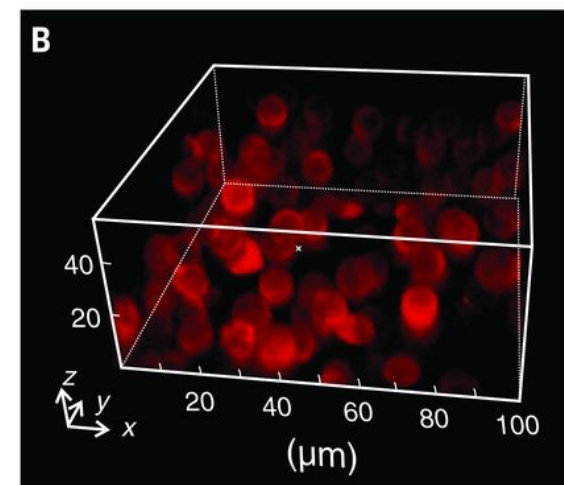
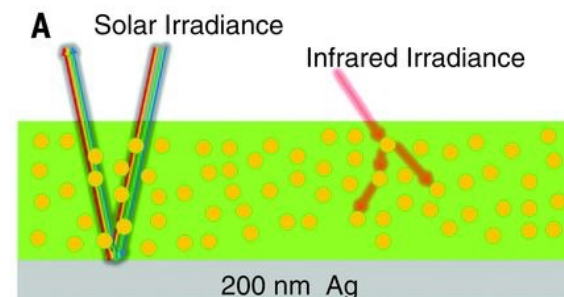


National Research Priority: DOE-Microelectronics

Fabrication of metamaterials for efficient passive cooling

Spectroscopic response of the hybrid metamaterial. **(A)** Schematic of the hybrid metamaterial backed with a thin silver film. The silver film diffusively reflects most of the incident solar irradiance, whereas the hybrid material absorbs all incident infrared irradiance and is highly infrared emissive. **(B)** Three-dimensional confocal microscope image of the hybrid metamaterial. The microspheres are visible because of the autofluorescence of SiO_2 .

We embedded resonant polar dielectric microspheres randomly in a polymeric matrix, resulting in a metamaterial that is fully transparent to the solar spectrum while having an infrared emissivity greater than 0.93 across the atmospheric window. When backed with a silver coating, the metamaterial shows a noontime radiative cooling power of 93 watts per square meter under direct sunshine. More critically, we demonstrated high-throughput, economical roll-to-roll manufacturing of the metamaterial, which is vital for promoting radiative cooling as a viable energy technology.

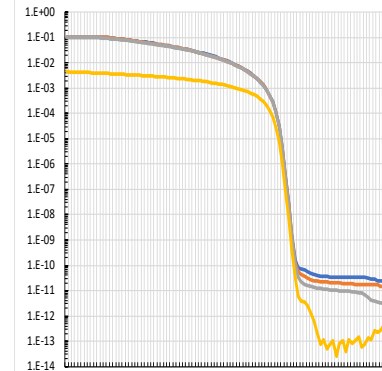
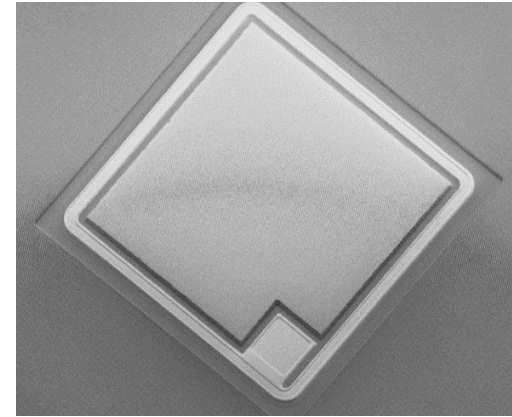


A Heltzel, PC Krause and Associates. Work performed at TNF Texas Materials Institute.

National Research Priority: DOE-Secure Energy Future

Thin Crystalline (~30 Microns) Silicon Vertical Power Transistor

AND Inc. has developed a thin crystalline technology that can peel off 20 - 50 μ m of silicon from semi-processed wafers and enable reuse of the parent wafer. Using this exfoliation technology, AND has recently demonstrated the world's first Thin Crystalline (~30 Microns) Silicon Vertical Power MOSFET fabricated without grinding away the substrate. The industry standard process for vertical power MOSFET and IGBTs is to use a back grinding process. The standard toolset provided by Disco for this process was used, and compared with the wafers fabricated with back grinding against the thin crystalline wafers fabricated by AND. The thin crystalline process has been scaled to 12" semi standard wafers. AND has developed a unique self-aligned vertical power MOSFET architecture. This architecture brings in significant process simplification and device benefits. AND is combining this device architecture with thin crystalline Si technology to target record device performance of power MOSFETs.



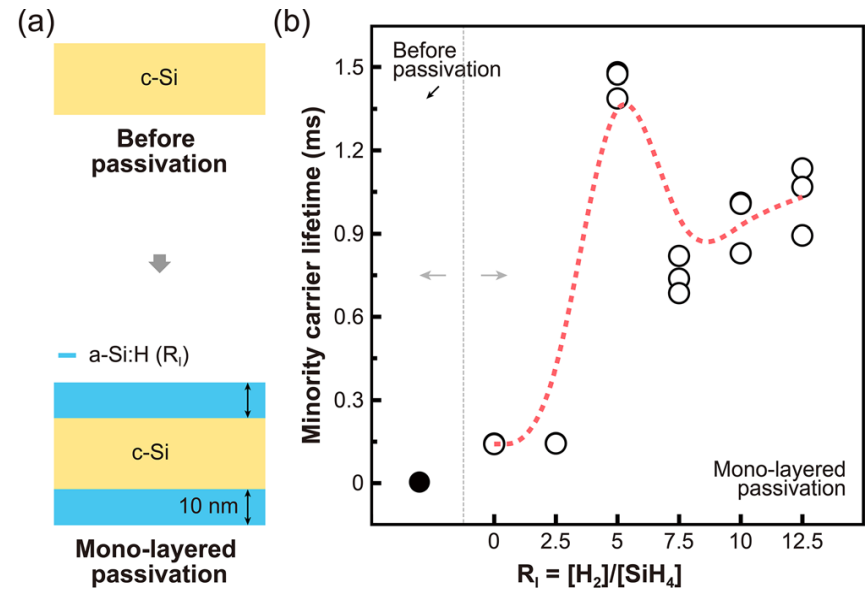
Leo Mathew and Rajesh Rao, Applied Novel Devices (AND). This work was performed at TNF.

This work was supported by NSF SBIR grant.

National Research Priority: DOE-Secure Energy Future

Highly improved passivation of c-Si surfaces using a gradient i a-Si:H layer

Surface passivation using intrinsic a-Si:H (i a-Si:H) films plays a key role in high efficiency c-Si heterojunction solar cells. In this study, we demonstrate improved passivation quality using i a-Si:H films with a gradient-layered structure consisting of interfacial, transition, and capping layers deposited on c-Si surfaces. The H₂ dilution ratio (R) during deposition was optimized individually for the interfacial and capping layers, which were separated by a transition layer for which R changed gradually between its values for the interfacial and capping layers. This approach yielded a significant reduction in surface carrier recombination, resulting in improvement of the minority carrier lifetime from 1480 μ s for mono-layered i a-Si:H passivation to 2550 μ s for the gradient-layered passivation approach.



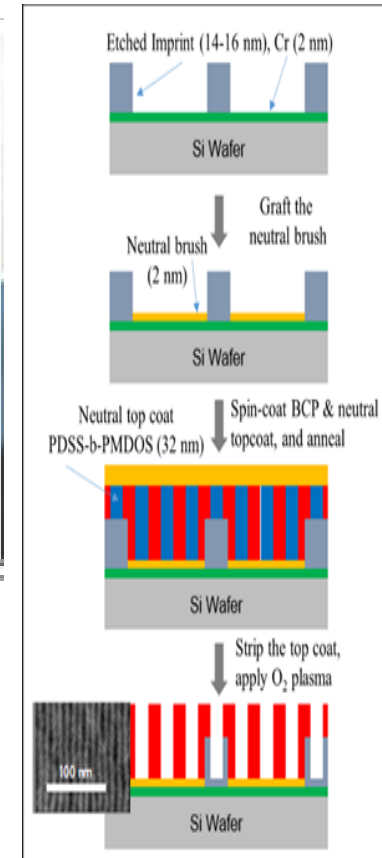
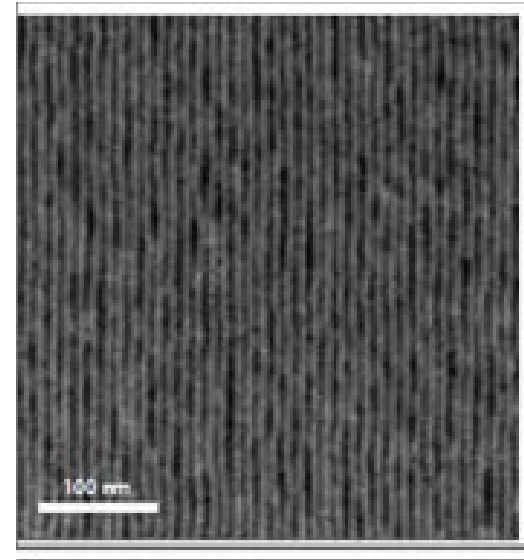
Soonil Lee, Jaehyun Ahn, Leo Mathew, Rajesh Rao, and Edward T. Yu, Univ. of Texas, Applied Novel Devices. Work performed at TNF.

This work was supported by U.S. Army Research Laboratory. *Journal of Applied Physics* 123, 163101 (2018).

National Research Priority: DOE-Secure Energy Future

Oriented lamellae of Si-containing BCP after selective RIE of one block

The directed self-assembly (DSA) of block copolymers (BCP) is a potentially lower cost lithography alternative to enable the continued scaling of devices to smaller dimensions. Organometallic block copolymers have been developed to form patterns down to 5 nm critical dimensions. Graphene nanoribbons have been fabricated using block copolymer lithography. Si-containing BCP material has been developed and incorporated into a process involving a nanoimprinted Cr layer to produce long-ranged parallel lines. Annealing, topcoat strip, and O₂ plasma etch has led to the demonstration of patterning with 5nm lines and spaces. DSA of BCP and our earlier results in nanoshape imprinting demonstrates unprecedented patterning capability that far exceeds the resolution of photo- and EUV lithography.



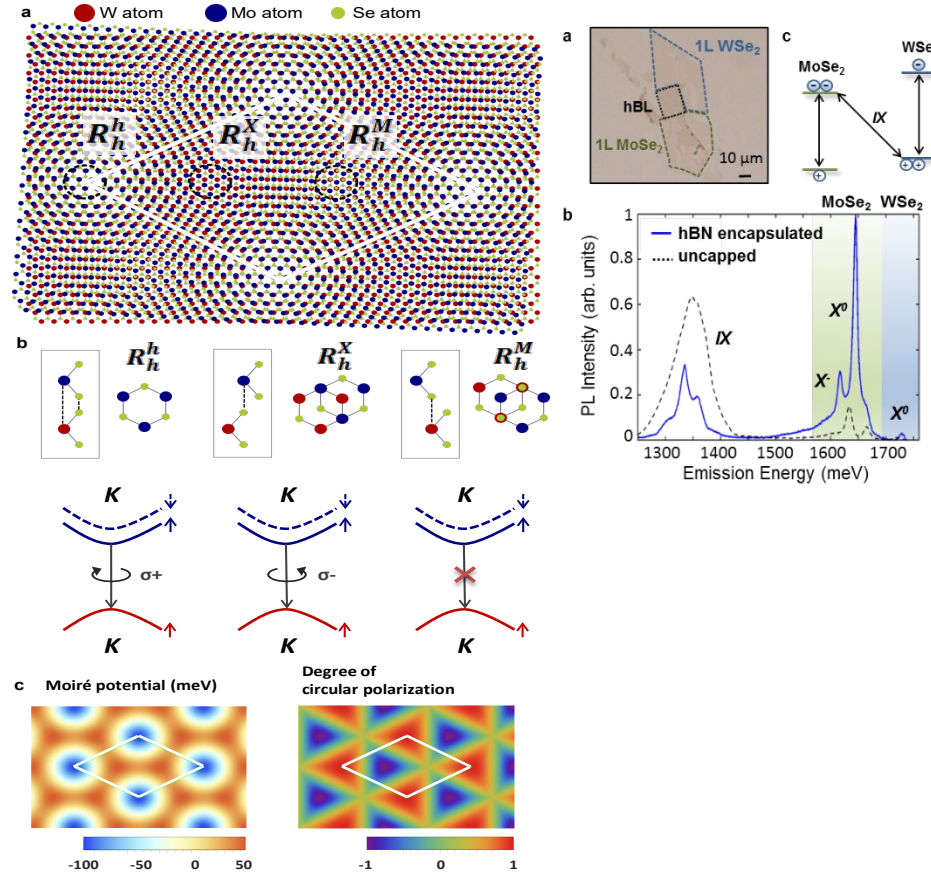
Steve Sirad, Lam Research. Work performed at TNF.

This work was supported by Lam Research Corporation.

National Research Priority: NSF-Quantum Leap

Moiré Excitons in Van der Waals Heterostructures

Moiré superlattice modulates the electronic and optical properties. (a) Different local atomic alignments occur in an MoSe₂/WSe₂ vertical heterostructure with small twist angle. The three highlighted regions correspond to local atomic configurations with three-fold rotational symmetry. (b) In the K valley, S_z = 0 interlayer exciton transitions occur between spin-up conduction-band electrons in the MoSe₂ layer and spin-up valence-band electrons in the WSe₂ layer. K-valley excitons obey different optical selection rules depending on the atomic configuration R_h^μ within the moiré pattern. R_h^μ refers to R-type stacking with the μ site of the MoSe₂ layer aligning with the hexagon center (h) of the WSe₂ layer. Exciton emission at the R_h^h (R_h^X) is left-circularly (right-circularly) polarized. Emission from site R_h^M is dipole-forbidden for normal incidence. (c) Left: The moiré potential of the interlayer exciton transition showing a local minimum at site R_h^h. Right: Spatial map of the optical selection rules for K-valley excitons. The high-symmetry points are circularly polarized and regions between are elliptically polarized.

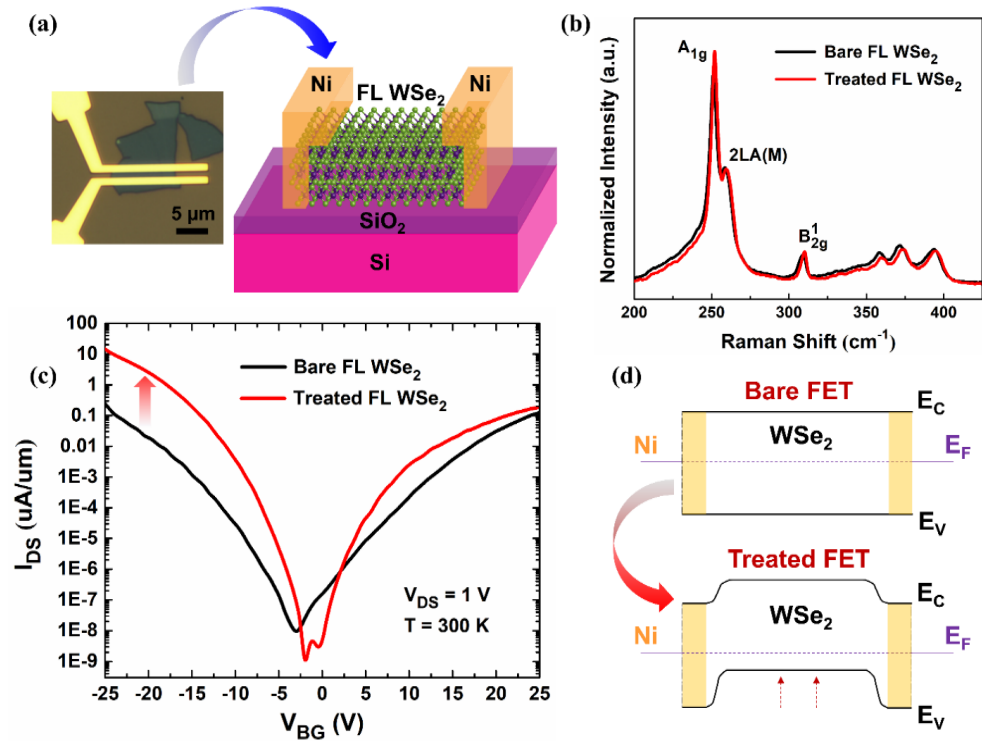


K. Tran, ... S.K. Banerjee... and X. Li, Work performed at TNF.
Nature, 567 (7746) March 7 2019

National Research Priority: NSF-Quantum Leap

Band Structure Engineering of Layered WSe₂ via One-Step Chemical Functionalization

Spectroscopic and electrical characterization of a FL WSe₂ FET. (a). Optical image and schematic diagram of the back-gated FL WSe₂ FET with Ni/Au top contact electrodes. (b). Raman spectra taken on a FL WSe₂ device flake (~ 4 nm thickness) before and after (NH₄)₂S(aq) treatment. (c). Room-temperature back-gated transfer characteristics of the FL WSe₂ FET shown in (a) before (black curve) and after (red curve) (NH₄)₂S(aq) treatment. A clear enhancement of I_{ON} in the p-branch is observed after (NH₄)₂S(aq) treatment. (d). Qualitative equilibrium band diagrams along the FL WSe₂ FET channel before (top) and after (bottom) (NH₄)₂S(aq) treatment explaining the measured FET current-voltage behavior.



J. Park, A.Rai, ...G. Xing, K. Cho, S. K. Banerjee and A. C. Kummel

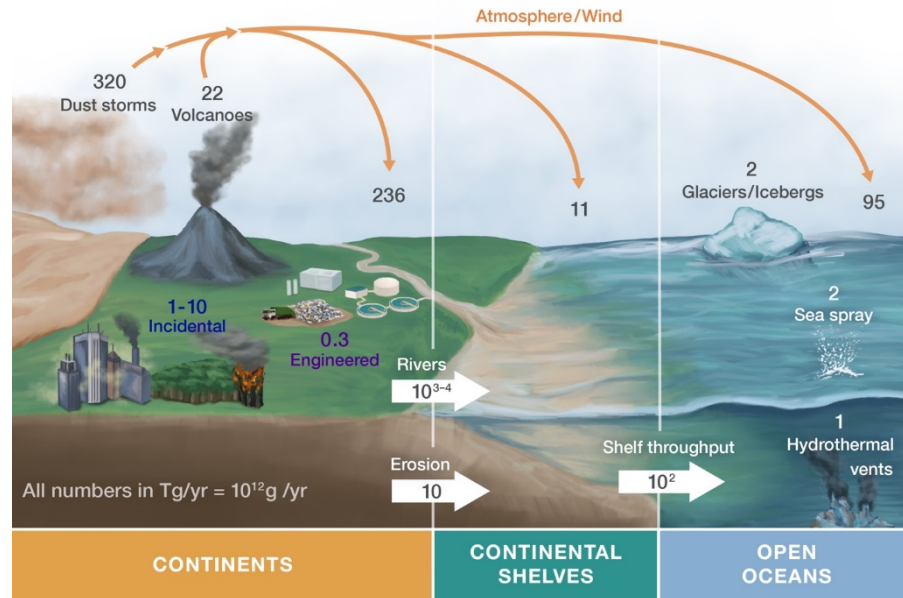
Device Research Conference, ACS Nano (2019)

National Research Priority: NSF-Quantum Leap

***Virginia Tech National Center for Earth and
Environmental Nanotechnology
Infrastructure (NanoEarth)***

Natural, incidental, and engineered nanomaterials and their impacts on the Earth system

Nanomaterials are critical components in the Earth system's past, present, and future. Natural, incidental, and engineered nanomaterials, regardless of their origin, have unique chemical and physical properties, clearly setting them apart from their macroscopic equivalents and necessitating careful study. Following major advances in experimental, computational, analytical, and field approaches, it is becoming possible to better assess and understand all types and origins of nanomaterials in the Earth system. It is also now possible to frame their immediate and long-term impact on environmental and human health at local, regional, and global scales.



An estimated global accounting for all natural, incidental, and engineered nanomaterials on/in Earth's surface and atmosphere.

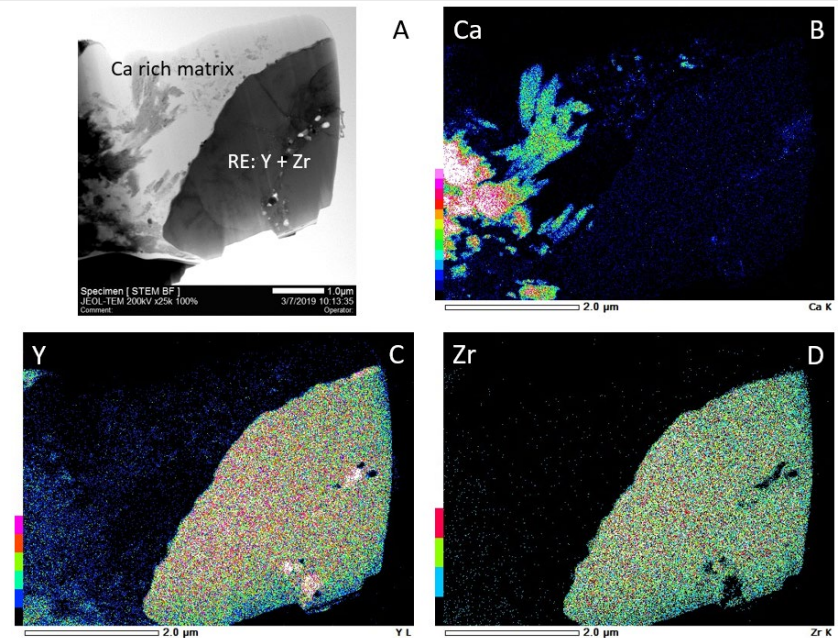
Hochella M.F. Jr., Mogk D.W., Ranville J., Allen I.C., Luther G.W., Marr L.C., McGrail B.P., Murayama M., Qafoku N.P., Rosso K.M., Sahai N., Schroeder P.A., Vikesland P., Westerhoff P., Yang Y. Work performed at NanoEarth.

This work was supported by NSF Awards # ECCS-1542100, 1542160, and 1542210, NSF Awards EAR-1822111, EAR-1331846, EAR-1331846, OCE-1558738, OCE-1558712, EF-0830093, and EEC-1449500. *Science*, 363, eaau8299, 2019.

National Research Priority: NSF-Growing Convergence Research

Detection of Rare Earth Elements in Coal Combustion Byproducts

Rare Earth Elements (REEs) are critical materials for the manufacture of modern electronics. This work is motivated to identify domestic reservoirs of REEs to improve supply chain security. Further, the utilization of coal fly ash for secondary purposes could reduce the environmental impact of the coal industry compared to conventional ash pond storage methods. Coal fly ash samples were examined using SEM / EDS to identify REEs grains. These were extracted using precision FIB milling to produce FIB lift-out sections for subsequent TEM analysis. Crystallographic and chemical analysis suggest the yttrium containing grain is a zircon.



Rare earth elements identified in coal fly ash

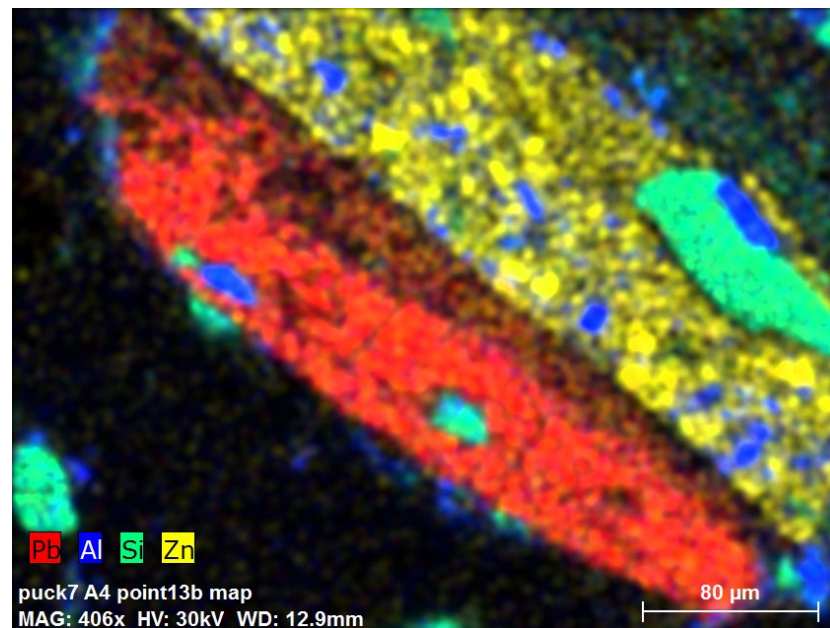
James C. Hower, Elizabeth Cantando, Ya-Peng Yu, Cortland F. Eble, and Gregorcy C. Coply, University of Kentucky Center for Applied Energy Research, Kentucky Geological Survey. Work performed at Virginia Tech's National Center for Earth and Environmental Nanotechnology Infrastructure.

This work was supported by NSF Award # ECCS-1542100. *International Journal of Coal Geology*, 213, 103260, 2019.

National Research Priority: NSF-Growing Convergence Research

Lead Contaminants in Soils in Residential Philadelphia Neighborhoods

Lead contaminated soil has been identified and collected throughout the city of Philadelphia using handheld X-ray fluorescence. The contaminated soils were analyzed using SEM / EDS to assess the location, size, and distribution of lead particles, which were observed as fine grains. The particles were targeted for precision FIB sectioning to produce a TEM lift-out cross section of the grain. The goal of this work is to determine the crystallographic and chemical nature of the lead contamination, which may reveal the source, characterize the biological threat, and inform decontamination efforts, if necessary.



Lead contaminated soils identified using SEM / EDS for targeted precision FIB sectioning, were further analyzed with HRTEM, STEM / EDS mapping and electron diffraction

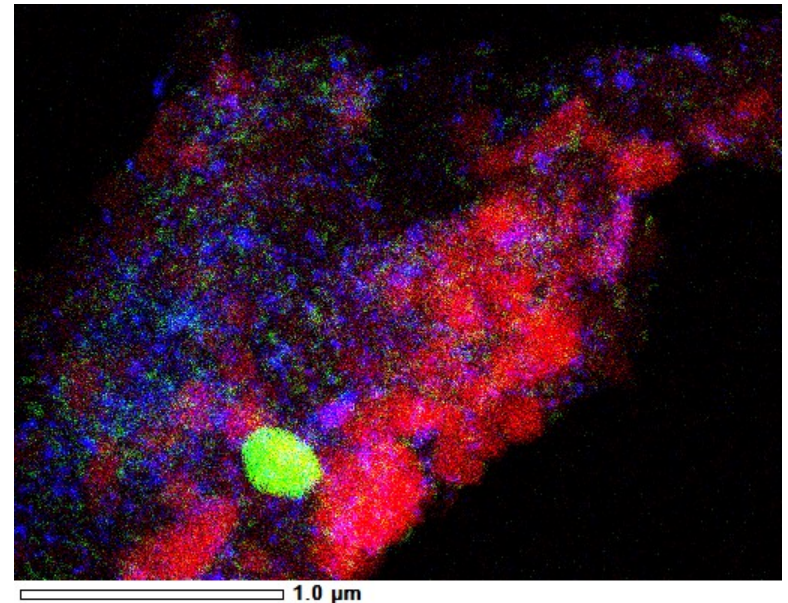
Cynthia Hall, Michael Schindler, Ya-Peng Yu, and Elizabeth Cantando, Laurentian University, West Chester University. Work performed at Virginia Tech's National Center for Earth and Environmental Nanotechnology Infrastructure.

This work was supported by NSF Award # ECCS-1542100.

National Research Priorities: NSF-Growing Convergence Research, NSF-Includes, EPA-Children's Environmental Health

Detecting Titanium Oxide Engineered Nanoparticles in Urban Water Runoff

Efforts to quantify the release of anthropogenic engineered TiO_2 nanoparticles into the environment have been hampered by the inability to distinguish natural from engineered nanoparticles. This research proposes to use the Nb to Ti ratios associated with naturally occurring TiO_2 to isolate the fractions of natural and engineered nanoparticles collected. The water sampled from Ballona Creek, CA was filtered and size fractionated prior to ICP-MS and further analyzed with HRTEM and STEM / EDS mapping to determine particle morphology. The TiO_2 particles were generally observed to range in size from 50-150 nm. TiO_2 is the most abundant engineered nanomaterial produced globally.



STEM / EDS mapping of pollutants sampled from Ballona Creek, CA with maps of Ti (green), Zn (blue), and O (red).

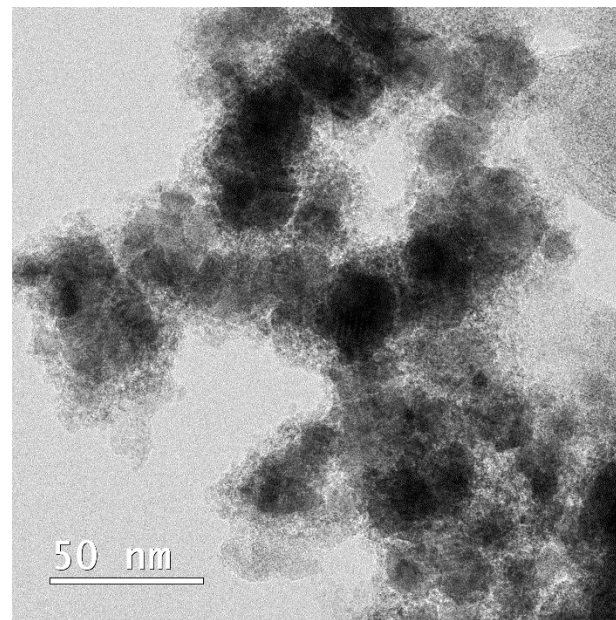
Jingjing Wang, Md. Mahmudun Nabi, Sanjay Mohanty, ARM Nabiul Afroz, Elizabeth Cantando, Nirupam Aich, and Mohammed Baalousha, University of South Carolina, University of Los Angeles, Southern California Coastal Research Project, University of Buffalo. Work performed at Virginia Tech's National Center for Earth and Environmental Nanotechnology Infrastructure.

This work was supported by NSF Award # ECCS-1542100. Submitted to *Chemosphere*.

National Research Priority: NSF-Growing Convergence Research

Precipitation and Transformation of Cobalt Sulfide Nanoparticles

Cobalt sulfide precipitates, key phases in the biogeochemical cycling of cobalt and in relevant remediation and resource recovery processes, remain poorly defined under low-temperature aqueous conditions. Here, we systematically studied the Co-(Fe-)sulfides precipitated and aged in environmentally-relevant solutions, defined by different combinations of pH, initial cobalt-to-iron ratios ($[\text{Co}]_{\text{aq}}/[\text{Fe(II)}]_{\text{aq}}$), with/without S_0 , and the presence/absence of sulfate-reducing bacteria. The revealed precipitation and transformation pathways of Co-(Fe-)sulfides in this study provide a framework for predicting the prevalent Co-bearing phases in various natural and engineered environments.



Biogenic Co-(Fe) sulfide nanoparticles

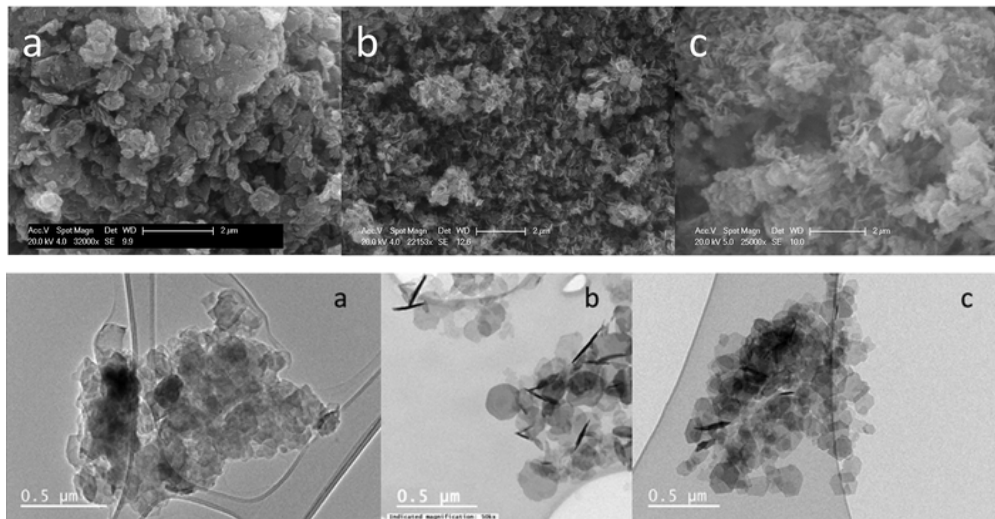
M. Mansor, E. Cantando, Y. Wang, J. Hernandez-Viezcas, J. Gardea-Torresdey, M. Hochella, and J. Xu, University of Texas at El Paso and Pacific Northwest National Laboratory. Work performed at Virginia Tech's National Center for Earth and Environmental Nanotechnology Infrastructure.

This work was supported by NSF Award # ECCS-1542100. M. Mansor et al. (2019). Insights into the biogeochemical cycling of cobalt: Precipitation and transformation of cobalt sulfide nanoparticles under low-temperature aqueous conditions. Submitted to *Environmental Science and Technology*.

National Research Priorities: NSF-Growing Convergence Research & USDA-Sustainable Use of Natural Resources

Continuous synthesis of Zn_2Al-CO_3 layered double hydroxides: a comparison of bench, pilot and industrial scale syntheses

Zn_2Al-CO_3 was produced continuously at bench ($g\ h^{-1}$), pilot ($100s\ g\ h^{-1}$) and industrial scale ($10s\ kg\ h^{-1}$). Crystal domain length and BET surface area were similar at all three scales although there was a small increase at pilot scale. Platelet size increased from 120 nm at bench to 177 nm and 165 nm at pilot scale and industrial scale, respectively. Overall this paper shows that the increase in scale by almost $2000\times$ does not impact on the overall product quality which is an excellent indicator that continuous hydrothermal synthesis is a route for nanomaterials synthesis.



TOP: SEM images of bench (a), pilot (b) and industrial (c) scale LDH samples.. BOTTOM: TEM images of bench (a), pilot (b) and industrial (c) scale LDH samples.

Edward Lester, Promethean Particles and Univ. of Nottingham with Chris Winkler and Matthew Hull of Virginia Tech. Work performed at Virginia Tech's National Center for Earth and Environmental Nanotechnology Infrastructure.

This work was supported in part by NSF Award # 1542100. *React. Chem. Eng.* 4: 663-666, 2019.

National Research Priority: NSF-Quantum Leap

Education and Outreach

International REU: A Network Collaboration for Development of Globally Aware Scientists

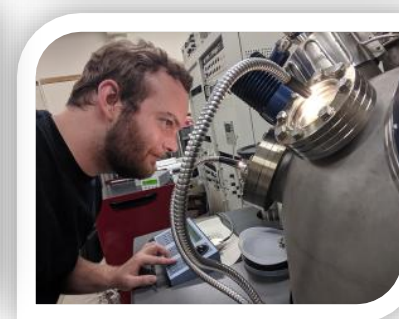
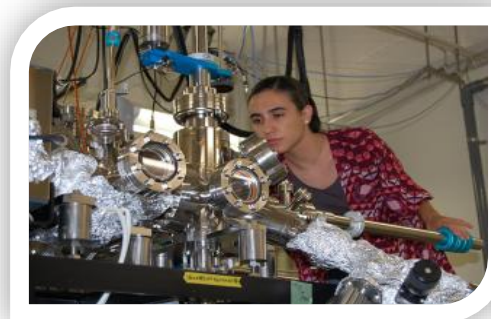
Research is a world-wide enterprise, and being able to thrive in a multicultural environment is a critical skill for 21st century scientists and engineers.

On behalf of NNCI, CNF conducts an international Research Experiences for Undergraduates in collaboration with the National Institute for Materials Science in Tsukuba, Japan. Each summer, six students are selected from the prior year NNCI REU participants for a 10 week advanced research experience at NIMS. This program has been shown to be effective in increasing the participants' "cultural intelligence" toward the goal of becoming more "Globally Aware Scientists":

Since 2008, 81 students have participated in this program. Fifty seven of those have completed or are working on Ph.D.s., and twenty two of those 57 have received NSF Graduate Fellowships. All report the experience has been formative in their professional career development.

Co-funded by CNF (NNCI:1542081) and NNCI Coordinating Office (NNCI:1626153) in 2019.

National Research Priority: NSF-NSF INCLUDES and OSTP-Broadening Participation in the STEM Workforce



Nanooze: A Free Nanotechnology Science Magazine for Children



CNF publishes NANOOZE, a colorful science magazine for children. It is produced by Prof. Carl Batt at Cornell and distributed free to classrooms around the country. It is also distributed to other NNCI sites as well as other laboratories, museums, and programs for use own in their own outreach activities.

It provides newsy content on topics related to nanotechnology but still in support of common middle school curriculum. Approximately 100,000 copies of each issue are printed; over 1.5 million copies have been distributed over the last 10 years.

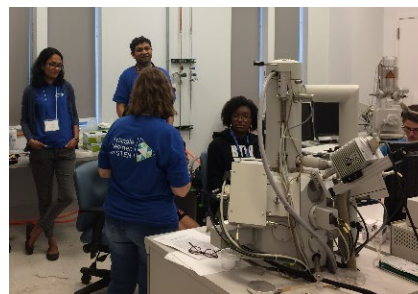
Production and distribution funded as part of the NSF CNF NNCI Cooperative Agreement NNCI:1542081



National Research Priority: NSF-NSF INCLUDES and OSTP-Broadening Participation in the STEM Workforce

Girls STEM Day @ Duke

- Girls participate and earn Girl Scout badges through hands-on STEM activities in topics of DNA, robotics/AI, and chemistry of cosmetics
- Includes parent-focused activities (e.g. financial sessions) for supporting girls' trajectory in the STEM pipeline
- Two years running (2018-2019)
- >140 girls and their families participated (2019)
- Collaboration between many partners with volunteers from STEM professions (43 companies/institutions)
- Assessment
 - 98% were satisfied or very satisfied with their experience
 - 81% felt the event had a great or a lot of impact on them
 - 85% were extremely or very likely to attend next year



Triangle
Women
in STEM



girl scouts



Faculty and staff at NC State, UNC-Chapel Hill, and Duke. Work performed at Duke's Shared Materials Instrumentation Facility.

Work supported by NSF Award # ECCS-1542015, IBM, Triangle Women in STEM, Credit Suisse, and Duke's Pratt School of Engineering and Trinity College of Arts and Sciences.

National Research Priority: NSF-NSF INCLUDES

Nanotechnology, A Maker's Course

- Massive Open Online Course on Coursera platform, providing education in nano-fabrication and -characterization
- Lectures and in-lab demonstrations of equipment in RTNN labs
- Launched September 2017
 - >70,000 visitors
 - >14,000 enrolled
 - > 2,000 completed all course components
 - Learners from >150 countries
- High satisfaction, e.g. course instruction rated 6.4 on a scale with 7 being the highest
- 90% of respondents “likely” or “very likely” to recommend course

coursera



“Gracias...me divertí mucho en este curso y definitivamente con mas ganas de seguir aprendiendo.”

Faculty, students, and staff at NC State, UNC-Chapel Hill, and Duke. Work performed at Duke's Shared Materials Instrumentation Facility, NC State's Analytical Instrumentation Facility, the NC State Nanofabrication Facility, and the Chapel Hill Analytical and Nanofabrication Laboratory.

Work supported by NSF Award # ECCS-1542015.

National Research Priority: NSF-NSF INCLUDES

Quantum Leap Symposium at MANTH

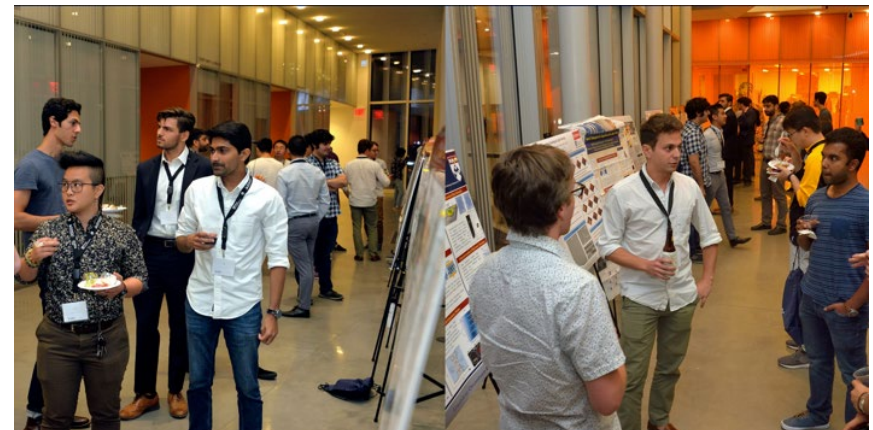


This NSF-Funded workshop at MANTH explored the needs and challenges involved in ensuring the advancement of quantum logic with improved low-dimensional materials operating at room temperature.

Attendees came from NSF and 17 Universities

Symposium: Enabling Quantum Leap: Achieving Room-Temperature Quantum Logic through Improved Low-Dimensional Materials

September 2019



National Research Priority: NSF-Quantum Leap

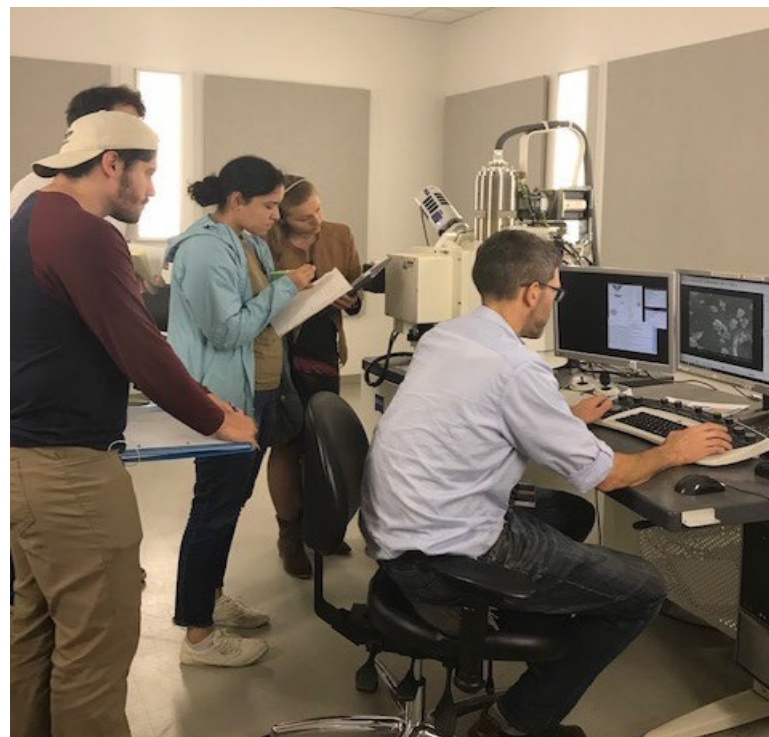
Demonstrations of Microscopic (SEM/TEM) and Surface Analysis Techniques

This work supported a site visit for ten students enrolled in GEOS 4042/6042, Environmental Analytical Instrumentations, at Georgia State University.

After learning the theory and operational procedures of each instrument, the students visited the Materials Characterization Facility (MCF) twice for demonstrations of SEM/TEM, AFM, XRD, XPS and TOF-MS.

The students, in groups of 3-4, rotated to each station and spent 30 minutes with each instrument specialist who went over basic terminology and results from a typical sample.

The demonstrations were very powerful for the students to visualize the concepts they learned in class. The graduate students in the class were pleased to learn of potential avenues to obtain characterization data they may need in their work.



Class demonstration for students enrolled in GEOS 6046, Environmental Analytical instrumentations, at Georgia State University.

Nadine Kabengi, Georgia State University. Work performed at Georgia Tech's Materials Characterization Facility.

This work was supported by a SENIC Catalyst Grant (funded by NSF ECCS-1542174).

National Research Priority: NSF-NSF INCLUDES

Nanotechnology Summer Institute for Middle School Teachers

In June 2019, GT organized a Nanotechnology Summer Institute for Middle School Teachers (Nano SIMST). Based on nano@Stanford's curriculum, 15 teachers from across GA spent 4 days learning about nanotechnology through lectures, hands-on activities, tours, and guest speakers. They were also tasked to develop their own lesson plans to bring back to their classrooms. Adaptations of the original program were included, such as a session on the social and ethical implications of nanotechnology, an opportunity to work on scopes in the Materials Characterization Facility, a remote access session through RAIN, and a career panel featuring reps from different local companies. Both GT and JSNN plan to host Nano SIMST in summer 2020.

Feedback from the workshop at SENIC was very positive: "(T)his workshop was absolutely phenomenal." "I learned so much about a topic I had no previous knowledge of and have easy ways to implement them in my classroom."



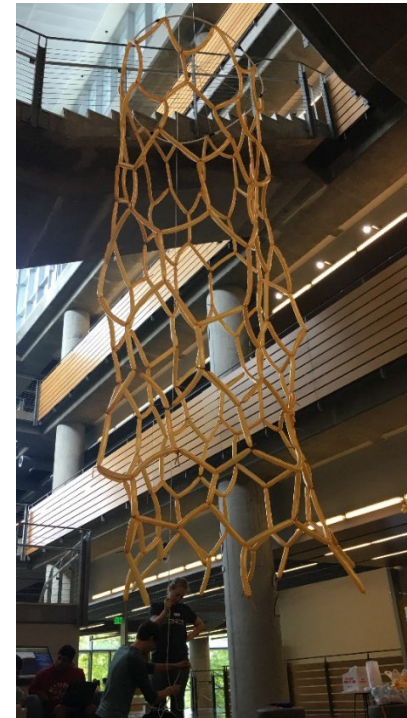
2019 Nano SIMST cohort (top); teachers working through a size sorting activity (bottom)

This work was supported by SENIC, NSF ECCS-1542174.

National Research Priority: NSF-NSF INCLUDES

Graduates In Nanotechnology

In the fall 2018, Georgia Tech started the Graduates in Nanotechnology (GIN) student group to support undergraduates through post-docs who are interested or doing research related to nanotechnology. GIN has hosted lunch-time speakers, Researchers Open-Mic Presentations (ROMP), outreach training session, and has an invited seminar speaker series. Lunch guests have discussed preparing for jobs in academia, how to launch a start-up company, job opportunities at national labs, and the students' own nanotechnology research. When possible, JSNN students join GIN meetings via teleconference. JSNN recently started a Materials Research Society Chapter. These two student groups plan to stream or teleconference events when relevant.



GIN sponsored seminar (left); GIN students in the GT student center building a balloon model of a CNT in honor of National Nanotechnology Day (above)

This work was supported by SENIC, NSF ECCS-1542174.

National Research Priority: NSF-NSF INCLUDES